NEW INSIGHTS INTO EXOSOME BIOGENESIS

by

Francis Kusi Fordjour

A dissertation submitted to The Johns Hopkins University in conformity with the requirements for the degree of Doctor of Philosophy

Baltimore, Maryland

March 2019

Abstract

Extracellular vesicles (EVs) are small membrane bound vesicles that bud from the plasma and endosomal membranes of nearly all cell types. EVs do not have a defined morphology but have the same topology as the cells they bud from. They have gained prominence over the years because of their involvement in intercellular communication; cells can transmit signals, nuclei acids, proteins, carbohydrates and lipids to other cells in a non-viral pathway via extracellular vesicles. EVs have been implicated in numerous physiological processes such as protein quality control, differentiation, and cell polarity. They have also been shown to play important roles in pathological processes (e.g. cancer, viral infections and neurodegenerative disorders).

The size and composition of extracellular vesicles vary significantly, and this has led to a proliferation of names for EVs, including exosomes, microvesicles, oncosomes, ectosomes, membrane particles, etc. Of these, the two most commonly used terms are exosomes and microvesicles. Some have proposed that exosomes be defined as vesicles that are released when multivesicular bodies (MVB) fuse with the plasma membrane, while microvesicles be defined as vesicles that bud directly from the plasma membrane. However, there is little empirical support for these distinctions, and the extent to which differences in EV size and composition are caused by stochastic variations or mechanistic differences is not yet known.

Our understanding of organelle biogenesis has been shaped by detailed studies of individual cargo proteins. My thesis work advanced our mechanistic understanding of EV biogenesis using the same type of cargo-based approach. Specifically, in chapter 1, I tested the endosomal hypothesis of the current model of exosome biogenesis in HEK293 cells using the classical exosomal cargoes

(CD63, CD81 and CD9). I observed that (i) majority of these proteins are localized on the plasma membrane, (ii) cargo proteins localized on the plasma membrane bud better than those in the endosomes, and lastly (iii) redirecting cargo proteins from the endosome to the plasma membrane enhances their budding significantly. The most parsimonious explanation for these observations is that the majority of protein budding occurs at the plasma membrane of HEK293 and NIH3T3 cells, two of the most commonly used cell lines in biomedical research.

In Chapter 2, I characterized the role of certain *trans*-acting factors that are required for the budding of classical exosomal markers. I showed that loss of tetraspanins, or other putative exosome factors such as alix and syntenin, do not cause a defect in the vesicular secretion of exosomal markers in HEK293 and 293T. Despite no defect in budding, I however noticed variation in the budding of exosome cargo proteins in some mutant clones. To identify the basis of this clonal heterogeneity in exosome biogenesis, I generated dozens of single cell clones (SCCs) from the parental HEK293 cell line and found that they varied by as much as 10-fold in their production of exosomes, demonstrating that the variation we observed in mutant cell lines was not due to the nature of the mutations we introduced or the other Cas9-induced mutations in our SCC lines. We next tested whether clonal heterogeneity in exosome biogenesis was a unique feature of HEK293 cells by generating multiple SCCs from several other human cell lines, again in the absence of any mutagenesis. These experiments revealed that SCCs derived 293T, K562, and Hap1 cells also displayed pronounced clonal heterogeneity. Furthermore, in collaboration with Louise Laurent, we found that SCCs derived from the human stem cell line WA09 also displayed pronounced clonal heterogeneity. We conclude from these results that the extent of exosome biogenesis in

human cultured cells is under a complex regulatory pathway that can switch from low to high activity and back as cells are subjected to single cell cloning.

Lastly, I described my observations in the differences in exosome composition and production in HEK293 and HEK293T cells. I report an increase in budding of CD63, CD81 and CD9 in HEK293T compared to HEK293, and propose that the increase in budding is a result of the elevated nSMase2 levels observed in HEK293T. The mechanisms for how nSMase2 affects budding of proteins is however not known.

Thesis Advisor: Stephen J. Gould, Ph.D.
Professor, Department of Biological Chemistry
The Johns Hopkins University School of Medicine

Thesis Reader: Daniel M. Raben, Ph.D.
Professor, Department of Biological Chemistry
The Johns Hopkins University School of Medicine

Dedication

This thesis is dedicated to my mother, Ms. Agnes Adusei Acheampong for her tireless contributions to my education and well-being. As a single mother, she has devoted most of her time to making sure that my brothers and I got the best education. She has been very inspirational and helpful throughout my graduate studies. She encouraged me whenever I had low moments along my journey and even came over to the lab some nights to keep me company while I worked.

I also dedicate this thesis to the many wonderful and driven teachers and professors who taught and encouraged me to pursue science especially Dr. Sharon Crary. Dr. Crary saw so much potential in me when I could not and recommended that I apply to Johns Hopkins for my Ph.D. while working in her lab as an undergraduate researcher. She continues to be a great mentor and role model to me.

Acknowledgements

I'm very grateful to my thesis advisor, Dr. Stephen J. Gould for the opportunity to work in his lab and train as a scientist. Steve took his time to train me on how to critically think through scientific problems and creatively develop solutions. He also encouraged me to be independent while providing the necessary supervision. I'm very grateful for the opportunities he gave me to present my research work at conferences every year.

Next, I would like to thank the members of the Gould lab who have been very supportive and provided great feedback on my experiments in the lab. I'm grateful to James C. Morrell for his help with most of the plasmids I used for my work and for teaching me about molecular cloning. A special thanks to Hayley Muendlein, Jerry Plange, Phillip Harding, Chris Hawk, Shawn Owiredu and Colin Fowler for their help and technical assistance on my thesis projects.

Thanks to my thesis committee members (Dr. Michael Caterina, Dr. Daniel Raben, Dr. Sin Urban, and Dr. Kenneth Witwer) for their guidance throughout my research work. Thanks a lot for making time to be present at all my thesis meetings and for providing me with constructive feedback and suggestions. I'm very grateful for all your help and in particular to Dr. Daniel Raben for reading my thesis.

I would also like to thank the Biological Chemistry Department at Johns Hopkins University School of Medicine for this great opportunity to be trained as a scientist. Lastly, I would like to thank my parents, my brothers Yaw and Philip, and my friends whose constant support made this journey worthwhile.

Table of Contents

List of Tables

List of Figures

Chapter 2

Chapter 3

Chapter 4

Chapter 1: Introduction

Background

Extracellular vesicles are small membrane bound organelles that are released from the plasma and endosomal membrane of eukaryotic cells. These vesicles were initially referred to as 'platelet dust' by Wolf in 1967 when he showed that plasma devoid of platelet still had small particulate platelet material that were bound in phospholipid-rich membranes and could be separated from the plasma by ultracentrifugation[1]. During that same time, Bonucci[2] and Anderson[3] described small roundish osmiophilic vesicles which were formed in the pericellular spaces prior to cartilage calcification. These vesicles contain crystallites and come together around collagenous fibrils and the cartilage matrix to initiate calcification. In 1980, Trams[4] proposed the term 'exosome' to describe ecto-enzyme containing vesicles from cultured cell lines that may have physiologic functions. The 'exosomes' isolated were enriched with phospholipids such as sphingomyelin and unsaturated fatty acids, so were concluded to probably bud from specific domains of the plasma membrane.

However, in the late 1980's, the term exosome was used to describe small membrane vesicles released by reticulocytes during differentiation[5]. Initial studies on reticulocyte maturation revealed that the transferrin receptor (TfR) could be detected in the intraluminal bodies of endosomes during its elimination from the plasma membrane, as well as its release on secreted vesicles[6]. These EM-based studies showed that TfR budding was a multi-step process involving its trafficking to the limiting membrane of the endosome, budding at that membrane to form MVBs, and subsequent release upon MVB fusion with the plasma membrane[7].

Morphology

Extracellular vesicles (EVs) have the same topology as the cell. The sizes can vary significantly, and this has led to a plethora of names in the field. Vesicles ranging from 30nm to 200nm in diameter are referred to as exosomes, while larger vesicles with diameters more than 200nm but less than 1000nm are classified as microvesicles. Oncosomes,[8,9] on the other hand are large vesicles that bud from cancer cells and can be up to 10um in size. However, the extent to which these variations in size are caused by stochastic or mechanistic effect is not fully known, even though it has been proposed that large vesicles such as microvesicles and oncosomes bud from the plasma membrane and exosomes strictly bud from the endosome, these hypotheses have not been fully tested. Furthermore, experimental techniques used in assaying the sizes of extracellular vesicles may indirectly alter vesicle sizes as some of these experiments entails fixing with formaldehyde, freezing under high pressure, and treating with heavy metal salts.

In addition to the size differences, there are variations in the shapes and structures of EVs. Exosomes isolated from HMC-1 cells were classified into nine different categories based on their shapes and structures when imaged using negative staining and cryo-EM[10]. The HMC-1 exosomes comprised of single vesicles which formed the majority, while double vesicles which contained a smaller vesicle enclosed in a larger vesicle, and triple vesicles where two vesicles were inside a larger one formed about 20%. They observed variations in the shape of the exosomes, while some had defined shapes such as round, oval, tubular, filamentous, they noticed some vesicles were pleomorphic. The heterogeneity in exosome morphologies could suggest that exosomes are made up of subpopulations which can have different functions and biochemistry. It is, however, important to note that there are currently no known mechanisms to explain the variations in shapes

and structures of exosomes, and there exist no protocols to isolate the different exosomal subpopulations.

The density of exosomes ranges between 1.11 and 1.19 g/ml as a result of the variations in protein-lipid content of exosomes[11]. For example, exosomes secreted from mouse tumor breast cell line where Rab27a is inhibited has been shown to be less dense (1.11g/ml) compared to exosomes released from the wild type cell lines[12]. Fang et al showed that expression of a single protein such as AcylTyA in human T-cells can considerably alter the density of exosomes, and even affect their sizes and shapes[13]. In conclusion, size, shape and density cannot be used as determinants of exosomes since these characteristics vary significant depending on the protein:lipid compositions, cell line that they are budding from, physiologic state of the cell and how the vesicles are assayed.

Exosome Composition

Exosomes are enriched with a wide repertoire of proteins, lipids, nuclei acids and carbohydrates. These exosomal components can vary significantly from one cell to another, and even within a single cell. The variations can further be enhanced depending on the physiologic state of the cell. For instance, we have observed that HEK293T has significantly higher relative abundance of tetraspanins in exosomes than HEK293 even though both cell lines are embryonic kidney cells with the major difference being that HEK293T is transformed with SV40 large T antigen. Exosome composition can also change depending on the cell's pathological state, as exosomes derived from diseased cells have significantly different composition compared to that of healthy cells[14]. Ling et al found that miR-195 is downregulated in LX2, human stellate cells

when co-cultured with human cholangiocarcinoma[15]. Extensive work done on the compositions of exosomes can be found in these databases: EVpedia[16], Exocarta[17], and Vesiclepedia[18].

Exosome Lipids

Lipidomic analyses have shown exosomes to be highly enriched in membrane lipids. These include phospholipids (phosphatidylcholine (PC), phosphatidylethanolamine (PE), phosphatidylserine (PS), phosphatidylinositol (PI), sphingomyelin), cholesterol, ceramides, and glycolipids (glycosphingolipids)[19-22]. The relative abundance of these lipids is however different from the whole cell membrane. Exosome membranes have high amount of PE and PS on the outer membrane, while whole cell membrane have them in their inner membrane due to the activity of phospholipid flippases[23,24]. Another difference in lipid distribution is that of exosomes and MVB which they are presumed to bud. Exosomes have been shown to have high amount of cholesterol and very low lysobisphosphatidic acid (LBPA), which is in sharp contrast to the lipid composition of the limiting membrane MVB[25]. It is possible that MVB might not be a major site of budding or the lipid composition of MVB changes as it matures and progresses to the plasma membrane to release the vesicles.

Lipids play roles in exosome biogenesis by enhancing secretion of exosomes. Increasing ceramide levels by overexpressing nSMase2 in oligodendroglial cells[26], HEK293[27], and T-cells[28] resulted in an increased in exosome budding. The mechanism by which ceramide enhances exosomal secretion is unknown but it has been proposed that ceramide induces inward curvature of the limiting membranes of the sites of budding. Pharmacologic or genetically induced accumulation of cholesterol in MVB of Oli-neu cells has been shown to enhance secretion of exosomes carrying specific cargoes such as ALIX and Flotillin-2[29]. It is important to note that the

mechanisms by which these lipids enhance exosome secretion is unknown even though it has been suggested that the lipids can induce membrane curvature or act as signal to stimulate a signaling pathway that enhances exosome biogenesis.

Exosome Carbohydrates

Complex polysaccharides are found on the surface of exosomes, attached to glycoproteins and lipids on the outer membranes. Glycomic analysis using lectin binding microarray has shown exosomes to be enriched with high mannose, polylactosamine, α-2,6 sialic acid, and complex N-linked glycans[30,31]. These enrichments however vary across exosomes secreted from different cell lines as some cancer cells exosomes are enriched for polymers of hyaluronic acid[32] and heparin sulfate glycans[33].

The presence or lack of these carbohydrates on the surface on exosomes can affect their uptake by recipient cells as they can change the physico-chemical properties of the membrane. Escrevente et al, showed that removal of N-acetylneuraminic acid (NeuAc) from the SKOV3 cancer cell exosomes led to an increase in their uptake by the same cell[34]. NeuAc, which is a negatively charged carbohydrate, when removed likely resulted in a change of membrane charge which enhanced their uptake. The absence of NeuAc could also expose new carbohydrate residues which might have been the preferred ligands for carbohydrate binding proteins on the surface of the recipient cells.

Exosome Nuclei Acids

Exosomes contain RNA and DNA, but these are not carried in large amount compared to other macromolecules. Despite the low abundance of these nuclei acids, sensitive methods of detection such as RNA-sequencing and reverse transcription and quantitative PCR analysis has shown exosomes to have single-stranded DNA, double-stranded DNA, genomic DNA, mitochondria DNA, coding RNAs (mRNA), and non-coding RNAs (miRNA, lncRNAs, circRNAs, snoRNAs, snRNAs, tRNAs, rRNAs)[35-42]. These nuclei acids expressed in exosomes are protected from nucleases and can be transferred to recipient cells or other parts of the same cell to be further expressed or to regulate expressions of other genes. Purified exosomes derived from Glioblastoma cancer cells expressing Gaussia luciferase (Gluc) mRNA increased the Gluc activity of human brain microvascular endothelial cells (HBMVECs) over 24 hours when co-cultured[43,44].

The process by which nuclei acids are incorporated into exosomes is not fully understood. DNA isolated and sequenced from pancreatic cancer cell derived exosomes reconstructed the entire genome of the producing cell without any bias for particular sequences. RNA on the other has been proposed to bud into exosomes by binding to other exosomal cargoes. For instance, Gag and Gag-like proteins binds their mRNA and co-import them into exosomes[44,45]. Ago-2 which is a protein involved in microRNA processing has been shown to bud into exosomes with other miRNAs[46,47]. Other proteins such as YBX1[36,48], SYNCRIP[49], Hu[50,51], and hnRNPA2B1[52] bind to motifs on miRNA and shuttle them into exosomes.

Exosome Proteins

Exosomes are highly enriched in selected proteins. These include integral membrane proteins, peripheral membrane proteins, lipid-anchored proteins and soluble proteins. It is important to note that just like the other macromolecules described earlier, the protein composition of exosomes varies significantly within clones of a single cell, and from one cell line to another.

Escola et al[53] were the first to show the presence of tetraspanins (4-transmembrane proteins) such as CD37, CD53, CD63, CD81, CD82, and CD86. Of these tetraspanins, CD81 was the most abundant and was enriched by 124-fold in exosomes while CD63 was the least enriched in exosomes by 7-fold. Other tetraspanins such as CD9, CD37, CD151, TSPAN7, TSPAN8, TSPAN16, etc. have been found in exosomes[54]. Tetraspanins act as molecular facilitators that interact with integrins and other transmembrane proteins to facilitate their trafficking in the cells[55]. These tetraspanins partners such as integrins[56], MHC Class II proteins[11], ICAM-1[57], syndecans[58] have been found in exosomes. It is likely that as tetraspanins are recruited into exosomes, their binding partners are automatically recruited too. Exosomes have been shown to also contain signal proteins, many of which tetraspanins interact with and facilitate their recruitments. Epidermal growth factor receptor (EGFR)[59], T-cell receptor[60], notch receptors[61,62], G-protein couple receptors[63,64], cytokine receptors[63] and vascular endothelial growth factor (VEGF) receptor type 2[65] are a few signal receptor molecules that have been identified in exosomes. Other signaling proteins such as tumor necrosis factor (TNF)[66], TRAIL[67], FAS ligand[68] and TGFß[69] have been found to be reside at the peripheral surface of exosomes. These signaling molecules can elicit functional signaling responses by binding to and activating receptors on recipient cells.

Exosomes are enriched with membrane proteins which are anchored by lipids to the inner and outer membranes. C-terminal glycosylphosphotidylinositol (GPI) anchor proteins such as

ectonucleotidases CD39 and CD73[70], decay accelerating factor CD55 and reactive lysis membrane inhibitor CD59[71], glypian-1[72], Juno[73] and prion proteins have been found in the outer leaflet of exosome membranes[74]. Proteins like Hedgehog (Hh), a secreted morphogen that is responsible for differentiation and patterning in developing animal tissues, has been shown to be linked to the outer membrane leaflet of exosomes by their cholesterol moiety[75]. The inner membrane leaflet is enriched with acylated proteins such as prenylated small GTPases like Rabs[76,77], palmitoylated proteins present in the inner membrane of tumor derived exosomes[78], and myristoylated signaling kinases like Src[79,80]. Scaffolding proteins have been found at the peripheral surface of the inner membrane lipids to crosslink the cytoplasmic tails of membrane proteins to one another and to other cargoes in the exosomes. These scaffolding proteins include Ezrin-Radixin-Moesin (ERM) a family protein which links membrane proteins to actin-based cytoskeleton[81,82]. Syntenin which has been found in exosomes secreted from MCF-7 cells and other cell lines binds to ALIX (ALG-2-interacting protein X) via its three $LYPX_nL$ motifs on the N-terminus and to syndecans via the PDZ domains[58,83]. ALIX is also a scaffold protein that is enriched in exosomes, it interacts with CHMP4a/b and TSG101 which are components of ESCRT-I and ESCRT-III respectively[84]. The endosomal sorting complex required for transport (ESCRT) machinery consists of ESCRT-0, ESCRT-I, ESCRT-II and ESCRT-III protein complexes and these have been shown to be involved in a number of membrane remodeling events such as retroviral budding, cytokinetic abscission, MVB biogenesis, nuclear membrane reformation and autophagy[85,86]. It has been thought to be involved in exosome budding because of its enrichment in exosomes[87], however silencing or deletion of ESCRT genes has not shown any significant defect in the budding of exosomes[88,89].

In addition to the membrane proteins, exosomes are enriched with soluble/cytosolic proteins such as chaperones[90-93], cytoskeleton[94-96], and enzymes[90,97-99]. These proteins are

surprisingly abundant in exosomes, however there is currently no evidence that they are involved in exosomes biogenesis or are selectively enriched in exosomes. It is therefore likely that they end up in exosomes non-selectively during cargo recruitment into exosomes. Chaperone proteins on the other hand bind to aggregated or misfolded proteins[100] so can be recruited into exosomes when these proteins buds into exosomes. For instance, HSP70 interacts with TfR during maturation of the red blood cells, and both are secreted together into exosomes[91].

Exosome Biogenesis

Sites of Exosome Budding

The current dogma of exosome biogenesis predicts that exosomes bud from endosomes. Proteins are targeted to the endosomal limiting membrane where they bud. The endosome becomes laden with vesicles and then moves to the plasma membrane to fuse with it and release the exosomes. The vesicle laden endosomes are referred to as multivesicular bodies (MVB). This model is based on electron microscopic data which showed the vesicular externalization of the transferrin receptor in sheep reticulocytes[6,7,101]. Subsequently other studies have confirmed that exosomes can bud from the endosomes[102]. Knocking down Rab27[77] or RAL-1[103] showed accumulation of MVBs in cells and reduction in exosome level. In addition, using RNAi to inactivate HRS inhibits the formation and secretion of exosomes in dendritic cells[89]. HRS is an ESCRT-0 protein which functions with ESCRT-1 to cluster ubiquitylated cargoes onto the limiting membrane of endosomes before they bud. Experiments involving pH-sensitive GFP-pHLuorin moiety inserted into the first extracellular loop of CD63 has been used to show the fusion of MVEs with cell surface[104]. Deleting target membrane SNARES such as SNAP23 and syntaxin-4 significantly inhibits the secretion of CD63-enriched exosomes in HeLa cells. Similarly, enhancing

activity of SNAP23 through the activation of H1R1 allows for rapid fusion of MVEs with plasma membrane[105].

While these experiments confirm exosomes can bud from the endosomes in some cells, other experiments indicate that exosomes also bud from the plasma membrane[106-108]. Exosomes from T-lymphocytes cells are secreted from the plasma membrane[13,23,109]; cargoes are targeted to discrete domains on the plasma membrane instead of the endosomes where they bud into the extracellular space[13,23,110-112]. Electron microscopy experiment has shown Glioblastoma cells (GBM20/3) shed most of their exosomes directly from the plasma membrane[113]. Juno protein which is the sperm surface receptor on egg also buds into exosomes from the egg surface immediately after fertilization[73]. Arrestin domain-containing protein (ARRDC) and G protein-coupled receptors (GPCRs) bud from the plasma membrane. GPCRs cluster onto the plasma membranes of cilia where they bud directly into the extracellular milieu[64]. ARRDC on the other hand interacts with TSG101 and relocalizes it from the endosome to the plasma membrane where they bud together into exosomes[114].

Fang et al.[13] showed in Jurkat T cells that inducing higher-order oligomerization of plasma membrane proteins, and attaching high-order oligomeric cytoplasmic proteins to the plasma membrane via a short N-terminal acylation tag were sufficient to target them to the exosomes. These lines of evidence provide support for the hypothesis that the plasma membrane is a site for exosome budding. Shen et al.[112] confirmed the budding of high-order cytosolic proteins from plasma membrane into exosomes using a variety of plasma membrane anchors such as (i) a myristoylation tag; (ii) a phosphatidylinositol-(4,5)-bisphosphate (PIP(2))-binding domain; (iii), a phosphatidylinositol-(3,4,5)-trisphosphate-binding domain; (iv) a prenylation/palmitoylation tag, and (v) a type-1 plasma membrane protein, CD43. It is important to note that targeting such cargoes

to the endosomal membrane budded rather poorly even though endosome membrane is the widely hypothesized site of exosome budding.

Machineries Involved in Exosomes Biogenesis

Exosomes biogenesis involves the targeting of cargoes to sites of budding (endosomes and plasma membranes), the budding of cargoes into small membrane bound vesicles, and their release into the extracellular space. A number of molecular machineries have been implicated in these processes.

Lipids play an important role in exosome biogenesis. In order for exosomes to bud, membrane curvature must be induced, and this is made possible by lipids such as PE and PS that are able to form cone-shapes and inverted-cone shapes. Exosome outer membranes have relatively high levels of PE and PS, and this is in sharp contrast to the outer leaflet of plasma membrane which has relatively low levels of PE and PS. The low abundance of these lipids is due to the activity of phospholipid flippases, which transport PE and PS from the outer leaflet to the inner leaflet. However, there are discrete domains of the plasma membrane that are enriched with PE on the outer leaflet, these domains serve as site for exosome budding[13,23]. Wehmann et al.[115] showed that deleting TAT-5 phospholipid flippase in *C. elegans* results in an increase in exosome secretion. They suggested that loss of TAT-5 exposes PE on the outer leaflet thereby inducing a membrane curvature that favors exosome secretion.

Exosomes secreted from MCF-7 and RBL-2H3 cells contain Phospholipase D2 (PLD2), an enzyme that catalyzes the hydrolysis of phosphocholine (PC) to choline and phosphatidic acid (PA), a cone shaped lipid. Laulagnier et al.[116] showed that increasing PLD2 levels in RBL-2H3 cells with an expression vector or by stimulating with ionomycin enhanced exosomes secretion.

The model suggested is that an increase in PLD2 will result in an increase in PA levels in the inner leaflet of MVB's limiting membrane which would induce membrane curvature and thus formation of vesicles[117,118]. Ceramide is another important lipid that has been implicated in exosome biogenesis. It has been shown that exosomes secretion is significantly impaired when neutral sphingomyelinase 2 (nSMase2) is inhibited with GW4869[26]. nSMase2 catalyzes the production of ceramide from the hydrolysis of sphingomyelin[119]. It has been proposed that ceramide induces membrane curvature that favors excision of vesicles from the cells. It is important to note that ceramide is also a second messenger so can activate a number of pathways which can in turn stimulate exosome production.

Endosomal Sorting Complexes Required for Transport (ESCRT)

ESCRT were identified in yeast as protein complexes involved in the sorting of cargoes into vesicles during the formation of MVB (multivesicular bodies)[85,120]. They have subsequently been found to be involved in envelope viral budding, cytokinesis, wound repair, neuron pruning, defective nuclear pore extraction, nuclear envelope reformation and autophagy[121]. ESCRT consists of five different protein complexes denoted as ESCRTs -0, -I, -II, -III, and AAA ATPase Vps4 complex. ESCRT-0 binds and sequesters ubiquitinated cargoes on the surface of the cell, ESCRT-I together with ESCRT-II are responsible for budding of membrane and protein, ESCRT-III drives vesicle scission, and AAA ATPase Vps4 is responsible for the disassembling and recycling of the ESCRT machinery[122].

The mechanisms for exosome biogenesis have been hypothesized to be dependent on ESCRT due to the similarities between the exosome biogenesis processes and other processes in which ESCRT machinery have been implicated. However, a number of independent studies have

shown a minimal reduction in exosome secretion when ESCRT-0 and -I components are depleted, and no effect on the budding of exosomes when the ESCRT function is blocked by inhibition of VPS4. For instance, inhibiting HRS, an ESCRT-0 protein in HeLa cells[88], HEK293[123], mouse dendritic cell[89], and head and neck squamous cell carcinoma[124] resulted in a defect in exosome secretion, but an RNA interference screen targeting ESCRT -II and -III proteins in HeLa cells showed no defect in exosome secretion[88]. It is possible that these effects might be cell line specific as depletion of CHMP4, an ESCRT-III protein showed some reduction in exosome secretion of MCF-7 cell line[58]. Also, inhibiting TSG101, an ESCRT-I protein resulted in a defect in exosome budding of HeLa[88], MCF-7[58] and RPE1[125] cells, but not in oligodendroglial cells[26].

AAA ATPase VPS4, the complex responsible for disassembling and recycling the ESCRT components has been shown in vivo to block all ESCRT-dependent processes when its catalytic activity is silenced. However, expressing a dominant negative VPS4 in human cells does not significantly affect budding of exosomal tetraspanins, even though it completely inhibits HIV budding and cytokinesis[13,88]. Trajkovic confirmed this observation in oli-neu cells[26]. It is important to note that VPS4 has two isoforms and inhibiting both isoforms has no significant effect on exosome secretion but inhibiting one of the isoforms (VPS4B) in HeLa cells has been shown to result in an increase in exosome secretion[88].

In conclusion, the mechanisms for exosome biogenesis cannot be said to be dependent on ESCRT since inactivation of VPS4 does not significantly affect exosome production. The mechanisms also vary among cell lines since while depleting or inhibiting a protein might have an effect on the biogenesis in one cell line, its inhibition might have the opposite or no effect at all in another cell line.

RAB Family

Rab GTPases are a large family of small GTPases that regulate membrane identity and control the steps involved in intracellular vesicle trafficking such as vesicle budding, vesicle transport along cytoskeletal elements, and membrane fusion[126]. Rab proteins have been identified in exosomes and implicated in exosome biogenesis but the precise mechanism of their involvement is not fully understood. Rab11 was the first Rab GTPase identified to affect exosome secretion. Savina et al showed that vesicular secretion of transferrin receptor, Lyn and chaperone protein HSC70 are impaired in K562 cells when overexpressed with a dominant negative Rab11 mutant[127]. Similarly, inhibiting Rab11 in *Drosophila* S2 cells reduced the budding of Evi-containing exosomes[128].

Subsequently, several other Rabs have been found to affect exosome secretion through genetic screens. Rab35, when inhibited in oli-neu cells impaired the budding of proteolipid proteins (PLP) in exosomes[76]. Fruhbeis et al. also noted a reduction in exosome secretion when Rab35 was silenced in oli-neu cells[129]. Ostrowski et al.[77] using RNA interference (RNAi) screen identified five different Rab GTPases that affect exosome secretion in HeLa cells. They found that depletion of Rab2b, Rab5a, Rab9a, Rab27a and Rab27b in HeLa cells resulted in a decrease in secretion of exosomes which was assayed using flow cytometry to detect anti-CD81 and anti-MHC exosomes bound on anti-CD63 beads. They observed using TIRF microscopy that silencing Rab27a resulted in an increase in the sizes of the MVE, while MVEs were redirected towards the perinuclear area when Rab27b is depleted. This same phenotype was observed when Slp4 and Slac2b which are effectors of Rab27. It was therefore proposed that Rab27 is an important of exosome biogenesis and it regulates the maturation of MVEs and their docking to the plasma membrane to release exosomes. It important to note that even though several studies have shown

the effects of Rab27 on exosome biogenesis in different cell lines[124,130-132], however some studies have shown no significant defect on exosome biogenesis when Rab27 is depleted[125,128]. Similarly, Rab7 has been shown by Baietti et al.[58] to affect the budding of syntenin, ALIX and syndecans in exosomes of MCF-7 cells but no effect was observed in exosome secretion in HeLa cells.

Syndecan-Syntenin-ALIX Pathway

Baietti et al.[58] observed that depleting syndecan, syntenin, and ALIX in MCF-7 cells significantly impair exosome secretion. They also established using electron microscopy, that knocking down syntenin affects the formation of intraluminal vesicles in the endosomes and proposed that syndecan interacts with syntenin which connects to ALIX, an accessory component of the ESCRT machinery that supports endosomal membrane budding and scission. Additional experiments have shown that the silencing of ALIX in dendritic[88] and muscle cells[133] result in a reduction of the budding of CD63 positive exosomes.

ARF6-PLD2 Pathway

ADP ribosylation factor 6 (ARF6) and its effector phospholipase D2 (PLD2) have been implicated in the exosome biogenesis pathway. Ghossoub et al.[117] showed that budding of syntenin, ALIX and CD63 is significantly reduced when MCF-7 cells are treated with a PLD-2 inhibitor, thereby implicating PLD-2 in exosome biogenesis. They also confirmed the effect of PLD-2 using confocal microscopy to assess enrichment of exogenous syntenin in the endosomal lumen of a PLD-2 depleted cell. They observed that syntenin is significantly reduced in the lumen when PLD-2 is silenced, and so suggested that PLD2 is involved in the packaging of syntenin in endosomal lumen before they bud into exosomes. Depleting of ARF6 significantly impairs the

vesicular secretion of syntenin, ALIX and CD63. In contrast, overexpressing ARF6 in MCF-7 enhances the budding of these cargoes. To investigate the role of ARF6 in exosome biogenesis, the authors performed electron microscopy to assess the ultrastructure of the endosomes of ARF6 depleted cells, and observed the lumen of the endosomes to be virtually empty with minimal ILVs at the periphery. They therefore proposed that ARF6 is involved in formation of the ILV.

It is important to note that ARF6 and PLD2 have also been implicated in the budding of exosomes from the plasma membrane in tumor cells. Vandhana et al.[134] observed a significant decrease in exosomes collected from multiple tumor cell lines expressing a mutant ARF6 where the GTPase activity is inhibited. Using microscopy, they observed an accumulation of more exosome structures within the cell and these were localized around the plasma membrane. They proposed that ARF6 activity stimulates PLD2 which in turn activates the ERK pathway, thus allowing the actomyosin-based budding of the exosomes into the extracellular space.

Biological Significance of Exosomes

Exosomes have been implicated in a number of physiological processes such as cellular homeostasis[135], calcification of extracellular matrix[2,3], cell polarity[111], migration[111], germ cell development[136] and cell-to-cell communication.

Exosomes may participate in intra-cellular homeostasis by selectively budding out toxic and obsolete macromolecules from the cell. Johnstone et al.[7] reported this role of exosomes when they described the mechanisms by which reticulocytes get rid of transferrin receptor during maturation into erythrocytes. They observed TfR was trafficked from the plasma membrane into small vesicles in the endosomes which were later secreted out of the cell. Cells can get rid of misfolded and aggregated proteins such Prions, Tau, α-synuclein and amyloid β by secreting via

exosomes[137,138]. Juno, the sperm receptor on the egg surface buds off into exosomes immediately after a sperm fuses with the egg in order to prevent polyspermy[73].

In addition to cellular homeostasis, exosomes play a role in establishing cell polarity. In leukocytes, exosomal biogenesis pathway generates a polarized protein sorting pathway where higher-order oligomerized proteins and proteins attached to the plasma membrane are trafficked to the posterior pole of cells. This overlap between exosomal proteins and the posterior pole of cells can generate anterior-posterior morphology in non-polarized cells, which is critical for directed cell migration[111].

Exosomes have been found to participate in cellular communications through their transmission of signals and molecules. Exosomes containing miRNA have been shown to reduce target mRNA expression levels in the recipient cells. Mittebrunn et al.[28] tested the functionality of T cell exosomes containing miR-335 in antigen-presenting cells (APC) using a SOX4 luciferase reporter assay. They found the internalization of miR-335 containing exosomes by APC led to a decrease in SOX4 luciferase activity. Exosomes secreted from dendritic cells have also been shown to enhance immunogenicity and differentiation of T helper cells. Choudhuri et al.[139] observed that T cells release exosomes containing T cell receptors (TCR) at the immunological synapses which engage with peptide-bound MHC molecules on B cells to initiate T cell signaling. These experiments underscore the involvement of exosomes in cellular communication.

Exosomes have been shown to be involved in many pathophysiological processes. They have been implicated in multiple human diseases such as HIV, Herpes, Hepatitis, cancer and neurodegenerative disorders. It has been postulated that HIV and other retroviruses exploit the exosome biogenesis pathway for the budding of their viral particles[140]. This hypothesis is based on the similarities in (i) lipids and proteins compositions of exosomes and retroviruses; (ii) protein

targeting and vesicle biogenesis; and (iii) the release of exosomes and viral particles from the cell. Fang et al. demonstrated that proteins bud into both exosomes and virus particles when targeted to discrete domains on the plasma membrane. They also showed that HIV Gag proteins possess exosomal sorting information, and that higher-order oligomerization is the principal factor for their budding into exosomes and viral particles[13].

Neurodegenerative disorders are characterized by the progressive loss of neurons and are linked with the accumulation of misfolded proteins and infectious isoforms. The aggregation of these proteins can target them to site of budding where they are secreted into exosomes. In prion diseases, both normal (PrP^{C}) and infectious isoforms (PrP^{Sc})of prion protein have been found in exosomes isolated from neuronal cells and blood[74,141]. Fevrier et al.[138] showed PrP^{Sc} can catalyze the infection of normal PrP^{C} when they incubated Rov cells with isolated exosomes from prion infected Rov cells. They observed the presence of PrP^{Sc} in normal cells after a number of passages which indicated the transfer of infectivity. They further confirmed this, by inoculating transgenic mice that were highly susceptible to prions, with PrP^{Sc} containing exosomes, and observed that all the inoculated mice died as a result of acute neurological disorder. Other proteins and nuclei acids related to neurodegenerative disorders such α-synucleins[142], tau[143], β-amyloids[144], and SOD1[145] have been found in exosomes and have demonstrated a prion-like infection. These findings suggest a role for exosomes in the transmission of diseases within a host cell and among organisms, even though the mechanisms are not fully understood.

Objectives

Exosomes have been shown to be of enormous biological importance in a number of physiological and pathological processes. However, the mechanisms by which exosomes are

made, and how cargoes are targeted to exosomes are not fully understood. The current dogma of exosome biogenesis is that cargoes are targeted to the limiting membrane of endosomes where they bud to form a vesicle laden endosome referred to as MVB, which then moves to fuse with the plasma membrane to release the vesicles, but this has not been rigorously tested. The objective of my thesis is to enhance our mechanistic understanding of exosome biogenesis by (i) identifying *cis*-acting signals on cargoes that target them to exosomes, and (ii) characterizing *trans*-acting factors that are required for budding of exosomes.

Specifically, in chapter 1, I investigated the endosomal trafficking of the current dogma of exosome biogenesis in HEK293 cells using the classical exosomal markers. I found that most of these markers (CD81 and CD9) are abundant on the plasma membrane and bud significantly better than CD63 which is localized in the endosomes. I observed that redirecting CD9 which is primarily localized on the plasma membrane to the endosomes resulted in a decrease in budding while CD63 budded significantly better when mislocalized to the plasma membrane. Using single-particle interferometry reflectance imaging and immunofluorescence microscopy, I showed that exosome composition can be determined by intracellular protein trafficking pathways, as misdirecting an exosomal cargo from the endosome to the plasma membrane results in an increase its its exosomal co-localization with plasma membrane-localized exosome cargoes. I also showed that the converse is true, that misdirecting a plasma membrane-enriched exosome cargo to endosomes results in a decrease in its exosomal co-localization with plasma membrane-localized exosome cargoes, and an increase in its exosomal co-localization with endosome-enriched exosome cargoes. I conclude that exosomes can bud from both the plasma and endosome membranes in HEK293 and NIH3T3 cells, bud even better from the plasma than endosome membranes in these two cell lines, and that

exosome engineering is best accomplished by targeting potentially new cargoes to the plasma rather than endosome membrane.

Chapter 2, I identified and characterized proteins that have been implicated in the budding of exosomes. I knocked out tetraspanins and other putative exosome factors using CRISPR/Cas9 technology in HEK293 and 293T cells and assessed the effects on relative budding of classical markers, synthetic cargoes and vesicle concentration. I observed that loss of CD63, CD81, CD9, Alix or Syntenin does not cause any significant defect in the budding of classical exosomal markers and exogenous cargoes. I also did not observe any significant effect in the budding of vesicles in HEK293 cells lacking CD63, CD81 or CD9. I however noticed significant clonal variations in the budding of markers as some clones of these mutants had enhanced budding even though none showed any defect. To explore this clonal variability, I single cell cloned wildtype HEK293 cells and found this same phenotype among the selected clones. I went on to single cell clone other cell lines and observed a similar phenotype where the relative budding of classical exosomal markers varied significantly from one clone to another in the same cell line. This indicates that the relative rate of exosome production can vary significantly among cells in the absence of mutagenesis and this can be inadvertently exposed during isolation of single cell clones.

In Chapter 3, I report my observations in the exosomal protein compositions of HEK293 and HEK293T, and suggest a mechanism for the significant differences in the budding of classical exosomal markers.

References

1 Wolf, P. The nature and significance of platelet products in human plasma. *Br J Haematol* **13**, 269-288 (1967).

2 Bonucci, E. Fine structure of early cartilage calcification. *J Ultrastruct Res* **20**, 33-50 (1967).

3 Anderson, H. C. Vesicles associated with calcification in the matrix of epiphyseal cartilage. *J Cell Biol* **41**, 59-72 (1969).

4 Trams, E. G., Lauter, C. J., Salem, N., Jr. & Heine, U. Exfoliation of membrane ecto-enzymes in the form of micro-vesicles. *Biochim Biophys Acta* **645**, 63-70 (1981).

5 Johnstone, R. M., Adam, M., Hammond, J. R., Orr, L. & Turbide, C. Vesicle formation during reticulocyte maturation. Association of plasma membrane activities with released vesicles (exosomes). *J Biol Chem* **262**, 9412-9420 (1987).

6 Harding, C., Heuser, J. & Stahl, P. Endocytosis and intracellular processing of transferrin and colloidal gold-transferrin in rat reticulocytes: demonstration of a pathway for receptor shedding. *Eur J Cell Biol* **35**, 256-263 (1984).

7 Pan, B. T., Teng, K., Wu, C., Adam, M. & Johnstone, R. M. Electron microscopic evidence for externalization of the transferrin receptor in vesicular form in sheep reticulocytes. *J Cell Biol* **101**, 942-948 (1985).

8 Minciacchi, V. R., Freeman, M. R. & Di Vizio, D. Extracellular vesicles in cancer: exosomes, microvesicles and the emerging role of large oncosomes. *Semin Cell Dev Biol* **40**, 41-51, doi:10.1016/j.semcdb.2015.02.010 (2015).

9 Di Vizio, D. *et al.* Large oncosomes in human prostate cancer tissues and in the circulation of mice with metastatic disease. *Am J Pathol* **181**, 1573-1584, doi:10.1016/j.ajpath.2012.07.030 (2012).

10 Zabeo, D. *et al.* Exosomes purified from a single cell type have diverse morphology. *J Extracell Vesicles* **6**, 1329476, doi:10.1080/20013078.2017.1329476 (2017).

11 Raposo, G. *et al.* B lymphocytes secrete antigen-presenting vesicles. *J Exp Med* **183**, 1161-1172 (1996).

12 Bobrie, A., Colombo, M., Krumeich, S., Raposo, G. & Thery, C. Diverse subpopulations of vesicles secreted by different intracellular mechanisms are present in exosome preparations obtained by differential ultracentrifugation. *J Extracell Vesicles* **1**, doi:10.3402/jev.v1i0.18397 (2012).

13 Fang, Y. *et al.* Higher-order oligomerization targets plasma membrane proteins and HIV gag to exosomes. *PLoS Biol* **5**, e158, doi:10.1371/journal.pbio.0050158 (2007).

14 Shah, R., Patel, T. & Freedman, J. E. Circulating Extracellular Vesicles in Human Disease. *N Engl J Med* **379**, 2180-2181, doi:10.1056/NEJMc1813170 (2018).

15 Li, L. *et al.* Extracellular vesicles carry microRNA-195 to intrahepatic cholangiocarcinoma and improve survival in a rat model. *Hepatology* **65**, 501-514, doi:10.1002/hep.28735 (2017).

16 Kim, D. K. *et al.* EVpedia: an integrated database of high-throughput data for systemic analyses of extracellular vesicles. *J Extracell Vesicles* **2**, doi:10.3402/jev.v2i0.20384 (2013).

17 Keerthikumar, S. *et al.* ExoCarta: A Web-Based Compendium of Exosomal Cargo. *J Mol Biol* **428**, 688-692, doi:10.1016/j.jmb.2015.09.019 (2016).

18 Kalra, H. *et al.* Vesiclepedia: a compendium for extracellular vesicles with continuous community annotation. *PLoS Biol* **10**, e1001450, doi:10.1371/journal.pbio.1001450 (2012).

19 Skotland, T., Sandvig, K. & Llorente, A. Lipids in exosomes: Current knowledge and the way forward. *Prog Lipid Res* **66**, 30-41, doi:10.1016/j.plipres.2017.03.001 (2017).

20 Llorente, A. *et al.* Molecular lipidomics of exosomes released by PC-3 prostate cancer cells. *Biochim Biophys Acta* **1831**, 1302-1309 (2013).

21 Brouwers, J. F. *et al.* Distinct lipid compositions of two types of human prostasomes. *Proteomics* **13**, 1660-1666, doi:10.1002/pmic.201200348 (2013).

22 Laulagnier, K. *et al.* Mast cell- and dendritic cell-derived exosomes display a specific lipid composition and an unusual membrane organization. *Biochem J* **380**, 161-171, doi:10.1042/BJ20031594 (2004).

23 Booth, A. M. *et al.* Exosomes and HIV Gag bud from endosome-like domains of the T cell plasma membrane. *J Cell Biol* **172**, 923-935, doi:10.1083/jcb.200508014 (2006).

24 Dillon, S. R., Mancini, M., Rosen, A. & Schlissel, M. S. Annexin V binds to viable B cells and colocalizes with a marker of lipid rafts upon B cell receptor activation. *J Immunol* **164**, 1322-1332 (2000).

25 Matsuo, H. *et al.* Role of LBPA and Alix in multivesicular liposome formation and endosome organization. *Science* **303**, 531-534, doi:10.1126/science.1092425 (2004).

26 Trajkovic, K. *et al.* Ceramide triggers budding of exosome vesicles into multivesicular endosomes. *Science* **319**, 1244-1247, doi:10.1126/science.1153124 (2008).

27 Kosaka, N. *et al.* Secretory mechanisms and intercellular transfer of microRNAs in living cells. *J Biol Chem* **285**, 17442-17452, doi:10.1074/jbc.M110.107821 (2010).

28 Mittelbrunn, M. *et al.* Unidirectional transfer of microRNA-loaded exosomes from T cells to antigen-presenting cells. *Nat Commun* **2**, 282, doi:10.1038/ncomms1285 (2011).

29 Strauss, K. *et al.* Exosome secretion ameliorates lysosomal storage of cholesterol in Niemann-Pick type C disease. *J Biol Chem* **285**, 26279-26288, doi:10.1074/jbc.M110.134775 (2010).

30 Batista, B. S., Eng, W. S., Pilobello, K. T., Hendricks-Munoz, K. D. & Mahal, L. K. Identification of a conserved glycan signature for microvesicles. *J Proteome Res* **10**, 4624-4633, doi:10.1021/pr200434y (2011).

31 Shimoda, A., Tahara, Y., Sawada, S. I., Sasaki, Y. & Akiyoshi, K. Glycan profiling analysis using evanescent-field fluorescence-assisted lectin array: Importance of sugar recognition for cellular uptake of exosomes from mesenchymal stem cells. *Biochem Biophys Res Commun* **491**, 701-707, doi:10.1016/j.bbrc.2017.07.126 (2017).

32 Rilla, K. *et al.* Hyaluronan production enhances shedding of plasma membrane-derived microvesicles. *Exp Cell Res* **319**, 2006-2018, doi:10.1016/j.yexcr.2013.05.021 (2013).

33 Thompson, C. A., Purushothaman, A., Ramani, V. C., Vlodavsky, I. & Sanderson, R. D. Heparanase regulates secretion, composition, and function of tumor cell-derived exosomes. *J Biol Chem* **288**, 10093-10099, doi:10.1074/jbc.C112.444562 (2013).

34 Escrevente, C., Keller, S., Altevogt, P. & Costa, J. Interaction and uptake of exosomes by ovarian cancer cells. *BMC Cancer* **11**, 108, doi:10.1186/1471-2407-11-108 (2011).

35 Wei, Z. *et al.* Coding and noncoding landscape of extracellular RNA released by human glioma stem cells. *Nat Commun* **8**, 1145, doi:10.1038/s41467-017-01196-x (2017).

36 Shurtleff, M. J. *et al.* Broad role for YBX1 in defining the small noncoding RNA composition of exosomes. *Proc Natl Acad Sci U S A* **114**, E8987-E8995, doi:10.1073/pnas.1712108114 (2017).

37 Koppers-Lalic, D. *et al.* Nontemplated nucleotide additions distinguish the small RNA composition in cells from exosomes. *Cell Rep* **8**, 1649-1658, doi:10.1016/j.celrep.2014.08.027 (2014).

38 Baglio, S. R. *et al.* Sensing of latent EBV infection through exosomal transfer of 5'pppRNA. *Proc Natl Acad Sci U S A* **113**, E587-596, doi:10.1073/pnas.1518130113 (2016).

39 Balaj, L. *et al.* Tumour microvesicles contain retrotransposon elements and amplified oncogene sequences. *Nat Commun* **2**, 180, doi:10.1038/ncomms1180 (2011).

40 Kahlert, C. *et al.* Identification of double-stranded genomic DNA spanning all chromosomes with mutated KRAS and p53 DNA in the serum exosomes of patients with pancreatic cancer. *J Biol Chem* **289**, 3869-3875, doi:10.1074/jbc.C113.532267 (2014).

41 Thakur, B. K. *et al.* Double-stranded DNA in exosomes: a novel biomarker in cancer detection. *Cell Res* **24**, 766-769, doi:10.1038/cr.2014.44 (2014).

42 Sansone, P. *et al.* Packaging and transfer of mitochondrial DNA via exosomes regulate escape from dormancy in hormonal therapy-resistant breast cancer. *Proc Natl Acad Sci U S A* **114**, E9066-E9075, doi:10.1073/pnas.1704862114 (2017).

43 Tannous, B. A., Kim, D. E., Fernandez, J. L., Weissleder, R. & Breakefield, X. O. Codon-optimized Gaussia luciferase cDNA for mammalian gene expression in culture and in vivo. *Mol Ther* **11**, 435-443, doi:10.1016/j.ymthe.2004.10.016 (2005).

44 Ashley, J. *et al.* Retrovirus-like Gag Protein Arc1 Binds RNA and Traffics across Synaptic Boutons. *Cell* **172**, 262-274 e211, doi:10.1016/j.cell.2017.12.022 (2018).

45 Pastuzyn, E. D. *et al.* The Neuronal Gene Arc Encodes a Repurposed Retrotransposon Gag Protein that Mediates Intercellular RNA Transfer. *Cell* **173**, 275, doi:10.1016/j.cell.2018.03.024 (2018).

46 Melo, S. A. *et al.* Cancer exosomes perform cell-independent microRNA biogenesis and promote tumorigenesis. *Cancer Cell* **26**, 707-721, doi:10.1016/j.ccell.2014.09.005 (2014).

47 McKenzie, A. J. *et al.* KRAS-MEK Signaling Controls Ago2 Sorting into Exosomes. *Cell Rep* **15**, 978-987, doi:10.1016/j.celrep.2016.03.085 (2016).

48 Shurtleff, M. J., Temoche-Diaz, M. M., Karfilis, K. V., Ri, S. & Schekman, R. Y-box protein 1 is required to sort microRNAs into exosomes in cells and in a cell-free reaction. *Elife* **5**, doi:10.7554/eLife.19276 (2016).

49 Santangelo, L. *et al.* The RNA-Binding Protein SYNCRIP Is a Component of the Hepatocyte Exosomal Machinery Controlling MicroRNA Sorting. *Cell Rep* **17**, 799-808, doi:10.1016/j.celrep.2016.09.031 (2016).

50 Teng, Y. *et al.* MVP-mediated exosomal sorting of miR-193a promotes colon cancer progression. *Nat Commun* **8**, 14448, doi:10.1038/ncomms14448 (2017).

51 Mukherjee, K. *et al.* Reversible HuR-microRNA binding controls extracellular export of miR-122 and augments stress response. *EMBO Rep* **17**, 1184-1203, doi:10.15252/embr.201541930 (2016).

52 Villarroya-Beltri, C. *et al.* ISGylation controls exosome secretion by promoting lysosomal degradation of MVB proteins. *Nat Commun* **7**, 13588, doi:10.1038/ncomms13588 (2016).

53 Escola, J. M. *et al.* Selective enrichment of tetraspan proteins on the internal vesicles of multivesicular endosomes and on exosomes secreted by human B-lymphocytes. *J Biol Chem* **273**, 20121-20127 (1998).

54 Hemler, M. E. Tetraspanin proteins mediate cellular penetration, invasion, and fusion events and define a novel type of membrane microdomain. *Annu Rev Cell Dev Biol* **19**, 397-422, doi:10.1146/annurev.cellbio.19.111301.153609 (2003).

55 Stipp, C. S., Kolesnikova, T. V. & Hemler, M. E. Functional domains in tetraspanin proteins. *Trends Biochem Sci* **28**, 106-112, doi:10.1016/S0968-0004(02)00014-2 (2003).

56 Rieu, S., Geminard, C., Rabesandratana, H., Sainte-Marie, J. & Vidal, M. Exosomes released during reticulocyte maturation bind to fibronectin via integrin alpha4beta1. *Eur J Biochem* **267**, 583-590 (2000).

57 Segura, E. *et al.* ICAM-1 on exosomes from mature dendritic cells is critical for efficient naive T-cell priming. *Blood* **106**, 216-223, doi:10.1182/blood-2005-01-0220 (2005).

58 Baietti, M. F. *et al.* Syndecan-syntenin-ALIX regulates the biogenesis of exosomes. *Nat Cell Biol* **14**, 677-685, doi:10.1038/ncb2502 (2012).

59 Al-Nedawi, K. *et al.* Intercellular transfer of the oncogenic receptor EGFRvIII by microvesicles derived from tumour cells. *Nat Cell Biol* **10**, 619-624, doi:10.1038/ncb1725 (2008).

60 Blanchard, N. *et al.* TCR activation of human T cells induces the production of exosomes bearing the TCR/CD3/zeta complex. *J Immunol* **168**, 3235-3241 (2002).

61 Gonzalez-King, H. *et al.* Hypoxia Inducible Factor-1alpha Potentiates Jagged 1-Mediated Angiogenesis by Mesenchymal Stem Cell-Derived Exosomes. *Stem Cells* **35**, 1747-1759, doi:10.1002/stem.2618 (2017).

62 Sheldon, H. *et al.* New mechanism for Notch signaling to endothelium at a distance by Delta-like 4 incorporation into exosomes. *Blood* **116**, 2385-2394, doi:10.1182/blood-2009-08-239228 (2010).

63 Li, M. *et al.* Horizontal transfer of exosomal CXCR4 promotes murine hepatocarcinoma cell migration, invasion and lymphangiogenesis. *Gene* **676**, 101-109, doi:10.1016/j.gene.2018.07.018 (2018).

64 Nager, A. R. *et al.* An Actin Network Dispatches Ciliary GPCRs into Extracellular Vesicles to Modulate Signaling. *Cell* **168**, 252-263 e214, doi:10.1016/j.cell.2016.11.036 (2017).

65 Jarad, M., Kuczynski, E. A., Morrison, J., Viloria-Petit, A. M. & Coomber, B. L. Release of endothelial cell associated VEGFR2 during TGF-beta modulated angiogenesis in vitro. *BMC Cell Biol* **18**, 10, doi:10.1186/s12860-017-0127-y (2017).

66 Sampey, G. C. *et al.* Exosomes from HIV-1-infected Cells Stimulate Production of Pro-inflammatory Cytokines through Trans-activating Response (TAR) RNA. *J Biol Chem* **291**, 1251-1266, doi:10.1074/jbc.M115.662171 (2016).

67 Munich, S., Sobo-Vujanovic, A., Buchser, W. J., Beer-Stolz, D. & Vujanovic, N. L. Dendritic cell exosomes directly kill tumor cells and activate natural killer cells via TNF superfamily ligands. *Oncoimmunology* **1**, 1074-1083, doi:10.4161/onci.20897 (2012).

68 Kim, S. H., Bianco, N. R., Shufesky, W. J., Morelli, A. E. & Robbins, P. D. MHC class II+ exosomes in plasma suppress inflammation in an antigen-specific and Fas ligand/Fas-dependent manner. *J Immunol* **179**, 2235-2241 (2007).

69 Borges, F. T. *et al.* TGF-beta1-containing exosomes from injured epithelial cells activate fibroblasts to initiate tissue regenerative responses and fibrosis. *J Am Soc Nephrol* **24**, 385-392, doi:10.1681/ASN.2012101031 (2013).

70 Clayton, A., Al-Taei, S., Webber, J., Mason, M. D. & Tabi, Z. Cancer exosomes express CD39 and CD73, which suppress T cells through adenosine production. *J Immunol* **187**, 676-683, doi:10.4049/jimmunol.1003884 (2011).

71 Rabesandratana, H., Toutant, J. P., Reggio, H. & Vidal, M. Decay-accelerating factor (CD55) and membrane inhibitor of reactive lysis (CD59) are released within exosomes during In vitro maturation of reticulocytes. *Blood* **91**, 2573-2580 (1998).

72 Melo, S. A. *et al.* Glypican-1 identifies cancer exosomes and detects early pancreatic cancer. *Nature* **523**, 177-182, doi:10.1038/nature14581 (2015).

73 Bianchi, E., Doe, B., Goulding, D. & Wright, G. J. Juno is the egg Izumo receptor and is essential for mammalian fertilization. *Nature* **508**, 483-487, doi:10.1038/nature13203 (2014).

74 Robertson, C. *et al.* Cellular prion protein is released on exosomes from activated platelets. *Blood* **107**, 3907-3911, doi:10.1182/blood-2005-02-0802 (2006).

75 Vyas, N. *et al.* Vertebrate Hedgehog is secreted on two types of extracellular vesicles with different signaling properties. *Sci Rep* **4**, 7357, doi:10.1038/srep07357 (2014).

76 Hsu, C. *et al.* Regulation of exosome secretion by Rab35 and its GTPase-activating proteins TBC1D10A-C. *J Cell Biol* **189**, 223-232, doi:10.1083/jcb.200911018 (2010).

77 Ostrowski, M. *et al.* Rab27a and Rab27b control different steps of the exosome secretion pathway. *Nat Cell Biol* **12**, 19-30; sup pp 11-13, doi:10.1038/ncb2000 (2010).

78 Chow, A. *et al.* Macrophage immunomodulation by breast cancer-derived exosomes requires Toll-like receptor 2-mediated activation of NF-kappaB. *Sci Rep* **4**, 5750, doi:10.1038/srep05750 (2014).

79 Imjeti, N. S. *et al.* Syntenin mediates SRC function in exosomal cell-to-cell communication. *Proc Natl Acad Sci U S A* **114**, 12495-12500, doi:10.1073/pnas.1713433114 (2017).

80 Di Noto, G. *et al.* C-src enriched serum microvesicles are generated in malignant plasma cell dyscrasia. *PLoS One* **8**, e70811, doi:10.1371/journal.pone.0070811 (2013).

81 Tsukita, S. & Yonemura, S. ERM (ezrin/radixin/moesin) family: from cytoskeleton to signal transduction. *Curr Opin Cell Biol* **9**, 70-75 (1997).

82 Wubbolts, R. *et al.* Proteomic and biochemical analyses of human B cell-derived exosomes. Potential implications for their function and multivesicular body formation. *J Biol Chem* **278**, 10963-10972, doi:10.1074/jbc.M207550200 (2003).

83 Friand, V., David, G. & Zimmermann, P. Syntenin and syndecan in the biogenesis of exosomes. *Biol Cell* **107**, 331-341, doi:10.1111/boc.201500010 (2015).

84 Hurley, J. H. & Odorizzi, G. Get on the exosome bus with ALIX. *Nat Cell Biol* **14**, 654-655, doi:10.1038/ncb2530 (2012).

85 Henne, W. M., Buchkovich, N. J. & Emr, S. D. The ESCRT pathway. *Dev Cell* **21**, 77-91, doi:10.1016/j.devcel.2011.05.015 (2011).

86 Schmidt, O. & Teis, D. The ESCRT machinery. *Curr Biol* **22**, R116-120, doi:10.1016/j.cub.2012.01.028 (2012).

87 Thery, C. *et al.* Proteomic analysis of dendritic cell-derived exosomes: a secreted subcellular compartment distinct from apoptotic vesicles. *J Immunol* **166**, 7309-7318 (2001).

88 Colombo, M. *et al.* Analysis of ESCRT functions in exosome biogenesis, composition and secretion highlights the heterogeneity of extracellular vesicles. *J Cell Sci* **126**, 5553-5565, doi:10.1242/jcs.128868 (2013).

89 Tamai, K. *et al.* Exosome secretion of dendritic cells is regulated by Hrs, an ESCRT-0 protein. *Biochem Biophys Res Commun* **399**, 384-390, doi:10.1016/j.bbrc.2010.07.083 (2010).

90 Li, J. *et al.* Identification and Characterization of 293T Cell-Derived Exosomes by Profiling the Protein, mRNA and MicroRNA Components. *PLoS One* **11**, e0163043, doi:10.1371/journal.pone.0163043 (2016).

91 Mathew, A., Bell, A. & Johnstone, R. M. Hsp-70 is closely associated with the transferrin receptor in exosomes from maturing reticulocytes. *Biochem J* **308 (Pt 3)**, 823-830 (1995).

92 Reddy, V. S., Madala, S. K., Trinath, J. & Reddy, G. B. Extracellular small heat shock proteins: exosomal biogenesis and function. *Cell Stress Chaperones* **23**, 441-454, doi:10.1007/s12192-017-0856-z (2018).

93 Takeuchi, T. *et al.* Intercellular chaperone transmission via exosomes contributes to maintenance of protein homeostasis at the organismal level. *Proc Natl Acad Sci U S A* **112**, E2497-2506, doi:10.1073/pnas.1412651112 (2015).

94 Sinha, S. *et al.* Cortactin promotes exosome secretion by controlling branched actin dynamics. *J Cell Biol* **214**, 197-213, doi:10.1083/jcb.201601025 (2016).

95 Cossetti, C. *et al.* Extracellular vesicles from neural stem cells transfer IFN-gamma via Ifngr1 to activate Stat1 signaling in target cells. *Mol Cell* **56**, 193-204, doi:10.1016/j.molcel.2014.08.020 (2014).

96 Graner, M. W. *et al.* Proteomic and immunologic analyses of brain tumor exosomes. *FASEB J* **23**, 1541-1557, doi:10.1096/fj.08-122184 (2009).

97 Bakhshian Nik, A., Hutcheson, J. D. & Aikawa, E. Extracellular Vesicles As Mediators of Cardiovascular Calcification. *Front Cardiovasc Med* **4**, 78, doi:10.3389/fcvm.2017.00078 (2017).

98 Nolte-'t Hoen, E., Cremer, T., Gallo, R. C. & Margolis, L. B. Extracellular vesicles and viruses: Are they close relatives? *Proc Natl Acad Sci U S A* **113**, 9155-9161, doi:10.1073/pnas.1605146113 (2016).

99 Ronquist, K. G., Ek, B., Stavreus-Evers, A., Larsson, A. & Ronquist, G. Human prostasomes express glycolytic enzymes with capacity for ATP production. *Am J Physiol Endocrinol Metab* **304**, E576-582, doi:10.1152/ajpendo.00511.2012 (2013).

100 Hartl, F. U., Bracher, A. & Hayer-Hartl, M. Molecular chaperones in protein folding and proteostasis. *Nature* **475**, 324-332, doi:10.1038/nature10317 (2011).

101 Harding, C., Heuser, J. & Stahl, P. Receptor-mediated endocytosis of transferrin and recycling of the transferrin receptor in rat reticulocytes. *J Cell Biol* **97**, 329-339 (1983).

102 Colombo, M., Raposo, G. & Thery, C. Biogenesis, secretion, and intercellular interactions of exosomes and other extracellular vesicles. *Annu Rev Cell Dev Biol* **30**, 255-289, doi:10.1146/annurev-cellbio-101512-122326 (2014).

103 Hyenne, V. *et al.* RAL-1 controls multivesicular body biogenesis and exosome secretion. *J Cell Biol* **211**, 27-37, doi:10.1083/jcb.201504136 (2015).

104 Sung, B. H., Ketova, T., Hoshino, D., Zijlstra, A. & Weaver, A. M. Directional cell movement through tissues is controlled by exosome secretion. *Nat Commun* **6**, 7164, doi:10.1038/ncomms8164 (2015).

105 Verweij, F. J. *et al.* Quantifying exosome secretion from single cells reveals a modulatory role for GPCR signaling. *J Cell Biol* **217**, 1129-1142, doi:10.1083/jcb.201703206 (2018).

106 Casado, S., Lobo, M. & Paino, C. L. Dynamics of plasma membrane surface related to the release of extracellular vesicles by mesenchymal stem cells in culture. *Sci Rep* **7**, 6767, doi:10.1038/s41598-017-07265-x (2017).

107 Bruno, S. *et al.* Microvesicles derived from mesenchymal stem cells enhance survival in a lethal model of acute kidney injury. *PLoS One* **7**, e33115, doi:10.1371/journal.pone.0033115 (2012).

108 Cantaluppi, V. *et al.* Microvesicles derived from endothelial progenitor cells protect the kidney from ischemia-reperfusion injury by microRNA-dependent reprogramming of resident renal cells. *Kidney Int* **82**, 412-427, doi:10.1038/ki.2012.105 (2012).

109 Anderson, H. C., Garimella, R. & Tague, S. E. The role of matrix vesicles in growth plate development and biomineralization. *Front Biosci* **10**, 822-837 (2005).

110 Gerber, P. P. *et al.* Rab27a controls HIV-1 assembly by regulating plasma membrane levels of phosphatidylinositol 4,5-bisphosphate. *J Cell Biol* **209**, 435-452, doi:10.1083/jcb.201409082 (2015).

111 Shen, B., Fang, Y., Wu, N. & Gould, S. J. Biogenesis of the posterior pole is mediated by the exosome/microvesicle protein-sorting pathway. *J Biol Chem* **286**, 44162-44176, doi:10.1074/jbc.M111.274803 (2011).

112 Shen, B., Wu, N., Yang, J. M. & Gould, S. J. Protein targeting to exosomes/microvesicles by plasma membrane anchors. *J Biol Chem* **286**, 14383-14395, doi:10.1074/jbc.M110.208660 (2011).

113 Shao, H. *et al.* Protein typing of circulating microvesicles allows real-time monitoring of glioblastoma therapy. *Nat Med* **18**, 1835-1840, doi:10.1038/nm.2994 (2012).

114 Nabhan, J. F., Hu, R., Oh, R. S., Cohen, S. N. & Lu, Q. Formation and release of arrestin domain-containing protein 1-mediated microvesicles (ARMMs) at plasma membrane by recruitment of TSG101 protein. *Proc Natl Acad Sci U S A* **109**, 4146-4151, doi:10.1073/pnas.1200448109 (2012).

115 Wehman, A. M., Poggioli, C., Schweinsberg, P., Grant, B. D. & Nance, J. The P4-ATPase TAT-5 inhibits the budding of extracellular vesicles in C. elegans embryos. *Curr Biol* **21**, 1951-1959, doi:10.1016/j.cub.2011.10.040 (2011).

116 Laulagnier, K. *et al.* PLD2 is enriched on exosomes and its activity is correlated to the release of exosomes. *FEBS Lett* **572**, 11-14, doi:10.1016/j.febslet.2004.06.082 (2004).

117 Ghossoub, R. *et al.* Syntenin-ALIX exosome biogenesis and budding into multivesicular bodies are controlled by ARF6 and PLD2. *Nat Commun* **5**, 3477, doi:10.1038/ncomms4477 (2014).

118 Egea-Jimenez, A. L. & Zimmermann, P. Phospholipase D and phosphatidic acid in the biogenesis and cargo loading of extracellular vesicles. *J Lipid Res* **59**, 1554-1560, doi:10.1194/jlr.R083964 (2018).

119 Shamseddine, A. A., Airola, M. V. & Hannun, Y. A. Roles and regulation of neutral sphingomyelinase-2 in cellular and pathological processes. *Adv Biol Regul* **57**, 24-41, doi:10.1016/j.jbior.2014.10.002 (2015).

120 Katzmann, D. J., Babst, M. & Emr, S. D. Ubiquitin-dependent sorting into the multivesicular body pathway requires the function of a conserved endosomal protein sorting complex, ESCRT-I. *Cell* **106**, 145-155 (2001).

121 Christ, L., Raiborg, C., Wenzel, E. M., Campsteijn, C. & Stenmark, H. Cellular Functions and Molecular Mechanisms of the ESCRT Membrane-Scission Machinery. *Trends Biochem Sci* **42**, 42-56, doi:10.1016/j.tibs.2016.08.016 (2017).

122 Henne, W. M., Stenmark, H. & Emr, S. D. Molecular mechanisms of the membrane sculpting ESCRT pathway. *Cold Spring Harb Perspect Biol* **5**, doi:10.1101/cshperspect.a016766 (2013).

123 Gross, J. C., Chaudhary, V., Bartscherer, K. & Boutros, M. Active Wnt proteins are secreted on exosomes. *Nat Cell Biol* **14**, 1036-1045, doi:10.1038/ncb2574 (2012).

124 Hoshino, D. *et al.* Exosome secretion is enhanced by invadopodia and drives invasive behavior. *Cell Rep* **5**, 1159-1168, doi:10.1016/j.celrep.2013.10.050 (2013).

125 Abrami, L. *et al.* Hijacking multivesicular bodies enables long-term and exosome-mediated long-distance action of anthrax toxin. *Cell Rep* **5**, 986-996, doi:10.1016/j.celrep.2013.10.019 (2013).

126 Stenmark, H. Rab GTPases as coordinators of vesicle traffic. *Nat Rev Mol Cell Biol* **10**, 513-525, doi:10.1038/nrm2728 (2009).

127 Savina, A., Vidal, M. & Colombo, M. I. The exosome pathway in K562 cells is regulated by Rab11. *J Cell Sci* **115**, 2505-2515 (2002).

128 Koles, K. *et al.* Mechanism of evenness interrupted (Evi)-exosome release at synaptic boutons. *J Biol Chem* **287**, 16820-16834, doi:10.1074/jbc.M112.342667 (2012).

129 Fruhbeis, C. *et al.* Neurotransmitter-triggered transfer of exosomes mediates oligodendrocyte-neuron communication. *PLoS Biol* **11**, e1001604, doi:10.1371/journal.pbio.1001604 (2013).

130 Peinado, H. *et al.* Melanoma exosomes educate bone marrow progenitor cells toward a pro-metastatic phenotype through MET. *Nat Med* **18**, 883-891, doi:10.1038/nm.2753 (2012).

131 Bobrie, A. *et al.* Rab27a supports exosome-dependent and -independent mechanisms that modify the tumor microenvironment and can promote tumor progression. *Cancer Res* **72**, 4920-4930, doi:10.1158/0008-5472.CAN-12-0925 (2012).

132 Webber, J. P. *et al.* Differentiation of tumour-promoting stromal myofibroblasts by cancer exosomes. *Oncogene* **34**, 290-302, doi:10.1038/onc.2013.560 (2015).

133 Romancino, D. P. *et al.* Identification and characterization of the nano-sized vesicles released by muscle cells. *FEBS Lett* **587**, 1379-1384, doi:10.1016/j.febslet.2013.03.012 (2013).

134 Muralidharan-Chari, V. *et al.* ARF6-regulated shedding of tumor cell-derived plasma membrane microvesicles. *Curr Biol* **19**, 1875-1885, doi:10.1016/j.cub.2009.09.059 (2009).

135 Takahashi, A. *et al.* Exosomes maintain cellular homeostasis by excreting harmful DNA from cells. *Nat Commun* **8**, 15287, doi:10.1038/ncomms15287 (2017).

136 Arienti, G., Carlini, E., Verdacchi, R., Cosmi, E. V. & Palmerini, C. A. Prostasome to sperm transfer of CD13/aminopeptidase N (EC 3.4.11.2). *Biochim Biophys Acta* **1336**, 533-538 (1997).

137 Quek, C. & Hill, A. F. The role of extracellular vesicles in neurodegenerative diseases. *Biochem Biophys Res Commun* **483**, 1178-1186, doi:10.1016/j.bbrc.2016.09.090 (2017).

138 Fevrier, B. *et al.* Cells release prions in association with exosomes. *Proc Natl Acad Sci U S A* **101**, 9683-9688, doi:10.1073/pnas.0308413101 (2004).

139 Choudhuri, K. *et al.* Polarized release of T-cell-receptor-enriched microvesicles at the immunological synapse. *Nature* **507**, 118-123, doi:10.1038/nature12951 (2014).

140 Gould, S. J., Booth, A. M. & Hildreth, J. E. The Trojan exosome hypothesis. *Proc Natl Acad Sci U S A* **100**, 10592-10597, doi:10.1073/pnas.1831413100 (2003).

141 Vella, L. J., Greenwood, D. L., Cappai, R., Scheerlinck, J. P. & Hill, A. F. Enrichment of prion protein in exosomes derived from ovine cerebral spinal fluid. *Vet Immunol Immunopathol* **124**, 385-393, doi:10.1016/j.vetimm.2008.04.002 (2008).

142 Emmanouilidou, E. *et al.* Cell-produced alpha-synuclein is secreted in a calcium-dependent manner by exosomes and impacts neuronal survival. *J Neurosci* **30**, 6838-6851, doi:10.1523/JNEUROSCI.5699-09.2010 (2010).

143 Yamada, K. *et al.* In vivo microdialysis reveals age-dependent decrease of brain interstitial fluid tau levels in P301S human tau transgenic mice. *J Neurosci* **31**, 13110-13117, doi:10.1523/JNEUROSCI.2569-11.2011 (2011).

144 Sharples, R. A. *et al.* Inhibition of gamma-secretase causes increased secretion of amyloid precursor protein C-terminal fragments in association with exosomes. *FASEB J* **22**, 1469-1478, doi:10.1096/fj.07-9357com (2008).

145 Gomes, C., Keller, S., Altevogt, P. & Costa, J. Evidence for secretion of Cu,Zn superoxide dismutase via exosomes from a cell model of amyotrophic lateral sclerosis. *Neurosci Lett* **428**, 43-46, doi:10.1016/j.neulet.2007.09.024 (2007).

Chapter 2: A shared pathway of exosome biogenesis operates at plasma and endosome membranes

This chapter is currently published on biorxiv as a preprint. doi: https://doi.org/10.1101/545228

A shared pathway of exosome biogenesis operates at plasma and endosome membranes

Francis K. Fordjour[1], George G. Daaboul[2], and Stephen J. Gould[1*]

[1]Department of Biological Chemistry

Johns Hopkins University

Baltimore, MD

USA

[2]Nanoview Biosciences

Boston, MA

USA

Corresponding author:

Stephen J. Gould, Ph.D.

Department of Biological Chemistry

Johns Hopkins University

Baltimore, MD USA

Email: sgould@jhmi.edu

Tel (01) 443 847 9918

Summary:

This study of exosome cargo protein budding reveals that cells use a common pathway for budding exosomes from plasma and endosome membranes, providing a new mechanistic explanation for exosome heterogeneity and a rational roadmap for exosome engineering.

Keywords:

Protein budding, tetraspanin, endosome, plasma membrane, extracellular vesicle, CD9, CD63, CD81, SPIR, interferometry

Abbreviations:

EV, extracellular vesicles; IB, immunoblot; IFM, immunofluorescence microscopy; IPMC, intracellular plasma membrane-connected compartment; MVB, multivesicular body; SPIR, single-particle interferometric reflectance; SPIRI, single-particle interferometric reflectance imaging

Abstract

Eukaryotic cells secrete exosomes, which are small (~30-200 nm dia.), single membrane-bound organelles that transmit signals and molecules to other cells. Exosome-mediated signaling contributes to diverse physiological and disease processes, rendering their biogenesis of high biomedical importance. The prevailing hypothesis is that exosomes bud exclusively at endosome membranes and are released only upon endosome fusion with the plasma membrane. Here we tested this hypothesis by examining the intracellular sorting and exosomal secretion of the exosome cargo proteins CD63, CD9, and CD81. We report here that CD9 and CD81 are both localized to the plasma membrane and bud >5-fold more efficiently than endosome-localized CD63. Furthermore, we show that redirecting CD63 from endosomes to the plasma membrane by mutating its endocytosis signal (CD63/Y235A) increased its exosomal secretion ~6-fold, whereas redirecting CD9 to endosomes by adding an endosome targeting signal (CD9/YEVM) reduced its exosomal secretion ~5-fold. These data demonstrate that the plasma membrane is a major site of exosome biogenesis, and more importantly, that cells possess a common pathway for exosome protein budding that operates at both plasma and endosome membranes. Using a combination of single-particle interferometry reflectance (SPIR) imaging and immunofluorescence (IF) microscopy, we also show that variations in exosome composition are controlled by differential intracellular protein trafficking rather than by separate mechanisms of exosome biogenesis. This new view of exosome biogenesis offers a simple explanation for the pronounced compositional heterogeneity of exosomes and a validated roadmap for exosome engineering.

Introduction

Exosomes are secreted by virtually all eukaryotic cells. These small vesicles are ~30-200 nm dia., have the same topology as the cell, and are enriched in selected proteins, lipids, and nucleic acids(Pegtel and Gould, 2019). Exosomes contribute to numerous physiological processes, including development, immunity, neuronal signaling, etc.(Ashley et al., 2018; Lindenbergh and Stoorvogel, 2018; McGough and Vincent, 2016; Pastuzyn et al., 2018), as well as a wide array human diseases, such as cancer, neurodegeneration, infectious disease, etc.(Becker et al., 2016; Cheng et al., 2018; Gould et al., 2003; van Dongen et al., 2016). Moreover, exosomes are abundant in all biofluids, can be used for clinical liquid biopsies, and are being developed as intrinsic therapeutics as well as drug delivery vehicles(Jia et al., 2014; Li et al., 2017; Phinney and Pittenger, 2017). This breadth of biological importance and translational potential highlights the importance of elucidating the mechanisms of exosome biogenesis.

In their landmark description of secreted vesicles, Trams et al.(Trams et al., 1981) defined exosomes as secreted vesicles that '*may serve a physiological purpose*' and showed that cells secrete two classes of extracellular vesicles (EVs), one that is small, ~40 nm dia., and another that is considerably larger, >500 nm dia. This ~10-fold difference in size allows their separation by differential centrifugation, which led to the eventual restriction of the term *exosome* to mean the smaller class of secreted vesicles, and adoption of the term *microvesicle* to describe the large class of secreted vesicles(Gould and Raposo, 2013). More recently, there has been a concerted effort to redefine these terms yet again, this time on the basis of biogenic mechanism. However, this effort has instead led to redefinition based on the site where an exosome originated in the cell, rather than the actual mechanism of biogenesis, and the now-commonplace dogma that that exosomes

arise only by budding into the endosome lumen(Colombo et al., 2014; Crenshaw et al., 2018; Desrochers et al., 2016; Mathieu et al., 2019; van Niel et al., 2018). While there is abundant evidence that exosomes can arise in this manner, the prevailing, 'endosome-only' hypothesis of exosomes biogenesis is not supported by clear evidence that exosomes and exosome cargoes cannot bud from the plasma membrane. In fact, it is fair to say that the 'endosome-only' hypothesis has yet to be tested.

Highly reductionist, cargo-based studies provided critical early insights into the biogenesis of the endoplasmic reticulum(Blobel and Dobberstein, 1975a; Blobel and Dobberstein, 1975b; Blobel and Sabatini, 1971), nucleus(Kalderon et al., 1984), mitochondria(Horwich et al., 1985), peroxisome(Gould et al., 1989) and other organelles(Blobel, 1980; Blobel, 1995). It is therefore reasonable to use a similar approach in studies of exosome biogenesis. This requires a focus on the most highly enriched exosomal proteins, as these show the strongest evidence of active sorting into exosomes, which are the tetraspanins CD63, CD9, and CD81(Escola et al., 1998; Thery et al., 1999), a trio of proteins that are widely used as exosome markers(Colombo et al., 2014; Crenshaw et al., 2018; Desrochers et al., 2016; Mathieu et al., 2019; van Niel et al., 2018). Like all tetraspanins, these proteins are co-translationally translocated into the ER lumen and membrane, span the membrane 4 times, and have their N-terminus and C-terminus oriented into the cytoplasm. The remainder of this paper tests several predictions of the 'endosome-only' hypothesis of exosome biogenesis by following the intracellular sorting and exosomal secretion of these cargo proteins, particularly CD63 and CD9. Our data represent argue against the 'endosome-only' model and instead indicate that cells make exosomes by a common mechanism that acts across the spectrum of plasma and endosome membranes.

Results

A key tenet of the 'endosome-only' hypothesis of exosome biogenesis is that exosome cargo proteins must be targeted to the limiting membrane of endosomes as a prerequisite to their exosomal secretion. To assess the validity of this prediction, we first examined the subcellular distribution of three well-established exosome marker proteins, CD63, CD9, and CD81(Escola et al., 1998; Thery et al., 1999). Using immunofluorescence microscopy (IFM), we observed that CD9 and CD81 were highly enriched at the plasma membrane instead of at endosomes, and that only CD63 displayed an endosomal localization (***Fig. 1A***). Although these distributions do not argue against the 'endosome-only' hypothesis of exosome biogenesis, they can only be reconciled with this hypothesis if CD63 buds more efficiently into exosomes than either CD9 or CD81. However, when we measured the relative budding of these proteins, we observed the exact opposite result. Specifically, we observed that CD9 displayed a relative budding that was ~5-fold higher than CD63 (4.9 +/- 0.53 fold higher; Student's t-test *p*-value (*p*) = 0.0053; n = 4) and that CD81 displayed a relative budding ~15-fold higher CD63 (15.7 +/- 2.9 fold higher; *p* = 0.015; n = 4) (***Fig. 1B***).

These observations are inconsistent with the 'endosome-only' model of exosome biogenesis and instead raise the possibility that exosome cargo proteins, and thus exosomes, also bud directly from plasma, and that in HEK293 cells they may bud more efficiently from the plasma membrane than from endosome membranes. To differentiate between these models of exosome biogenesis we redirected CD63 from endosomes to the plasma membrane by eliminating it consitiutive endocytosis signal. If the endosome-only hypothesis is correct, then this shift should cause a severe reduction in the exosomal secretion of CD63. However, if HEK293 cells bud exosomes from

plasma membranes, the budding of plasma membrane-localized CD63 should remain strong. To execute this experiment, we created plasmids designed to express either WT CD63 or CD63/Y235A, a mutant form of CD63 carrying a mutation that disrupts its clathrin-mediated endocytosis ($\underline{Y}EVM_{COOH}$, where the Y235 reside critical for binding to the clathrin AP-2 adaptor complex is underlined(Bonifacino and Traub, 2003)). These plasmids were then transfected into $CD63^{-/-}$ cells(Fordjour et al., 2016) and the resulting cells were subsequently processed by IFM to assess the subcellular distribution of WT CD63 and CD63/Y235A. As expected, WT CD63 was localized primarily in endosomes, whereas CD63/Y235A was localized primarily at the plasma membrane (***Fig. 2A***). Exosome and cell lysates were also collected from these cultures, and subsequent IB analysis to assess the relative budding of these proteins. Once again, the data were the exact opposite of that predicted by the endosome-only hypothesis of exosome biogenesis (***Fig. 2B***). Specifically, the plasma membrane-localized CD63/Y235A protein displayed ~6-fold higher relative budding than endosome-localized, WT CD63 (6.1-fold; +/- 1.3-fold, $p = 0.0038$; $n = 9$).

The most parsimonious interpretation of these data is that cells can make exosomes at both plasma and endosome membranes, and that the plasma membrane is the predominant site of exosome budding in HEK293 cells. If this interpretation is correct, then WT CD63-containing exosomes should be the same size as CD63/Y235A-containing exosomes. To test this prediction, we used single-particle interferometry reflectance (SPIR) imaging(Avci et al., 2015; Daaboul et al., 2017; Daaboul et al., 2016; Sevenler et al., 2017; Sevenler et al., 2018) and immunofluorescence microscopy (IFM) to measure the sizes of thousands of WT CD63 exosomes and CD63/Y235A exosomes. SPIRI-IFM is a novel analytical approach that combines traditional IFM of immunolabeled exosomes with label-free visualization of exosomes using a single-particle

interferometric reflectance imaging sensor, in which the interference of light reflected from the sensor surface is (***i***) modified by the presence of a chip-bound exosome, (***ii***) varies in relation to the diameter of the chip-bound exosome, and (***iii***) allows measurement of exosome diameter to a resolution of 0.5 nm. In these experiments, exosomes were collected from the conditioned media of $CD63^{-/-}$ cells expressing either WT CD63 or CD63/Y235A. These were then incubated with SPIRI chips that had been previously functionalized with anti-CD63 antibodies. The chips were washed, the chip surface was incubated with fluorescently labeled antibodies specific for CD63, washed again, and the bound exosomes analyzed by SPIRI-IFM to (a) measure the sizes of thousands of individual exosomes and (b) confirm the exosomal nature of each exosome by the presence of anti-CD63 fluorescence. The resulting data revealed that WT CD63 exosomes and CD63/Y235A exosomes have size distribution profiles that are virtually identical (***Fig. 2C***), and average diameters that are nearly the same (69 nm for WT CD63 exosomes (n = 3686) and 65 nm for CD63/Y235A exosomes (n = 5569)).

These findings show that cells will bud CD63 in exosomes of the same size, regardless of whether CD63 is localized at endosome membranes or localized at the plasma membrane. The result represents strong evidence that cells possess a common pathway for budding exosomes from both plasma and endosome membranes. If this interpretation is correct, then the composition of individual exosomes will be heavily influenced by the local concentration of exosome cargo molecules. To test this prediction, we asked if WT CD63 exosomes and CD63/Y235A exosomes differed in their inclusion of CD9, a plasma membrane-localized exosome cargo. Specifically, we incubated these two exosome populations on SPIRI chips functionalized with either anti-CD63 or anti-CD9 antibodies, and then probed them with fluorescently-tagged antibodies specific for both

CD63 and CD9. The resulting data support this new view of exosome biogenesis as they show pronounced increase in the exosomal co-localization of these proteins on CD63/Y235A-containing exosomes (***Fig. 2D***). For example, when exosomes were captured on anti-CD63 antibodies and interrogated for the presence of CD9, only 20% of WT CD63-containing exosomes stained positive for CD9 (20% +/- 1%) whereas >80% of CD63/Y235A exosomes stained positive for CD9 (86% +/- 21%), a 4.3-fold increase ($p = 0.00011$; n = 3). Similar results were observed when these exosomes were captured on anti-CD9 antibodies and stained for CD63, which revealed an exosomal co-localization of CD63 on a quarter (25% +/- 7%) of CD9-captured exosomes from WT CD63-expressing cells, and an exosomal co-localization of CD63 on >90% of CD9-captured exosomes from cells expressing CD63/Y235 (91% +/- 5%), a 3.6-fold increase ($p = 0.032$; n = 3).

The pronounced increase in the exosomal co-localization of CD9 on CD63/Y235A exosomes vs WT CD63 exosomes can also be visualized by plotting fluorescence intensity for thousands of individual exosomes (***Fig. 2E, F***). This is evident from comparing plots of anti-CD9 fluorescence intensity for (left panel) WT CD63 exosomes captured on anti-CD63 antibodies to those of (right panel) CD63/Y235A exosomes captured on anti-CD63 antibodies (***Fig. 2E***). It can also be seen in plots of anti-CD63 fluorescence intensity for (left panel) WT CD63 exosomes captured on anti-CD9 antibodies and (right panel) CD63/Y235A exosomes captured on anti-CD9 antibodies (***Fig. 2F***).

The simplest interpretation of the above data is that CD63 and CD9 bud by a common mechanism that operates across the spectrum of endosome and plasma membranes, and that the composition of any individual exosome is determined in large part by the local concentration of other exosome

cargoes. If this model is correct, then the same trends should be observed upon redirecting CD9 from plasma to endosome membrane. Towards this end, we generated $CD9^{-/-}$ HEK293 cells (***supplementary figure S1***) and then transfected them with with plasmids designed to express either WT CD9 or CD9/YEVM, a form of CD9 that carries the constitutive endocytosis signal from CD63 ($\underline{Y}EVM_{COOH}$). Immunofluorescence microscopy of these cells confirmed that WT CD9 was correctly localized to the plasma membrane and that CD9/YEVM was redirected to endosome membranes (***Fig. 3A***). Furthermore, IB analysis of cell and exosome fractions prepared from these cell populations revealed that redirecting CD9 from the plasma membrane to endosomes resulted in an ~5-fold reduction in its relative budding compared to that of WT CD9 (***Fig. 3B***; 5.5-fold difference; p = 0.00019; n = 9), demonstrating once again that the plasma membrane-localized form of a protein buds better than its endosome-targeted counterpart.

To further characterize WT CD9 exosomes and CD9/YEVM exosomes, we once again employed SPIRI-IFM. WT CD9 exosomes and CD9/YEVM exosomes were incubated with to anti-CD9 antibody-functionalized SPIRI chips, bound exosomes were then stained with anti-CD9 antibodies, and the chips were interrogated by SPIRI-IFM. The resulting data revealed that WT CD9 exosomes and CD9/YEVM exosomes have similar size distribution profiles (***Fig. 3C***) and average diameters (67 nm for WT CD9 exosomes (n = 15,684) and 65 nm for CD9/YEVM exosomes (n = 18,232)), demonstrating that these proteins bud from the cell in bona fide exosomes.

The budding of both CD9 and CD9/YEVM in exosomes of the same size supports the idea that cells make exosomes from both plasma and endosome membranes. If this interpretation is correct, then the antigenic character of WT CD9 exosomes and CD9/YEVM exosomes should differ in

respect to CD81 and CD63, with WT CD9 exosomes showing a higher degree of exosomal co-localization with plasma membrane-enriched CD81, and CD9/YEVM showing a higher degree of exosomal co-localization with endosome-localized CD63. To test this prediction, WT CD9 exosomes and CD9/YEVM exosomes were bound to anti-CD9-functionalized SPIRI chips, incubated with antibodies specific for CD81 and CD63, and subjected to SPIRI-IFM (***Fig. 3D***). The resulting data revealed that the ratio of CD81-positive exosomes to CD63-positive exosomes was 2.8 (+/- 0.3) for WT CD9 exosomes, but fell 5.5-fold for CD9/YEVM exosomes to 0.51 (+/- 0.06), a decrease of high significance (p = 0.000020; n = 9). This shift in antigenic character is also reflected in a 4-fold decrease (p = 0.0037; n = 9) in the percentage of CD9-containing exosomes that contain CD81 (from 23% +/- 4% for WT CD9 exosomes to 5.4% +/- 0.7% for CD9/YEVM exosomes). It is also evident in a 1.7-fold increase (p = 0.011, n = 9) in the percentage of CD63-captured exosomes that contain CD9 (from 26% +/- 3% for WT CD9 exosomes to 41% +/- 2% for CD9/YEVM exosomes).

These changes in the exosomal co-localization of CD81, CD63 and CD9 can also be visualized by scatter plots of fluorescence intensity for thousands of individual exosomes (***Fig. 3E, F***). This is particularly evident from plotting anti-CD81 fluorescence intensity (a.u.) for (left panel) WT CD9-exosomes captured on anti-CD9 antibodies and (right panel) CD9/YEVM exosome captured on anti-CD9 antibodies (***Fig. 3E***). It can also be seen by plotting anti-CD9 fluorescence intensity (a.u.) for (left panel) WT CD9 exosomes captured on anti-CD63 antibodies and (right panel) CD9/YEVM exosomes captured on anti-CD63 antibodies (***Fig. 3F***).

Our model is agnostic on the point of whether cells bud exosomes predominantly from the plasma or endosome membranes, as we presume that both are possible. Nevertheless, the observation that HEK293 cells display such a pronounced preference for making exosomes from the plasma membrane raises the question of whether this is also true for any other cell types. To answer this question we expressed the WT CD63, CD63/Y235A, WT CD9, and CD9/YEVM proteins in mouse NIH3T3 fibroblasts and followed their intracellular sorting and exosomal secretion (***Fig. 4***). More specifically, we transfected NIH3T3 cells with plasmids designed to express each protein, selected for G418-resistant clones, and assayed each for levels of expression to obtain matched pairs of cell lines that express similar levels of each cargo protein. Each cell line was then subjected to IFM to determine the subcellular distribution of the protein of interest, and immunoblot analysis was used assess their relative budding. As expected, CD63/Y235A and WT CD9 were enriched at the plasma membrane whereas WT CD63 and CD9/YEVM were targeted to endosomes (***Fig. 4A-D***). Furthermore, we observed that redirecting CD63 from endosomes to the plasma membrane of NIH3T3 cells led to a significant increase in its relative budding from the cell (5.7 +/- 0.7 fold, $p = 0.00058$, n = 7; ***Fig. 4E***), similar to what we observed for HEK293 cells. The same was true for the CD9 experiments, as and redirecting CD9 from the plasma membrane to endosomes of NIH3T3 cells once again led to a significant decrease in its relative budding from the cell (3.3 +/- 0.6 fold, $p = 0.0056$, n = 8; ***Fig. 4F***). Thus, NIH3T3 resemble HEK293 cells in their preferential exosomal secretion of plasma membrane-targeted exosome cargoes.

Discussion

Testing the 'endosome-only' hypothesis

A wide array of reviews and research articles assert that exosomes arise solely by budding into endosomes, followed by endosome-plasma membrane fusion(Colombo et al., 2014; Crenshaw et al., 2018; Desrochers et al., 2016; Mathieu et al., 2019; Thery et al., 2018; van Niel et al., 2018). We find this perplexing, in part because there is no compelling body of evidence that exosomes cannot bud from the plasma membrane, and in part because no study has even attempted to test this prevailing, 'endosome-only' hypothesis. Here we subjected this hypothesis to experimental interrogation, primarily by testing its core tenet that exosomal cargoes must be targeted to endosomes before they can be secreted in exosomes.

The foundation of the 'endosome-only' hypothesis is belied by the fact that CD9 and CD81, which display the highest relative budding of any exosomal cargo proteins yet reported, are localized primarily at the plasma membrane, whereas endosome-targeted CD63 buds 5-15-fold less efficiently that either CD9 or CD81. After all, if exosomes only bud via endosomal budding, then cargoes that are enriched at endosomes should bud more efficiently than plasma membrane-localized cargoes. This tenet is also contradicted by the consequences of redirecting CD63 to the plasma membrane. Under the prevailing paradigm, this change in subcellular distribution should reduce or eliminate the exosomal secretion of CD63, while in reality it led to a ~6-fold increase in its exosomal secretion. The prevailing paradigm was similarly unable to predict or explain the consequence of redirecting CD9 from the plasma membrane to endosome membranes, which resulted in an ~5-reduction in CD9's exosomal secretion. In fact, every observation in this paper

runs counter to the assertion that exosomes are generate exclusively by budding from the endosome membrane. Given its consistent inability to predict the outcome of simple empirical tests, one cannot help but wonder whether the prevailing paradigm is based on anything more than a circular argument in which exosomes are believed to arise by endosomal budding for the sole reason that exosomes have been defined in that manner.

Exosomes arise from plasma and endosome membranes

The simplest interpretation of our data is that cells possess a shared mechanism of exosome biogenesis that operates at plasma and endosome membranes, and that HEK293 and NIH3T3 cells make most of their exosomes at the plasma membrane. This hypothesis predicts or explains all major observations in this report, including:

(i) the steady-state enrichment of exosome cargoes at both plasma and endosome membranes;

(ii) the ~5-15-fold higher relative budding of CD9 and CD81 relative to CD63;

(iii) the exosomal secretion of CD63/Y235A;

(iv) the ~6-fold higher exosomal secretion of CD63/Y235A compared to WT CD63;

(v) the ~5-fold lower exosomal secretion of CD9/YEVM compared to WT CD9;

(vi) the exosomal co-localization of CD9 and CD63 on WT CD63 exosomes;

(vii) the ~4-fold increase in exosomal co-localization of CD9 and CD63 on CD63/Y235A exosomes compared to WT CD63 exosomes;

(viii) the ~4-fold decrease in exosomal co-localization of CD81 on CD9/YEVM exosomes compared to WT CD9 exosomes; and

(ix) the ~1.7-fold increase in CD63 on CD9/YEVM exosomes compared to WT CD9 exosomes.

The model of exosome biogenesis posited here is also consistent with prior observations of exosome biogenesis via the plasma membrane(Anderson, 1969; Anderson et al., 2005; Bianchi et al., 2014; Booth et al., 2006; Cantaluppi et al., 2012; Casado et al., 2017; Fang et al., 2007; Shen et al., 2011a; Shen et al., 2011b) as well as prior observations of exosome biogenesis via endosome membranes(Colombo et al., 2014; Crenshaw et al., 2018; Desrochers et al., 2016; Harding et al., 1983; Harding et al., 1984; Mathew et al., 1995; Mathieu et al., 2019; Pan and Johnstone, 1983; Pegtel and Gould, 2019; van Niel et al., 2018). Furthermore, it adheres to the principle of maximum parsimony by offering a simpler explanation for a wider array of data than is possible under the 'endosome-only' hypothesis of exosome biogenesis.

Implications for exosome composition and heterogeneity

Although our data indicate that a single mechanism of exosome biogenesis operates across the spectrum of endosome and plasma membranes, this model does not predict a uniform composition of secreted exosomes. To the contrary, it predicts that the composition of each individual exosome will be determined primarily by the local, nanometer-scale concentrations of exosome cargoes in the immediate vicinity of each nascent exosome, which are then fixed by its scission from its parent membrane. This prediction is supported by several of our observations, including the increased exosomal co-localization of CD9 on CD63/Y235A exosomes, the decreased exosomal co-localization of CD81 on CD9/YEVM exosomes, and the increased exosomal co-localization of CD63 on CD9/YEVM exosomes.

This model also provides a simple yet elegant explanation for the pronounced compositional heterogeneity of exosomes as the vesicular manifestation of nanometer-scale heterogeneities in the plasma and endosome membranes that give rise to exosomes. Compositional heterogeneity of these membranes is an established fact(Bernardino de la Serna et al., 2016; Sevcsik et al., 2015; Sevcsik and Schutz, 2016; Specht et al., 2017), and these heterogeneities are generated by both mechanistic and stochastic forces. For example, the protein sorting machineries that distribute cargoes along the spectrum of endosome and plasma membranes display significant-to-subtle differences in affinity for virtually every protein with which they interact(Traub and Bonifacino, 2013), resulting a spectrum of large-scale distribution patterns of these proteins along the spectrum of plasma and endosome membranes. In addition, each cargo molecule will experience a range of stochastic forces further affecting their nanometer-scale concentration at these membranes, including diffusion, structural fluctuations, and various intermolecular interactions. The combination of these forces, together with the varied size of exosomes, indicates that each exosome cargo molecule will emerge at various levels on exosomes of varied size, with few if any having the exact same size and amount of any one protein. This prediction corresponds rather well with our SPIRI-IFM data, in which we interrogated thousands of HEK293-derived exosomes for just two parameters, size and CD9 abundance, and found that each exosome had a nearly unique combination of size and CD9 staining. If one assumes that a similar heterogeneity is seen for the thousands of proteins, nucleic acids, and lipids that are incorporated into exosomes by a single cell line(Li et al., 2016), it may be that no two exosomes are alike.

It should be noted that this model predicts additional contributors to structural and functional heterogeneity. For example, exosomes that arise by budding from the plasma membrane are likely influenced by the high complexity of the extracellular milieu, whereas those that bud into endosomes are affected by its low pH and abundance of hydrolytic products (e.g. peptides, lipids, etc.). Exosomes may also arise by budding into intracellular plasma membrane-connected compartments (IPMCs), and this environment may also affect exosome composition and function(Nkwe et al., 2016; Pelchen-Matthews et al., 2012). IPMCs are virtually indistinguishable from multivesicular bodies (MVBs) but are not endosomes at all, as their lumens are contiguous with the extracellular space and their membranes are continuous with the cell surface. These different sites of origin can also impart a temporal heterogeneity in exosome release, as vesicles retained within MVBs or IPMCs can be released in a delayed and pulsatile manner via endosome fusion with the plasma membrane(Sung et al., 2015; Verweij et al., 2018) and IPMC opening(Pelchen-Matthews et al., 2012), respectively.

Applications to exosome engineering

The mechanisms of exosome biogenesis have important implications for the more prosaic topic of exosome engineering. Exosomes are being developed as therapeutics and drug-delivery vehicles for a number of applications(Gilligan and Dwyer, 2017; Kamerkar et al., 2017; Li et al., 2017), some of which involve genetic engineering of exosome-producing cells(Yim et al., 2016). Efficient exosome engineering requires a solid understanding of exosome biogenesis, as the pathway of exosome biogenesis is the blueprint for exosome design. From this perspective, the 'endosome-only' hypothesis of exosome biogenesis does not appear to be particularly helpful, as it wrongly

predicts that putative new exosome cargoes should be sent to the endosome membrane. In contrast, the hypothesis posited here provides a validated roadmap for the first two steps in exosome engineering. Specifically, it suggests that exosome engineers (i) test whether the exosome producing cell line of choice makes exosomes predominantly from plasma or endosome membranes, and then (ii) engineers the putative new exosomal cargo so that cells direct it too that location. However, additional steps are also likely involved, in part because most plasma membrane proteins are not targeted to exosomes(Escola et al., 1998; Thery et al., 1999) and in part because protein targeting to exosomes is induced by high-order oligomerization of plasma membrane-anchored proteins(Fang et al., 2007).

Two-pathway alternatives

It is also useful to consider whether a two-mechanism model could explain the biogenesis of exosomes. For example, is it possible that cells possess one pathway that mediates the exosomal secretion of 'class A' cargoes, such as CD9 and CD81, and a second, separate pathway that mediates the budding of 'class B' cargoes, such as CD63? To answer this question it is first necessary to accept that the word *separate* means distinct and non-overlapping. This is obvious from its dictionary definition, but also from the cell biological principle of protein topogenesis(Blobel, 1980; Blobel, 1995), in which separate organelles are defined in large part by their mechanistic connection to separate protein sorting pathways. This means that two-pathway models of exosome biogenesis demands that the exosomal co-localization of Class A and Class B cargoes is either minimal or absent.

The data in our paper argue strongly against a two-pathway model of exosome biogenesis, for the simple reason that we detected significant exosomal co-localization of Class A and Class B cargoes in every exosome sample we examined. For example, exosomal co-localization of CD9 and CD63 was observed on a relatively low but nonetheless highly significant percentage of exosomes, as ~25% of WT CD63 exosomes contained both of these Class A and Class B cargoes. Furthermore, their exosomal co-localization could be increased further, rising to ~90% merely by redirecting CD63 to the plasma membrane. Significant exosomal co-localization of Class A and B cargoes was also evident on a significant percentage (~20%) of WT CD9 exosomes, which was doubled to ~40% by redirecting CD9 to endosomes.

Another possible permutation of the two-pathway model would be to restate the Class A pathway as mediates the budding of proteins from the plasma membrane while a Class B pathway mediates protein budding from endosomes. This version of the two-pathway model posits that misdirecting plasma membrane cargoes to the endosome should inhibit its exosomal secretion, which actually matches the data we obtained by redirecting CD9 to endosomes (a 5-fold reduction in CD9 budding). However, this hypothesis also predicts that CD63 budding should also decrease upon its redistribution to the plasma membrane, which runs counter to the fact that it induced a ~6-fold increase in its exosomal secretion. It also predicts a dearth of exosomal co-localization of CD9 and CD63, and is similarly undermined by the contradictory observations outlined in the preceding paragraph.

In light of these considerations it seems that the only way to square our data with a two-mechanism model of exosome biogenesis would be to: (i) reject the conventional meaning of the word

'separate' and redefine it to mean 'pretty much the same'; (ii) ignore the well-established principles of protein topogenesis, in which organelle identity is driven by non-overlapping protein sorting pathways(Blobel, 1980; Blobel, 1995); and (iii) posit that cells somehow evolved two separate pathways of exosome biogenesis that accept the same sets of cargo proteins, secrete them from the cell in exosomes of the same size and molecular characteristics, and have no discernable difference. It seems far more logical to adhere to the principle of maximum parsimony and go with the far simpler model, in which cells use a shared pathway for exosome biogenesis from plasma and endosome membranes.

Acknowledgments

We thank Colin Fowler, James Morrell, and Jerry Plange of the Gould lab and Aditya Dhande of Nanoview Sciences for expert technical assistance. This work was supported by NIH (U19CA179563).

Author contributions

F.K.F. performed all experiments other than the coupled SPIRI-IFM analyses, contributed to the experimental design, data interpretation and writing of the paper; G.G.D. performed all SPIRI-IFM analyses and contributed to the experimental design, data interpretation and writing of the paper; S.J.G. conceived of the project, contributed to the experimental design, data interpretation, performed the majority of the SPIRI-IFM analysis, and composition of the manuscript.

Competing interests

F.K.F. receives royalties from the commercial use of mutant HEK293 cell lines and altered exosomes described in this paper.

G.G.D. is co-founder, CSO, co-owner, and employee of Nanoview Biosciences, which produces and sells the Exoview imaging system and related materials.

S.J.G. receives royalties from the commercial use of mutant HEK293 cell lines and altered exosomes described in this paper.

Materials & Correspondence

Correspondence and material requests should be addressed to:

Dr. Stephen Gould

Professor of Biological Chemistry

Johns Hopkins University

Room 409, Physiology Building

Baltimore, MD

21205

USA

Email: sgould@jhmi.edu

Tel: (01) 443 847 9918

Methods

Plasmids

The CD9 knock-out plasmid pJM1084 was generated by inserting CD9 gene-specific guide RNA-encoding sequences specific for CD9 exons 1 and 3, respectively, were inserted downstream of the 7sk and H1 promoters, respectively, of pFF4(Fordjour et al., 2016). Plasmids pCF1, pCF2, pCF6, and pCF7 were created by inserting the ORFs encoding CD63, CD63/Y235A, CD9, and CD9/YEVM downstream of the CMV promoter of pcDNA3. Plasmids were amplified by growth in *E. coli* DH10 and purified by ion exchange chromatography from bacterial cell lysates.

Cells, transfections

HEK293 cells (ATCC CRL1573), HEK293 CD63$^{-/-}$ cells(Fordjour et al., 2016), HEK293 CD9$^{-/-}$ cells and NIH3T3 cells (ATCC CRL-1658) were grown in DMEM supplemented with 10% fetal calf serum (FCS) or 10% exosome-free FCS, with all exosome-related studies performed using cells grown in the latter. HEK293 cells carrying null mutations in CD9 (CD9$^{-/-}$) were generated by transfecting HEK293 cells with pJM1084, selecting for puromycin-resistant cells (7 days), followed by limiting cell dilution into 96 well plates and expansion of single cell clones (SCCs). Multiple independent SCCs were screened by IB using anti-CD9 antibodies, followed by genomic DNA extraction, PCR analysis using oligos that flank both sides to the exon 1 and exon 3 target sites, and sequence analysis of individual PCR products. The CD9$^{-/-}$ cell line selected for further analysis here was found to carry only null alleles in the CD9 gene. Transfections were performed using lipofectamine 2000 (ThermoFisher) according to the manufacturer's instruction. NIH3T3 cells expressing WT CD63, CD63/Y235A, WT CD9 or CD9/YEVM were selected in 400 □g/ml

G418 (ThermoFisher), clones expressing similar level of each pair protein were identified, and then used for subsequent experiments.

Exosome purification and immunoblot

For each trial, 6 x 10^6 cells were seeded onto 2 x 150 mm dishes in a total volume of 60 ml of DMEM supplemented with 10% exosome-free FCS and grown for 72 hrs. For all exosome studies, the tissue culture media was spun at 5000 x *g* for 15 min. The pellet was discarded and the supernatants (SN) were passed through 0.22 um filter. For exosome analysis by SPIRI and IFM, the filtrate was concentrated by angular flow filtration (Centricon Plus-70; EMDMillipore) to a final volume of to 500ul. Exosomes were purified by size exclusion chromatography (Izon qEV column), 500ul fraction samples were collected, and fractions 4, 5, and 6 were assayed by immunoblot (IB) to confirm the presence of exosome markers, pooled, and interrogated by SPIRI and IFM. For exosome analysis by IB, the clarified tissue culture supernatant was spun twice at 10,000 x *g* for 30 mins to remove contaminating microvesicles, and the resulting supernatant was spun at 70,000 x *g* for 2 hrs at 4^{o}C to pellet exosomes. Cell lysates were generated by addition of 2 ml of 2x SDS-PAGE sample buffer. Exosome pellets were resuspended in 600ul of 2x SDS-PAGE sample buffer. Immunoblots were performed at a constant ratio of exosome:cell lysates. IB analysis was performed by separating cell and exosome lysates by SDS-PAGE. Proteins were then transferred to Immobilon membranes (EMDMillipore), followed in sequence by incubation with block solution (0.2% non-fat dry milk in TBST), primary antibody solution, 5 washes with TBST, secondary antibody solution, and 5 washes with TBST. Antigens were visualized by chemiluminescence and detected using an Amersham Imager 600 (GE Healthcare Life Sciences) gel imaging system. The resulting digitized IB images were then processed in Image J by

converting them to 8-bit grayscale files followed by background subtraction. Measurement parameter and scale were set to integrated density and pixel, respectively. Images were then inverted, bands were delineated using the freehand selection tool, and signal densities were converted to relative protein abundance by multiplying by the dilution factor for each sample. Relative budding was calculated by dividing the protein abundance in exosome lysate by the sum of the protein abundance in the cell lysate and the protein abundance in exosome lysate.

Immunofluorescence microscopy

Immunofluorescence microscopy (IFM) was performed on cells grown on cover glasses. Cells were fixed (3.7% formaldehyde in PBS for 15 min.), permeabilized (1% Triton X-100 in PBS for 5 min.), incubated with primary antibodies in PBS (15 min.), washed 3 times with PBS, incubated with fluorescently-labeled secondary antibody and DAPI, washed 3 times with PBS, mounted on glass slides, and visualized by confocal microscopy. Antibodies were diluted in PBS (1:200 dilution for CD63 (clone E-12, #sc-365604, Santa Cruz Biotechnology), 1:200 dilution for CD9 (clone H19a, #312102, Biolegend), 1:1000 dilution of fluorescein (FITC) AffiniPure Goat Anti-Mouse IgG (H+L) (#115-095-003 Jackson Laboratory). Confocal images were acquired using a Zeiss AxioObserver inverted microscope with LSM700 confocal module and 63x, 1.4 aperture AxioPlan objective. Images were acquired using Zen software, converted to tiff files, and imported into Adobe Photoshop and Illustrator to create final images. Standard immunofluorescence imaging of NIH3T3 cells was performed at room temperature on a BH2-RFCA microscope (Olympus) equipped with an Olympus S-plan Apo 63× 0.40 oil objective and a Sensicam QE (Cooke) digital camera using IPLab 3.6.3 software (Scanalytics, Inc.). Again, tiff images were imported into Adobe Photoshop and Illustrator to create final images.

SPIRI and IFM analysis

Each exosome sample was diluted ten-fold in SPIRI incubation buffer (50mM HEPES, 150 mM NaCl and 0.05% Tween-20, pH 7.3). 35 μL of each sample were then incubated on the ExoView Tetraspanin Chip (EV-TC-TTS-01) placed in a sealed 24 well plate for 16 hours at room temperature. Each chip was then washed on an orbital shaker once with PBST (PBS supplemented with 0.05% Tween-20) for 3 minutes, then washed three additional times with PBS for 3 minutes each Chips were then incubated with one or more of Alexa-55-labeled anti-CD81, Alexa-488-labeled anti-CD63, and Alexa-647anti-CD9 antibodies in PBST supplemented with 2% BSA in a volume of 250 μL for 2 hours at room temperature without shaking. Each chip was then washed once with PBST, 3 times with PBS, once in filtered deionized water, and then dried at room temperature for 1 hour. The chips were then imaged with the ExoView R100 reader using the ExoScan 2.5.5 acquisition software (Nanoview Biosciences). The resulting size and fluorescence intensity information for each individual exosome was exported to Excel for statistical analyses. Fluorescence values are reported in arbitrary units.

Data analysis and presentation

All quantitative data is reported as average +/- standard error of the mean. The statistical significance of differences between different data sets was assessed using Student's t-test (two-tailed, paired). Histograms and scatter plots were generated using Excel. Images were imported into Adobe photoshop and figures were assembled in Adobe Illustrator. Image data was adjusted for brightness only.

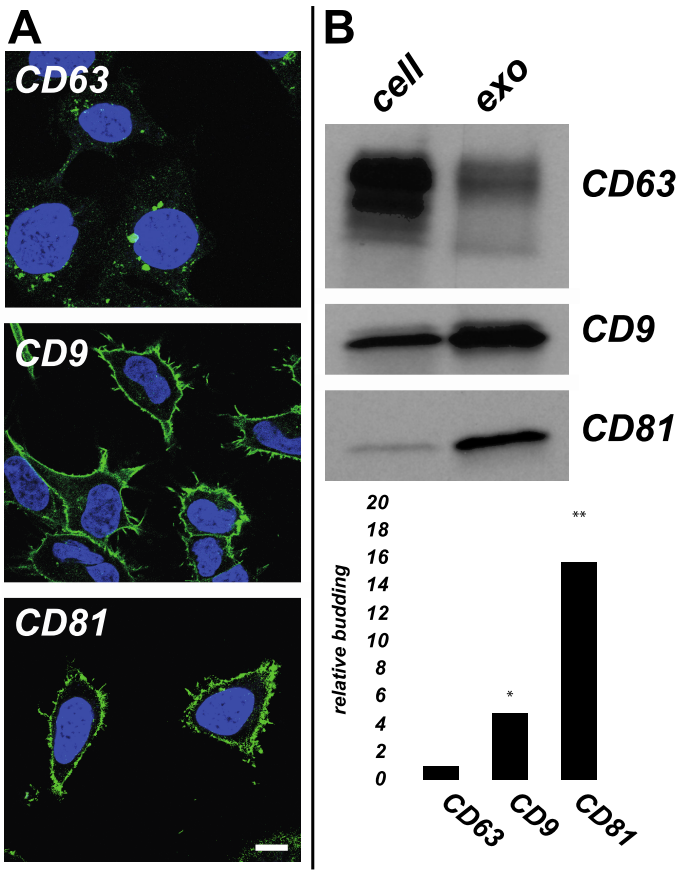

Figure 1. Plasma membrane-localized exosome cargoes CD9 and CD81 display higher relative budding than endosome-localized CD63. (**A**) HEK293 cells were fixed, permeabilized, and stained with antibodies specific for CD63, CD9, or CD81, as well as with DAPI (blue), and then imaged by confocal microscopy. bar, 10 um. (**B**) Immunoblot analysis of HEK293 exosome and cell lysates reveals that the relative budding of CD63 is 5-fold less than that of CD9 and 16-fold less than that of CD81. The bar graph shows the average +/- s.e.m. (n = 4) of the relative budding of CD63, CD9, and CD81 proteins. * denotes a *p*-value less than 0.05, ** denotes a *p*-value less than 0.005.

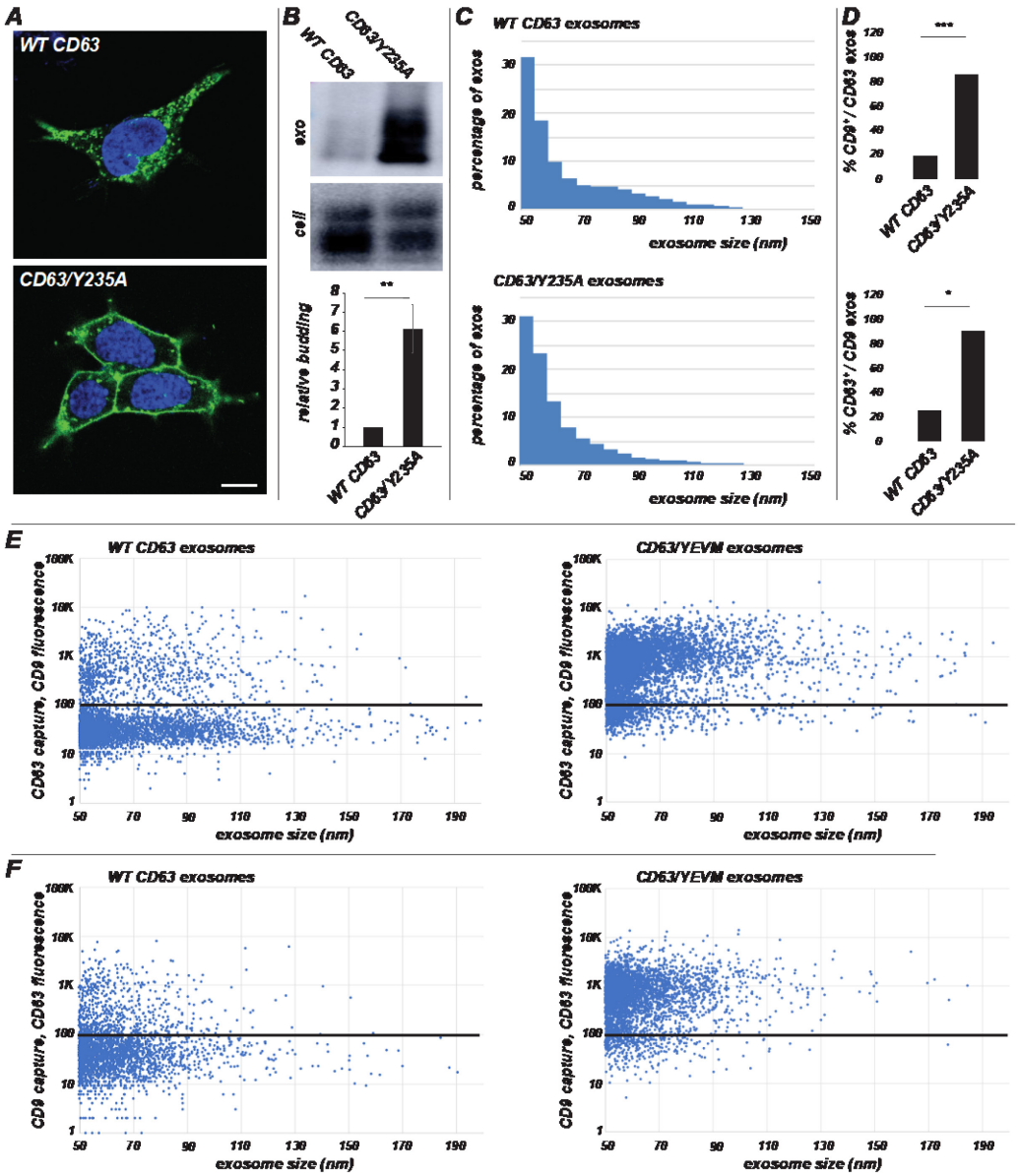
A
WT CD63
CD63/Y235A
B
WT CD63
CD63/Y235A
exo
cell
relative budding
**
WT CD63
CD63/Y235A
C
WT CD63 exosomes
percentage of exos
exosome size (nm)
CD63/Y235A exosomes
percentage of exos
exosome size (nm)
D
***
% CD9+/ CD63 exos
WT CD63
CD63/Y235A
*
% CD63+/ CD9 exos
WT CD63
CD63/Y235A
E
WT CD63 exosomes
CD63 capture, CD9 fluorescence
exosome size (nm)
CD63/YEVM exosomes
CD63 capture, CD9 fluorescence
exosome size (nm)
F
WT CD63 exosomes
CD9 capture, CD63 fluorescence
exosome size (nm)
CD63/YEVM exosomes
CD9 capture, CD63 fluorescence
exosome size (nm)

Figure 2. Redirecting CD63 to the plasma membrane enhances its exosomal secretion and its exosomal co-localization with the plasma membrane-enriched exosome marker, CD9. (**A**) Confocal microscopy of HEK293 $CD63^{-/-}$ cells transfected with plasmids expressing either (upper panel) WT CD63 or (lower panel) CD63/Y235A, stained with (green) antibodies specific for CD63 and (blue) DAPI. bar, 10 um. (**B**) Immunoblot analysis of exosome and cell lysates from HEK293 $CD63^{-/-}$ cells expressing either CD63 or CD63/Y235A. Bar graph shows average relative budding +/- s.e.m. (n = 9) of WT CD63 and CD63/Y235A compared to wildtype CD63; *p*-value < 0.005. (**C**) Coupled SPIRI and IFM reveal that (upper graph) WT CD63 exosomes and (lower graph) CD63/Y235A exosomes have similar size distribution profiles. (**D**) Bar graphs showing the percentages (average +/- s.e.m.) of (upper graph) CD9-captured exosomes that stain positive for CD63 and (lower graph) CD63-captured exosomes that stain positive for CD9. Statistical significance is denoted by one asterisk (p <0.05), two asterisks (p <0.005) or three asterisks (p <0.005). (**E**) Scatter analysis plotting CD9 fluorescence (a.u.) vs. exosome size on exosomes captured on anti-CD63 antibodies for (left plot) WT CD63 exosomes and (right plot) CD63/Y235A exosomes. Solid black line denotes the threshold of background fluorescence, as determined by staining samples with non-immune IgG. Black line denotes fluorescence background level of 100. (**F**) Scatter analysis plotting CD63 fluorescence (a.u.) vs. exosome size on exosomes captured on anti-CD9 antibodies for (left plot) WT CD63 exosomes and (right plot) CD63/Y235A exosomes. Black line denotes fluorescence background level of 100.

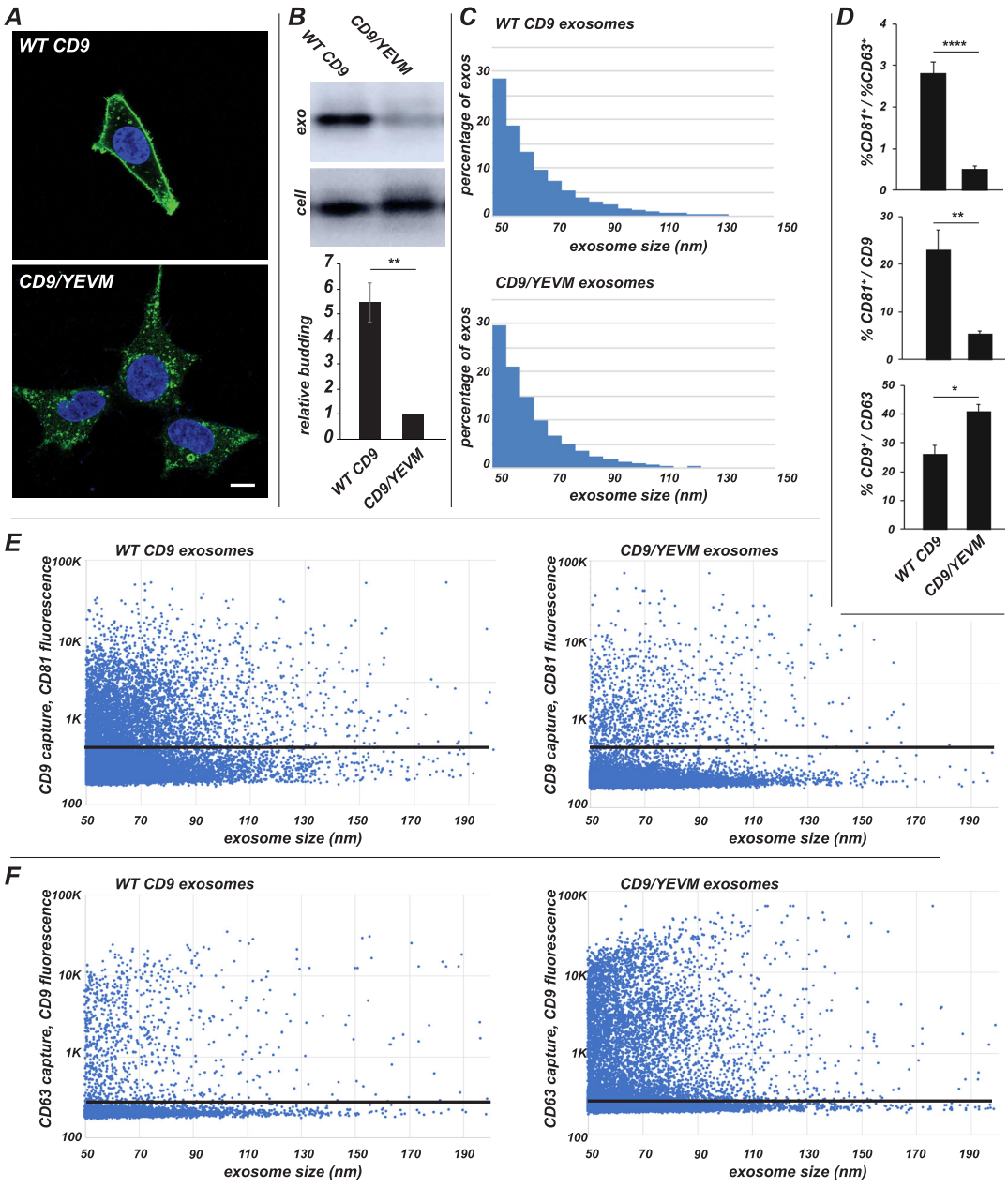
A
WT CD9
CD9/YEVM
B
WT CD9
CD9/YEVM
exo
cell
relative budding
**
C
WT CD9 exosomes
percentage of exos
exosome size (nm)
CD9/YEVM exosomes
D
%CD81+ / %CD63+
****
% CD81+ / CD9
**
% CD9+ / CD63
*
E
WT CD9 exosomes
CD9/YEVM exosomes
CD9 capture, CD81 fluorescence
exosome size (nm)
F
WT CD9 exosomes
CD9/YEVM exosomes
CD63 capture, CD9 fluorescence
exosome size (nm)

Figure 3. Redirecting CD9 to endosomes inhibits its exosomal secretion, reduces its exosomal co-localization with CD81, and increases its exosomal co-localization with CD63. (**A**) Confocal microscopy of HEK293 $CD9^{-/-}$ cells transfected with plasmids expressing either (upper panel) wildtype CD9 or (right panel) CD9/YEVM, stained with (green) antibodies specific for CD9 and (blue) DAPI. bar, 10 um. (**B**) Immunoblot analysis of cell and exosome fractions from HEK293 $CD9^{-/-}$ cells expressing either CD9 or CD9/YEVM. Graph shows average relative budding +/- s.e.m. (n = 9) of CD9 compared to CD9/YEVM; *p*-value <0.0005. (**C**) Size distribution of (upper graph) CD9-containing exosomes (upper graph) and (lower graph) CD9/YEVM-containing exosomes, as determined by coupled SPIRI and IFM. (**D**) Bar graphs showing (upper graph) the ratio of CD81-positive exosomes to CD63-positive exosomes captured by anti-CD9 antibodies from CD9 exosomes and CD9/YEVM exosomes; (middle graph) the percentage of CD81-positive exosomes captured on anti-CD9 antibodies from CD9 exosomes and CD9/YEVM exosomes; and (lower graph) the percentage of CD9-positive exosomes captured on anti-CD63 antibodies from CD9 exosomes and CD9/YEVM exosomes. Each value represents that average +/- s.e.m., and the degree of statistical significance is denoted by one asterisk ($p < 0.05$), two asterisks ($p < 0.005$) or four asterisks ($p < 0.0005$). (**E**) Scatter analysis of CD81 fluorescence intensity (a.u.) plotted against exosome diameter, of exosomes captured on anti-CD9 antibodies from (left plot) WT CD9 exosomes and (right plot) CD9/YEVM exosomes. Black line denotes fluorescence background level of 300. (**F**) Scatter analysis of CD9 fluorescence intensity (a.u.) plotted against exosome diameter, of exosomes captured on anti-CD63 antibodies from (left plot) WT CD9 exosomes and (right plot) CD9/YEVM exosomes. Black line denotes fluorescence background level of 250.

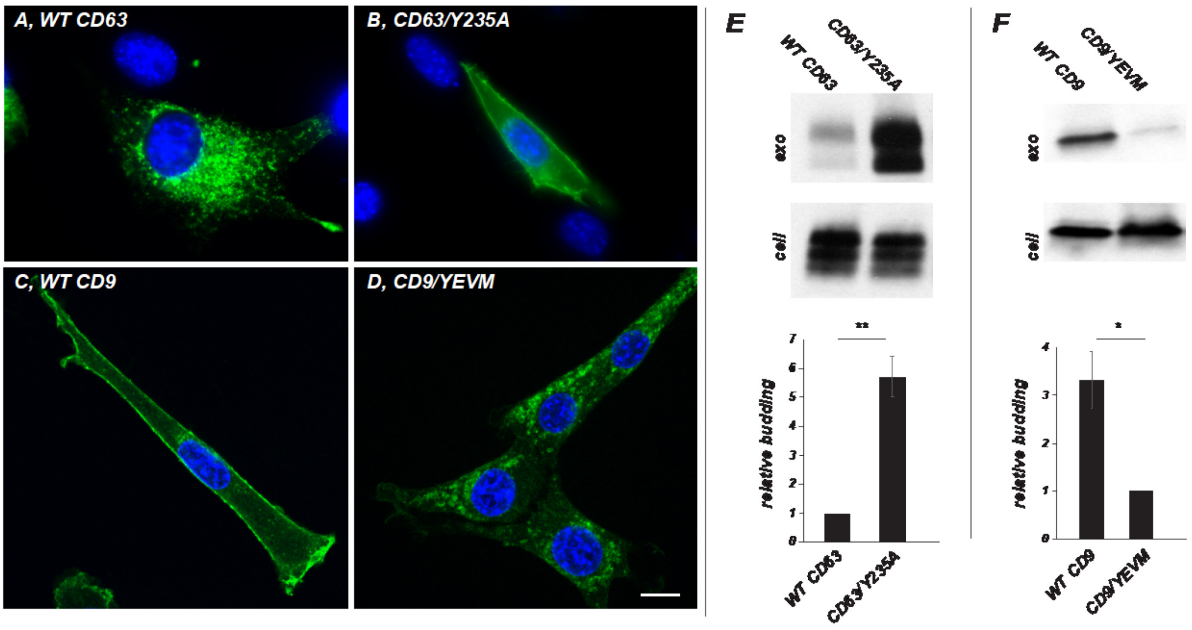

Figure 4: *NIH3T3 cells bud exosome cargoes preferentially from plasma membranes*. (**A-D**) IFM of NIH3T3 cells stably expressing (A) WT human CD63, (B) human CD63/Y235A, (C) WT human CD9, or (D) human CD9/YEVM. Cells were fixed, permeabilized, incubated with monoclonal antibodies specific for (A,B) human CD63 or (C,D) human CD9, stained with secondary antibodies specific for mouse IgG and also with DAPI to detect the nucleus. Bar, 10 um. (**E**) Immunoblot analysis of cell and exosome fractions collected from NIH3T3 cells stably expressing WT CD63 or CD63/Y235A, followed by calculation of relative budding and appropriate statistical analysis. (**F**) Immunoblot analysis of cell and exosome fractions collected from NIH3T3 cells stably expressing WT CD9 or CD9/YEVM, followed by calculation of relative budding and statistical analysis.

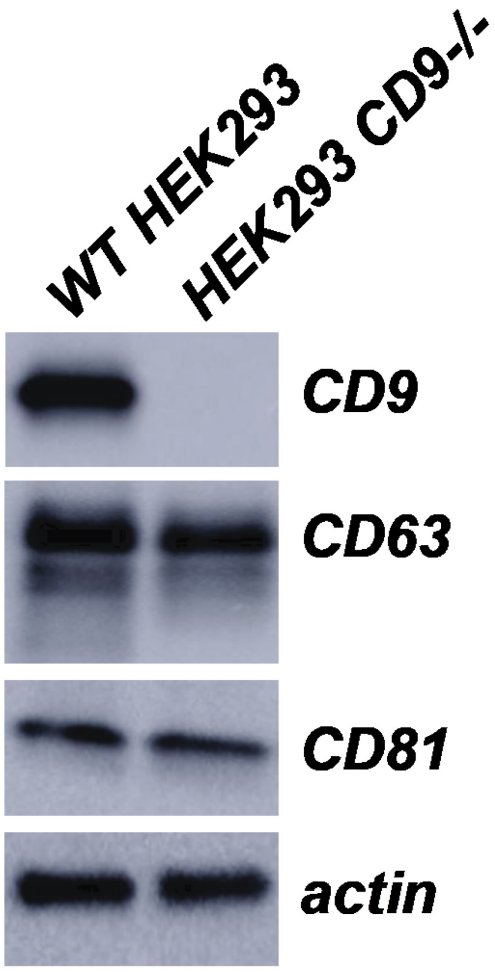

Supplementary Figure 1: CD9$^{-/-}$ HEK293 cells do not express CD9 protein. Immunoblot analysis of WT HEK293 cells and HEK293 CD9$^{-/-}$ cells using antibodies specific for CD98, CD63, CD81, and actin shows that CD9$^{-/-}$ cells do not produce CD9 protein but exhibit no apparent change in the expression of CD63, CD81, or actin.

References

Anderson, H.C. 1969. Vesicles associated with calcification in the matrix of epiphyseal cartilage. *J Cell Biol*. 41:59-72.

Anderson, H.C., R. Garimella, and S.E. Tague. 2005. The role of matrix vesicles in growth plate development and biomineralization. *Front Biosci*. 10:822-837.

Ashley, J., B. Cordy, D. Lucia, L.G. Fradkin, V. Budnik, and T. Thomson. 2018. Retrovirus-like Gag Protein Arc1 Binds RNA and Traffics across Synaptic Boutons. *Cell*. 172:262-274 e211.

Avci, O., N.L. Unlu, A.Y. Ozkumur, and M.S. Unlu. 2015. Interferometric Reflectance Imaging Sensor (IRIS)--A Platform Technology for Multiplexed Diagnostics and Digital Detection. *Sensors (Basel)*. 15:17649-17665.

Becker, A., B.K. Thakur, J.M. Weiss, H.S. Kim, H. Peinado, and D. Lyden. 2016. Extracellular Vesicles in Cancer: Cell-to-Cell Mediators of Metastasis. *Cancer Cell*. 30:836-848.

Bernardino de la Serna, J., G.J. Schutz, C. Eggeling, and M. Cebecauer. 2016. There Is No Simple Model of the Plasma Membrane Organization. *Front Cell Dev Biol*. 4:106.

Bianchi, E., B. Doe, D. Goulding, and G.J. Wright. 2014. Juno is the egg Izumo receptor and is essential for mammalian fertilization. *Nature*. 508:483-487.

Blobel, G. 1980. Intracellular protein topogenesis. *Proc Natl Acad Sci U S A*. 77:1496-1500.

Blobel, G. 1995. Unidirectional and bidirectional protein traffic across membranes. *Cold Spring Harb Symp Quant Biol*. 60:1-10.

Blobel, G., and B. Dobberstein. 1975a. Transfer of proteins across membranes. I. Presence of proteolytically processed and unprocessed nascent immunoglobulin light chains on membrane-bound ribosomes of murine myeloma. *J Cell Biol*. 67:835-851.

Blobel, G., and B. Dobberstein. 1975b. Transfer of proteins across membranes. II. Reconstitution of functional rough microsomes from heterologous components. *J Cell Biol*. 67:852-862.

Blobel, G., and D.D. Sabatini. 1971. Ribosome-membrane interaction in eucaryotic cells. *In* Biomembranes. L.A. Manson, editor. Plenum, New York. 193-195.

Bonifacino, J.S., and L.M. Traub. 2003. Signals for sorting of transmembrane proteins to endosomes and lysosomes. *Annu Rev Biochem*. 72:395-447.

Booth, A.M., Y. Fang, J.K. Fallon, J.M. Yang, J.E. Hildreth, and S.J. Gould. 2006. Exosomes and HIV Gag bud from endosome-like domains of the T cell plasma membrane. *J Cell Biol*. 172:923-935.

Cantaluppi, V., S. Gatti, D. Medica, F. Figliolini, S. Bruno, M.C. Deregibus, A. Sordi, L. Biancone, C. Tetta, and G. Camussi. 2012. Microvesicles derived from endothelial progenitor cells protect the kidney from ischemia-reperfusion injury by microRNA-dependent reprogramming of resident renal cells. *Kidney Int*. 82:412-427.

Casado, S., M. Lobo, and C.L. Paino. 2017. Dynamics of plasma membrane surface related to the release of extracellular vesicles by mesenchymal stem cells in culture. *Sci Rep*. 7:6767.

Cheng, L., W. Zhao, and A.F. Hill. 2018. Exosomes and their role in the intercellular trafficking of normal and disease associated prion proteins. *Mol Aspects Med*. 60:62-68.

Colombo, M., G. Raposo, and C. Thery. 2014. Biogenesis, secretion, and intercellular interactions of exosomes and other extracellular vesicles. *Annu Rev Cell Dev Biol*. 30:255-289.

Crenshaw, B.J., L. Gu, B. Sims, and Q.L. Matthews. 2018. Exosome Biogenesis and Biological Function in Response to Viral Infections. *Open Virol J*. 12:134-148.

Daaboul, G.G., D.S. Freedman, S.M. Scherr, E. Carter, A. Rosca, D. Bernstein, C.E. Mire, K.N. Agans, T. Hoenen, T.W. Geisbert, M.S. Unlu, and J.H. Connor. 2017. Enhanced light

microscopy visualization of virus particles from Zika virus to filamentous ebolaviruses. *PLoS One*. 12:e0179728.

Daaboul, G.G., P. Gagni, L. Benussi, P. Bettotti, M. Ciani, M. Cretich, D.S. Freedman, R. Ghidoni, A.Y. Ozkumur, C. Piotto, D. Prosperi, B. Santini, M.S. Unlu, and M. Chiari. 2016. Digital Detection of Exosomes by Interferometric Imaging. *Sci Rep*. 6:37246.

Desrochers, L.M., M.A. Antonyak, and R.A. Cerione. 2016. Extracellular Vesicles: Satellites of Information Transfer in Cancer and Stem Cell Biology. *Dev Cell*. 37:301-309.

Escola, J.M., M.J. Kleijmeer, W. Stoorvogel, J.M. Griffith, O. Yoshie, and H.J. Geuze. 1998. Selective enrichment of tetraspan proteins on the internal vesicles of multivesicular endosomes and on exosomes secreted by human B-lymphocytes. *J Biol Chem*. 273:20121-20127.

Fang, Y., N. Wu, X. Gan, W. Yan, J.C. Morrell, and S.J. Gould. 2007. Higher-order oligomerization targets plasma membrane proteins and HIV gag to exosomes. *PLoS Biol*. 5:e158.

Fordjour, F.K., S. Owiredu, H. Muendlein, J. Plange, J.C. Morrell, J. Han, and S.J. Gould. 2016. Creation of CD63-deficient HEK293 cell lines using a polycistronic CAS9/EGFP/HSVtk/PuroR expression vector. *Matters*

.

Gilligan, K.E., and R.M. Dwyer. 2017. Engineering Exosomes for Cancer Therapy. *Int J Mol Sci*. 18.

Gould, S.J., A.M. Booth, and J.E. Hildreth. 2003. The Trojan exosome hypothesis. *Proc Natl Acad Sci U S A*. 100:10592-10597.

Gould, S.J., G.A. Keller, N. Hosken, J. Wilkinson, and S. Subramani. 1989. A conserved tripeptide sorts proteins to peroxisomes. *J Cell Biol*. 108:1657-1664.

Gould, S.J., and G. Raposo. 2013. As we wait: coping with an imperfect nomenclature for extracellular vesicles. *J Extracell Vesicles*. 2.

Harding, C., J. Heuser, and P. Stahl. 1983. Receptor-mediated endocytosis of transferrin and recycling of the transferrin receptor in rat reticulocytes. *J Cell Biol*. 97:329-339.

Harding, C., J. Heuser, and P. Stahl. 1984. Endocytosis and intracellular processing of transferrin and colloidal gold-transferrin in rat reticulocytes: demonstration of a pathway for receptor shedding. *Eur J Cell Biol*. 35:256-263.

Horwich, A.L., F. Kalousek, I. Mellman, and L.E. Rosenberg. 1985. A leader peptide is sufficient to direct mitochondrial import of a chimeric protein. *EMBO J*. 4:1129-1135.

Jia, S., D. Zocco, M.L. Samuels, M.F. Chou, R. Chammas, J. Skog, N. Zarovni, F. Momen-Heravi, and W.P. Kuo. 2014. Emerging technologies in extracellular vesicle-based molecular diagnostics. *Expert Rev Mol Diagn*. 14:307-321.

Kalderon, D., B.L. Roberts, W.D. Richardson, and A.E. Smith. 1984. A short amino acid sequence able to specify nuclear location. *Cell*. 39:499-509.

Kamerkar, S., V.S. LeBleu, H. Sugimoto, S. Yang, C.F. Ruivo, S.A. Melo, J.J. Lee, and R. Kalluri. 2017. Exosomes facilitate therapeutic targeting of oncogenic KRAS in pancreatic cancer. *Nature*. 546:498-503.

Li, J., X. Chen, J. Yi, Y. Liu, D. Li, J. Wang, D. Hou, X. Jiang, J. Zhang, J. Wang, K. Zen, F. Yang, C.Y. Zhang, and Y. Zhang. 2016. Identification and Characterization of 293T Cell-Derived Exosomes by Profiling the Protein, mRNA and MicroRNA Components. *PLoS One*. 11:e0163043.

Li, L., K. Piontek, M. Ishida, M. Fausther, J.A. Dranoff, R. Fu, E. Mezey, S.J. Gould, F.K. Fordjour, S.J. Meltzer, A.E. Sirica, and F.M. Selaru. 2017. Extracellular vesicles carry microRNA-195 to intrahepatic cholangiocarcinoma and improve survival in a rat model. *Hepatology*. 65:501-514.

Lindenbergh, M.F.S., and W. Stoorvogel. 2018. Antigen Presentation by Extracellular Vesicles from Professional Antigen-Presenting Cells. *Annu Rev Immunol*. 36:435-459.

Mathew, A., A. Bell, and R.M. Johnstone. 1995. Hsp-70 is closely associated with the transferrin receptor in exosomes from maturing reticulocytes. *Biochem J*. 308 (Pt 3):823-830.

Mathieu, M., L. Martin-Jaular, G. Lavieu, and C. Thery. 2019. Specificities of secretion and uptake of exosomes and other extracellular vesicles for cell-to-cell communication. *Nat Cell Biol*. 21:9-17.

McGough, I.J., and J.P. Vincent. 2016. Exosomes in developmental signalling. *Development*. 143:2482-2493.

Nkwe, D.O., A. Pelchen-Matthews, J.J. Burden, L.M. Collinson, and M. Marsh. 2016. The intracellular plasma membrane-connected compartment in the assembly of HIV-1 in human macrophages. *BMC Biol*. 14:50.

Pan, B.T., and R.M. Johnstone. 1983. Fate of the transferrin receptor during maturation of sheep reticulocytes in vitro: selective externalization of the receptor. *Cell*. 33:967-978.

Pastuzyn, E.D., C.E. Day, R.B. Kearns, M. Kyrke-Smith, A.V. Taibi, J. McCormick, N. Yoder, D.M. Belnap, S. Erlendsson, D.R. Morado, J.A.G. Briggs, C. Feschotte, and J.D. Shepherd. 2018. The Neuronal Gene Arc Encodes a Repurposed Retrotransposon Gag Protein that Mediates Intercellular RNA Transfer. *Cell*. 172:275-288 e218.

Pegtel, D.M., and S.J. Gould. 2019. Exosomes. *Annu Rev Biochem*. 88:in press.

Pelchen-Matthews, A., S. Giese, P. Mlcochova, J. Turner, and M. Marsh. 2012. beta2 integrin adhesion complexes maintain the integrity of HIV-1 assembly compartments in primary macrophages. *Traffic*. 13:273-291.

Phinney, D.G., and M.F. Pittenger. 2017. Concise Review: MSC-Derived Exosomes for Cell-Free Therapy. *Stem Cells*. 35:851-858.

Sevcsik, E., M. Brameshuber, M. Folser, J. Weghuber, A. Honigmann, and G.J. Schutz. 2015. GPI-anchored proteins do not reside in ordered domains in the live cell plasma membrane. *Nat Commun*. 6:6969.

Sevcsik, E., and G.J. Schutz. 2016. With or without rafts? Alternative views on cell membranes. *Bioessays*. 38:129-139.

Sevenler, D., O. Avci, and M.S. Unlu. 2017. Quantitative interferometric reflectance imaging for the detection and measurement of biological nanoparticles. *Biomed Opt Express*. 8:2976-2989.

Sevenler, D., G.G. Daaboul, F. Ekiz Kanik, N.L. Unlu, and M.S. Unlu. 2018. Digital Microarrays: Single-Molecule Readout with Interferometric Detection of Plasmonic Nanorod Labels. *ACS Nano*.

Shen, B., Y. Fang, N. Wu, and S.J. Gould. 2011a. Biogenesis of the posterior pole is mediated by the exosome/microvesicle protein-sorting pathway. *J Biol Chem*. 286:44162-44176.

Shen, B., N. Wu, J.M. Yang, and S.J. Gould. 2011b. Protein targeting to exosomes/microvesicles by plasma membrane anchors. *J Biol Chem*. 286:14383-14395.

Specht, E.A., E. Braselmann, and A.E. Palmer. 2017. A Critical and Comparative Review of Fluorescent Tools for Live-Cell Imaging. *Annu Rev Physiol*. 79:93-117.

Sung, B.H., T. Ketova, D. Hoshino, A. Zijlstra, and A.M. Weaver. 2015. Directional cell movement through tissues is controlled by exosome secretion. *Nat Commun*. 6:7164.

Thery, C., A. Regnault, J. Garin, J. Wolfers, L. Zitvogel, P. Ricciardi-Castagnoli, G. Raposo, and S. Amigorena. 1999. Molecular characterization of dendritic cell-derived exosomes. Selective accumulation of the heat shock protein hsc73. *J Cell Biol*. 147:599-610.

Thery, C., K.W. Witwer, E. Aikawa, M.J. Alcaraz, J.D. Anderson, R. Andriantsitohaina, A. Antoniou, T. Arab, F. Archer, G.K. Atkin-Smith, D.C. Ayre, J.M. Bach, D. Bachurski, H. Baharvand, L. Balaj, S. Baldacchino, N.N. Bauer, A.A. Baxter, M. Bebawy, C. Beckham, A. Bedina Zavec, A. Benmoussa, A.C. Berardi, P. Bergese, E. Bielska, C. Blenkiron, S. Bobis-Wozowicz, E. Boilard, W. Boireau, A. Bongiovanni, F.E. Borras, S. Bosch, C.M. Boulanger, X. Breakefield, A.M. Breglio, M.A. Brennan, D.R. Brigstock, A. Brisson, M.L. Broekman, J.F. Bromberg, P. Bryl-Gorecka, S. Buch, A.H. Buck, D. Burger, S. Busatto, D. Buschmann, B. Bussolati, E.I. Buzas, J.B. Byrd, G. Camussi, D.R. Carter, S. Caruso, L.W. Chamley, Y.T. Chang, C. Chen, S. Chen, L. Cheng, A.R. Chin, A. Clayton, S.P. Clerici, A. Cocks, E. Cocucci, R.J. Coffey, A. Cordeiro-da-Silva, Y. Couch, F.A. Coumans, B. Coyle, R. Crescitelli, M.F. Criado, C. D'Souza-Schorey, S. Das, A. Datta Chaudhuri, P. de Candia, E.F. De Santana, O. De Wever, H.A. Del Portillo, T. Demaret, S. Deville, A. Devitt, B. Dhondt, D. Di Vizio, L.C. Dieterich, V. Dolo, A.P. Dominguez Rubio, M. Dominici, M.R. Dourado, T.A. Driedonks, F.V. Duarte, H.M. Duncan, R.M. Eichenberger, K. Ekstrom, S. El Andaloussi, C. Elie-Caille, U. Erdbrugger, J.M. Falcon-Perez, F. Fatima, J.E. Fish, M. Flores-Bellver, A. Forsonits, A. Frelet-Barrand, et al. 2018. Minimal information for studies of extracellular vesicles 2018 (MISEV2018): a position statement

of the International Society for Extracellular Vesicles and update of the MISEV2014 guidelines. *J Extracell Vesicles*. 7:1535750.

Trams, E.G., C.J. Lauter, N. Salem, Jr., and U. Heine. 1981. Exfoliation of membrane ecto-enzymes in the form of micro-vesicles. *Biochim Biophys Acta*. 645:63-70.

Traub, L.M., and J.S. Bonifacino. 2013. Cargo recognition in clathrin-mediated endocytosis. *Cold Spring Harb Perspect Biol*. 5:a016790.

van Dongen, H.M., N. Masoumi, K.W. Witwer, and D.M. Pegtel. 2016. Extracellular Vesicles Exploit Viral Entry Routes for Cargo Delivery. *Microbiol Mol Biol Rev*. 80:369-386.

van Niel, G., G. D'Angelo, and G. Raposo. 2018. Shedding light on the cell biology of extracellular vesicles. *Nat Rev Mol Cell Biol*. 19:213-228.

Verweij, F.J., M.P. Bebelman, C.R. Jimenez, J.J. Garcia-Vallejo, H. Janssen, J. Neefjes, J.C. Knol, R. de Goeij-de Haas, S.R. Piersma, S.R. Baglio, M. Verhage, J.M. Middeldorp, A. Zomer, J. van Rheenen, M.G. Coppolino, I. Hurbain, G. Raposo, M.J. Smit, R.F.G. Toonen, G. van Niel, and D.M. Pegtel. 2018. Quantifying exosome secretion from single cells reveals a modulatory role for GPCR signaling. *J Cell Biol*. 217:1129-1142.

Yim, N., S.W. Ryu, K. Choi, K.R. Lee, S. Lee, H. Choi, J. Kim, M.R. Shaker, W. Sun, J.H. Park, D. Kim, W.D. Heo, and C. Choi. 2016. Exosome engineering for efficient intracellular delivery of soluble proteins using optically reversible protein-protein interaction module. *Nat Commun*. 7:12277.

Chapter 3: *Trans*-acting factors involved in exosome biogenesis

Sections of this chapter are derived from:

Francis K Fordjour, Shawn Owiredu, Hayley Muendlein, Jerry Plange, James Morrell, Jingnan Han, Stephen J Gould. Creation of CD63-deficient HEK293 cell lines using a polycistronic CAS9/EGFP/HSVtk/PuroR expression vector. Journal Article published 21 Apr 2016 in Matters (Zürich). doi:10.19185/matters.201604000004

Abstract

Genetic analysis of a cell biological process presumes that the process occurs at a relatively constant steady state in the parental cell line, as it allows one to associate changes in the process (or lack thereof) to the loss of one or more specific genes and gene functions. Using HEK293 cells as our 'parental' human cell line, we used Cas9/sgRNA-based mutagenesis technology to generate null mutants in genes encoding (a) common exosomal protein cargoes (e.g. CD9, CD63, CD81, etc.) and (b) proteins thought to be involved in exosome biogenesis (e.g. Alix, syntenin). Our results demonstrate that cell lines lacking these (and other factors) showed no significant decrease in exosome concentration and the vesicular budding of known exosomal cargo proteins. However, we also observed significant clone-to-clone variability in the relative budding of several exosomal cargo proteins. Given that the high frequency with which we observed this 'enhanced exosome production' phenotype was inconsistent with its being caused by either the introduced mutations, or of Cas9-induced second-site mutations, we tested whether the parental HEK293 cell line contained cells that varied significantly in exosome biogenesis. It did, as different single-cell clones (SCCs) derived from unmutated HEK293 cells varied up to 5-fold in exosome biogenesis. These high-producing (HP) and low-producing (LP) phenotypes were semi-stable over period of up to 2 months in culture. However, when we generated a new round of SCCs from the cloned HP and LP derivatives of HEK293 cells, we observed significant variations in exosome production between clones. To test whether the secondary clones were stable or whether the heterogeneity breeds through, we single cell cloned the secondary clones and noticed significant variations in exosome production. We further observed that this phenotype was not peculiar to HEK293 as wildtype 293T, K562, LX-2, HAP1 and WA09 hESC showed significant heterogeneity in exosome production when single cell cloned. These results indicate that the relative rate of exosome

production can vary significantly in the absence of mutagenesis and be inadvertently exposed during the isolation of SCCs. The mechanistic basis of this semi-stable phenotype switching remains to be determined.

Introduction

Exosomes are small membrane bound organelles that are released from the plasma and endosome membranes of eukaryotic cells(Pegtel and Gould, 2019). These vesicles are enriched for proteins, lipids, carbohydrates and nuclei acids and have the same topology as the cell. Exosomes have been shown to play important roles in a number of physiological and pathological processes but the mechanisms by which they are made are not fully understood.

Several genes/proteins have been reported to have some sort of influence on EV biogenesis(Baietti et al., 2012; Colombo et al., 2013; Ghossoub et al., 2014; Ostrowski et al., 2010; Perez-Hernandez et al., 2013; Roucourt et al., 2015; Savina et al., 2002; Trajkovic et al., 2008). Most of these studies have not employed cell lines lacking the gene of interest, and the results have instead been based on addition of chemical inhibitors, overexpression of dominant negative proteins, or gene silencing techniques using transfected siRNAs and/or shRNA expression vectors. Another complication of these studies is that they have been performed in a wide array of cell lines with no systematic analysis of all genes in a single experimental system.

In this paper, we improve our mechanistic understanding of exosome biogenesis using the CRISPR (Clustered Regulatory Interspaced Short Palindromic Repeats)/Cas9 technology in a defined system (HEK293) to generate null mutants of candidate genes that have been implicated in exosome biogenesis. We then assessed their effects on the budding of exosomal marker proteins, primarily CD63, CD81, and CD9.

The CRISPR/Cas9 technology is an RNA-dependent DNA endonucleases system for genome editing(Cong et al., 2013; Mali et al., 2013). Typically, a type II CRISPR system functions by the CRISPR RNA (crRNA) interacting with a trans-activating crRNA (tracrRNA) to form a crRNA:tracrRNA duplex [this RNA duplex could be replaced with a single guide RNA (sgRNA)], which directs Streptococcus pyogenes Cas9 (SpyCas9) to specific sites, thereby generating a DNA strand break(Jinek et al., 2012). This break is then repaired in an error prone non-homologous end joining resulting in an insertion and /or deletion; when a template is introduced to the area of breakage, a homology directed repair could be achieved(Aird et al., 2018).

Results & Discussion

Creating plasmids to target specific genes implicated in exosome biogenesis

As discussed in Fordjour et al. 2016, we designed a base plasmid for generating Cas9-induced mutations. This plasmid expresses (a) two sgRNAs from the PolIII 7sk(Murphy et al., 1986) and H1(Baer et al., 1990) promoters, and (b) a large, polycistronic ORF from the CMV promoter that encodes Cas9-3xNLS(Cong et al., 2013), EGFP(Zhang et al., 1996), HSV-TK(McKnight, 1980), and Puro(Vara et al., 1985), each separated by the p2a peptide(Kim et al., 2011) to mediate their release as separate polypeptides (Fig. 1). The rationale for expressing two sgRNAs/gene is that it should (a) induce deletions between the two targeting sites, and (b) allow for mutations at one site if the sgRNA targeting the other site is ineffective. To generate mutants in a particular gene, we altered the base plasmid by inserting gene-specific sequences that direct the two sgRNAs to two different sites in the target gene. For CD9, we designed the sgRNAs targeting exons 1 and 3, and exons 2 and 3 for CD81. We targeted exons 1 and 8 in Alix gene, and exons 2 and 3 of syntenin.

Generating null mutant cell lines

We generated cell lines lacking the classical exosomal markers and other putative cargoes using the protocol described in Fordjour et al., 2016. Specifically, we transfected HEK293 cells with the expressing plasmid, selected in media containing puromycin after 48 hours, and expanded them into single cell clones. We screened single cell clones emerging from this process first by immunoblot (IB), to identify SCCs lacking expression of the protein (Figure 2). We then determined the mutations at each allele in cell lines by isolating genomic DNA, performing PCR using primers specific to the targeted exons, generating multiple subclones from each PCR reaction product, and sequencing multiple independent gDNA amplification products. Our mutational analysis is shown on Table 1. Consistent with our preselection for SCCs that lack cross-reactive material (CRM), we found that most of the targeted alleles contained short indels resulting in non-sense, frameshift, or splice site mutations that are predicted to inactivate the allele through a combination of non-functional ORF, nonsense mediated RNA decay and/or protein instability(Kurosaki and Maquat, 2016).

Loss of CD63, CD9 or CD81 does not cause a defect in budding of classical exosomal markers

To test whether the loss of CD63, CD9 or CD81inhibits the budding of exosomal marker proteins, we measured the relative budding of endogenously expressed, highly enriched exosomal cargo proteins by immunoblot (IB) analysis. Specifically, we collected cell and exosome fractions from each mutant cell lines, used IB to measure the level of each marker in cell and exosome samples, and calculated the relative budding of each marker in the knockout cell line by dividing the amount in the exosome fraction by the sum of the amount in cell and exosome fractions. Our results demonstrate robust budding of these markers in each mutant, and no significant difference from

the amount of budding detected in the parental HEK293 cell line (Figure 3). Interestingly, observed a variable increase in exosomal marker protein budding in selected knockout clones. For example, in Figure 4, we observed a significantly higher relative budding of CD9 and CD81 in 3 out of 4 HEKCD63KO mutant clones. Due to the significant differences in budding of classic markers between clones of the same mutant cell lines, we do not think the enhanced budding is a result of the absence of gene.

Exosome biogenesis is unaffected by the loss of CD63, CD9, or CD81

To determine whether the loss of CD63, CD81 or CD9 affects the budding of vesicles in HEK293 cells, we cultured cells in DMEM+10% Exo-free FBS for 3 days and isolated the exosomes by ultracentrifugation. We then measured the concentration of exosomes using the Particle Metrix ZetaView Nanoparticle Tracking device(Dragovic et al., 2011). This instrument captures the Brownian motion of vesicles in a video, and its concentration is calculated from analyzing the video frames for observed vesicle numbers and then normalizing to the volume loaded and cell count(Gercel-Taylor et al., 2012). We did not observe any significant differences in the concentration of vesicles isolated from HEK293 cells lacking CD63, CD81 or CD9 to vesicles from wildtype HEK293 (Figure 5).

Budding of exogenous AcylTyA is not affected by the loss of classical exosomal markers

To investigate whether the loss of CD63, CD9 or CD81 had any effect on the budding of other exosomal proteins, we expressed AcylTyANeonGreen (AcylTyAmNG), a synthetic exosomal cargo, in parental and mutant cells lacking CD63, CD81 or CD9 by transfecting these cells with an expression vector and selecting for transgenic cell lines by addition of antibiotic. IB analysis

revealed that the exosomal secretion of AcylTyAmNG was not reduced by loss of CD63, CD9, or CD81. In fact, we noticed a higher relative budding of this exosomal marker protein in both HEK293CD63KO and HEK293CD81KO mutant cells compared to parental HEK293 cells (Figure 6).

Unmutated HEK293 cell display significant heterogeneity in budding when single cell clone

We hypothesized that the random elevations in budding which we observed in some clones of the mutant cell lines were as a result of the parental cell line having a heterogenous population of cells. To test this hypothesis, we single cell cloned wildtype HEK293 and measured the relative budding of CD63 by immunoblot. We observed that the relative budding of CD63 varied from one clone to another even in the absence of mutagenesis (Figure 7). To test if a single clone is stable and can generate a homogenous population, we sub-cloned one of the high exosome producing cell (HXP) (Figure 8a) and one low exosome producing cell (LXP) (Figure 8b). We observed the new clones whether from the HXP or LXP had different relative budding. We however noticed that majority of the clones from the HXP were still high exosomes producers and a high frequency of the clones from the LXP still had low relative budding of CD63. We generated tertiary clones from the one of HXP and LXP subclones, and observed the same phenotype (Figure 9a & 9b). We concluded that single cell cloning exposes heterogeneity in budding of cargoes even in the absence of mutagenesis. To investigate if there were other cell lines which we could get a homogenous population of cell for our work, we generated multiple single cell clones (SCCs) of K562 (Figure 10a), HAP1 (Figure 10b), LX-2 and human embryonic stem cell line WA09 (Figure 11). In each case, we identified SCCs that displayed pronounced cone-to-clone heterogeneity in exosome biogenesis, indicating that all human cell lines tested display clonal heterogeneity, making a

genetic analysis of exosome biogenesis difficult to achieve through standard approaches.

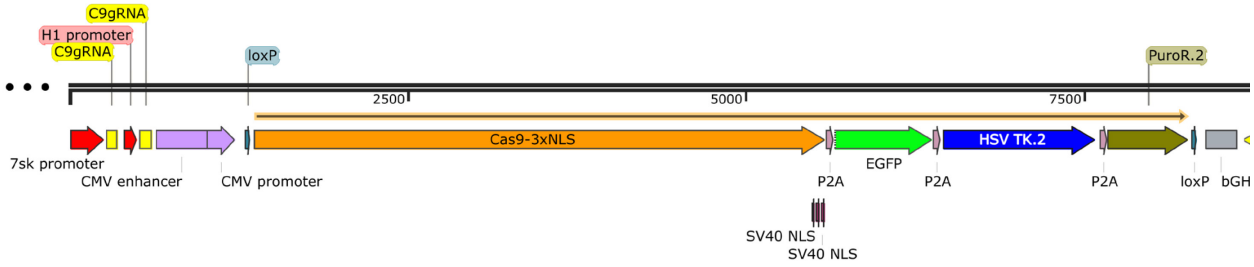

Figure 1: *Plasmid map*. The two guide RNAs (yellow) are designed to be expressed from the 7sk and H1 PolIII promoters marked in red arrow. The CMV promoter (purple) drives expression of a single long ORF (yellow/black line) that encodes Cas9-3xNLS (orange), EGFP (bright green), HSV-tk (blue) and Puro (olive green) each separated by p2a peptide to mediate their release as separate polypeptides. The ORF is flanked by loxP sites so can be excised with Cre.

Clone	Allele	Mutational Analysis
CD81-1	1	deletion between exon 2 and 3, 139bp deletion in ORF, frameshift
CD81-1	2	1 bp deletion in exon 2, 95 bp deletion in exon 3/intron 3
CD81-4	1	deletion between exon 2 and 3, 139 deletion in ORF, frameshift
CD81-4	2	deletion between exon 2 and 3, 139 deletion in ORF, frameshift
CD81-8	1	1 bp deletion in exon 3
CD81-8	2	in-frame deletion between exon 2 and 3
CD9-2	1	2 nt insertion in exon 1, 4 nt insertion and 27 bp deletion at the 5' end of exon 3
CD9-2	2	58 bp deletion at 3' end of exon 1, 19 bp deletion of 5' end of exon 3 and 109 deletion of exon 2; in-frame
Alix-1	1	85 nt insertion from Chr17 at the first cut site resulting in an in-frame STOP, and 6 nt deletion at the second cut site
Alix-1	2	deletion of 824 bp between exons 1 and 8, frameshift
Alix-4	1	1 nt deletion at the 3' of exon 1, frameshift resulting in a STOP
Alix-4	2	deletion of 824 bp between exons 1 and 8, frameshift
Alix-6	1	58bp insertion from the transfected plasmid includes STOP codon at the first cut site, and 10 nt deletion at the second cut site, frameshift
Alix-6	2	deletion of 824 bp between exons 1 and 8, frameshift
Syntenin-6	1	1 nt deletion in exon 2 and 2 bp insertion in exon 3, frameshift
Syntenin-6	2	7 nt deletion in exon 2 and 102 bp deletion in exon 3, frameshift
Syntenin-14	1	deletion between exon 2 and 5' end of intron 3, insertion of 736 bp
Syntenin-14	2	deletion of 107nt in ORF, frameshift
Syntenin-20	1	deletion between exon 2 and intron 3, insertion of 283bp of intron 2 in an anti-sense orientation
Syntenin-20	2	deletion between exon 2 and 5' end of intron 3, insertion of 736 bp

Table 1: Mutational analysis of each allele of the various mutant clones. Exon-specific PCR was performed on genomic DNA isolated from each mutant cell line. The PCR product was cloned and sequenced.

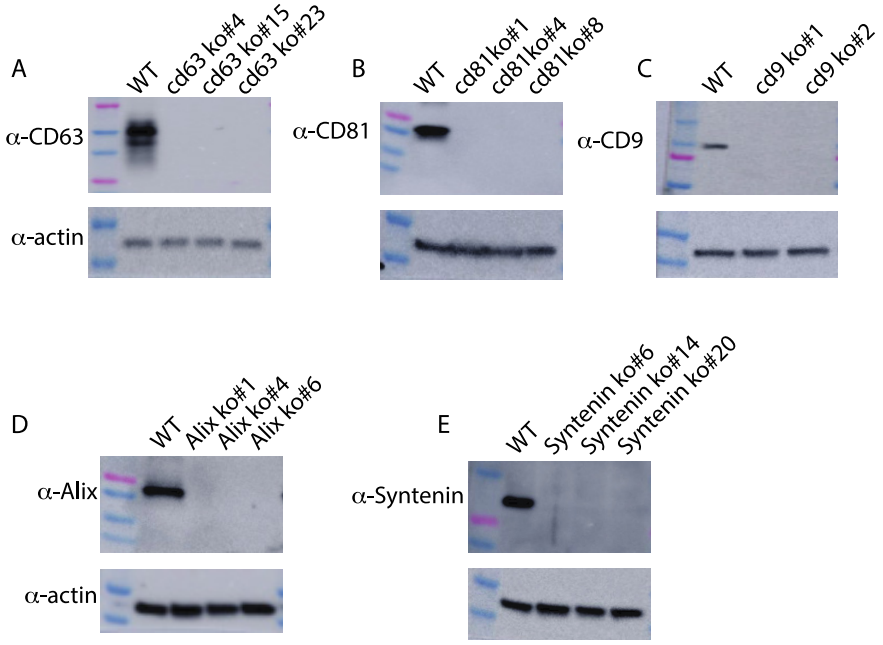

Figure 2: *Generating null mutant cell lines*, Immunoblot analysis of whole-cell protein lysates isolated from multiple independently grown and lysed cultures of HEK293 cells and of SCCs (A) CD63ko-4, -15, -23 blotted with antibodies specific for CD63 and beta-actin. CD63 has a predicted molecular mass of 26 kDa but runs on non-reducing SDS-PAGE gels as a mixture of products of ~35–55 kDa due to heterogeneous glycosylation. In contrast, actin migrates at its predicted molecular mass of 42 kDa. (B) CD81ko-1, -4, -8 blotted with antibodies specific for CD81 and beta-actin. CD81 has a molecular weight of 24kDa. (C) CD9ko-1, and -2 blotted with antibodies specific for (upper panels) CD9 and (lower panels) beta-actin. CD9 has a molecular weight of 24kDa. (D) Alixko-1, -4, -6 blotted with antibodies specific for Alix and beta-actin. Alix has a molecular weight of 96kDa. (E) Syntenінko-6, -14, -20 blotted with antibodies specific for syntenin and beta-actin. CD81 has a molecular weight of 32kDa.

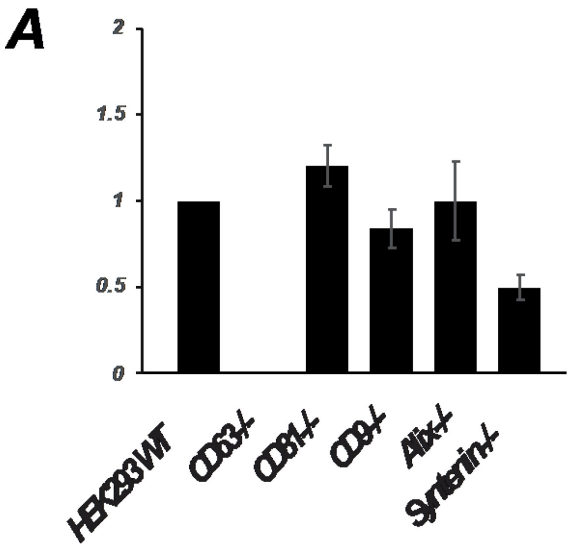
A
2
1.5
1
0.5
0
HEK293WT
CD63-/-
CD81-/-
CD9-/-
Alix-/-
Syntenin-/-

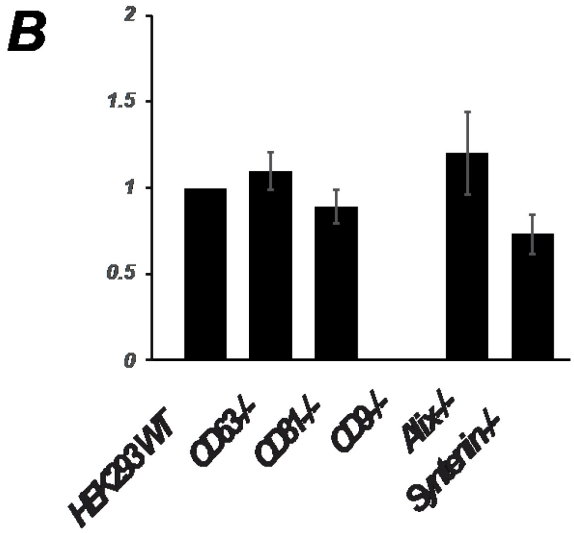
B
2
1.5
1
0.5
0
HEK293WT
CD63-/-
CD81-/-
CD9-/-
Alix-/-
Syntenin-/-

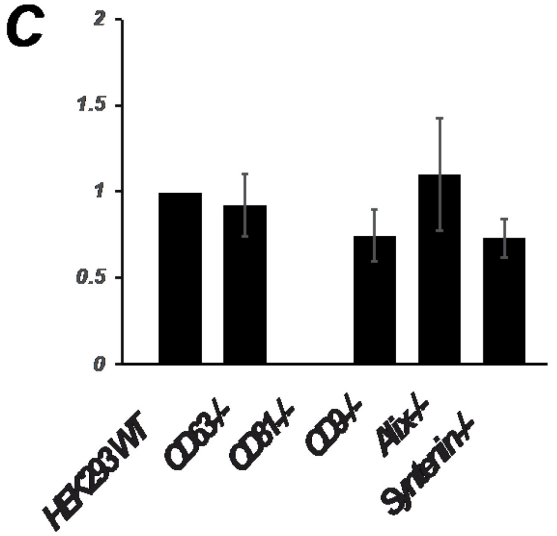
C
2
1.5
1
0.5
0
HEK293WT
CD63-/-
CD81-/-
CD9-/-
Alix-/-
Syntenin-/-

Figure 3: *Relative budding of CD63, CD9 and CD81 in HEK293 and null mutant cell lines*, The bar graphs show the average +/- s.e.m. of the relative budding of (**A**) CD63, (**B**) CD9, and (**C**) CD81 proteins in HEK293 WT, HEK293 CD63$^{-/-}$ (n=23), HEK293 CD81$^{-/-}$ (n=25), HEK293 CD9$^{-/-}$ (n=12), HEK293 Alix$^{-/-}$ (n=9), HEK293 Syntenin$^{-/-}$ (n=9).

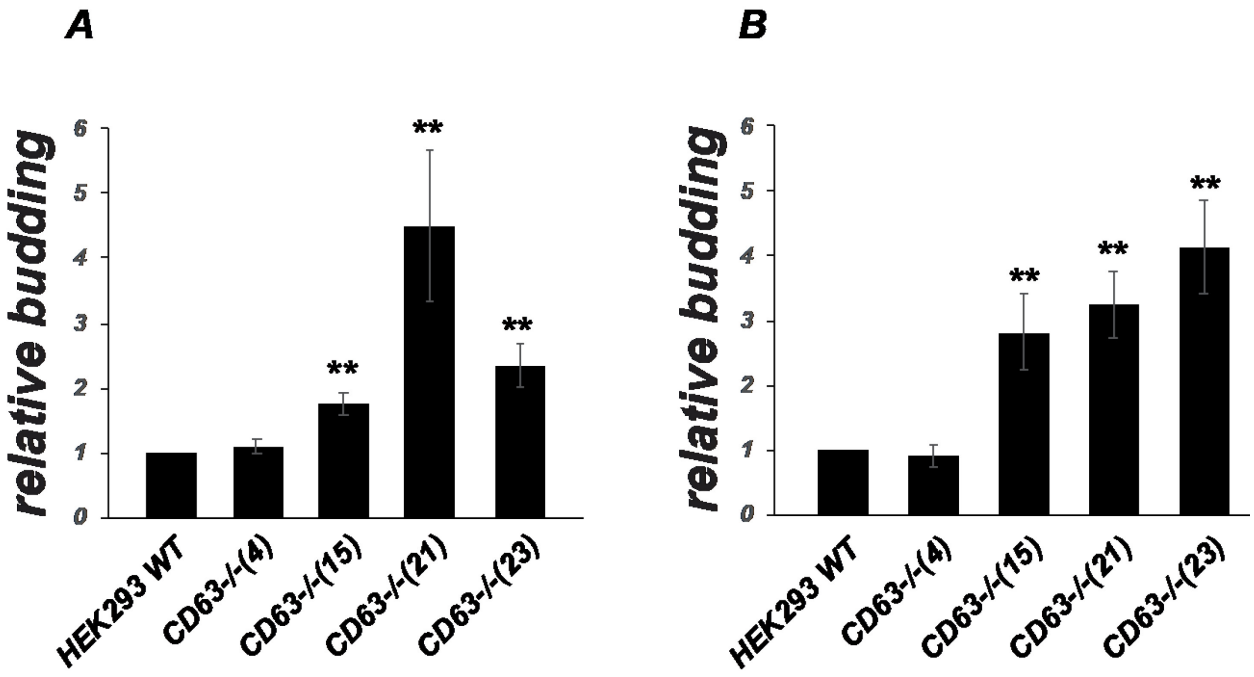

Figure 4: Elevated budding is observed in some mutant clones, The bar graphs show the average +/- s.e.m. of the relative budding of (**A**) CD9 and (**B**) CD81 proteins in HEK293 $CD63^{-/-}$ mutant clones -4, -15, -21 and -23. (n=23) * denotes a *p*-value less than 0.05, ** denotes a *p*-value less than 0.005.

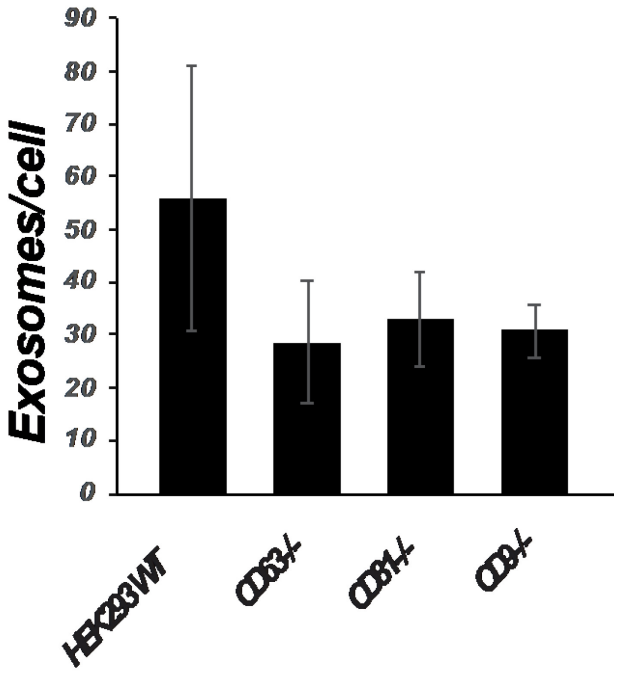

Figure 5: Exosome biogenesis is unaffected by the loss of CD63, CD81 or CD9. The bar graph shows the average +/- s.e.m. number of exosomes per cell of HEK293 WT, HEK293 CD63$^{-/-}$, HEK293 CD81$^{-/-}$, HEK293 CD9$^{-/-}$ (n=6)

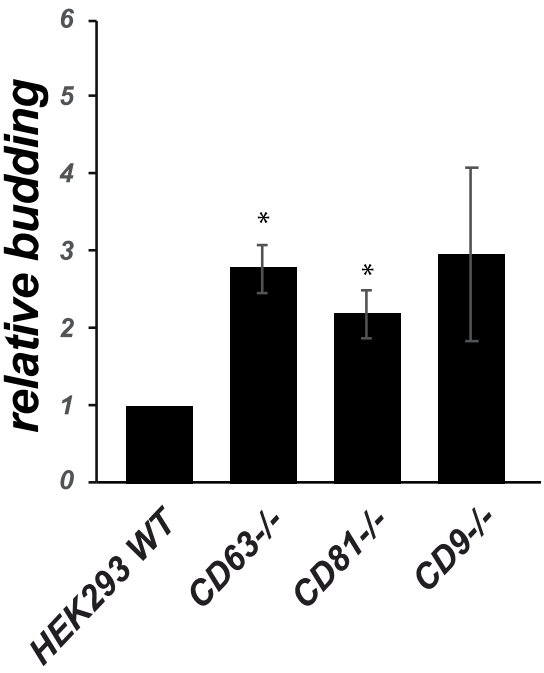

Figure 6: There is no defect in budding of exogenous cargoes. The bar graphs show the average +/- s.e.m. of the relative budding of AcylTyAmNG from HEK293 WT, HEK293 CD63$^{-/-}$, HEK293 CD81$^{-/-}$, HEK293 CD9$^{-/-}$ transfected with an expression vector. * denotes a *p*-value less than 0.05.

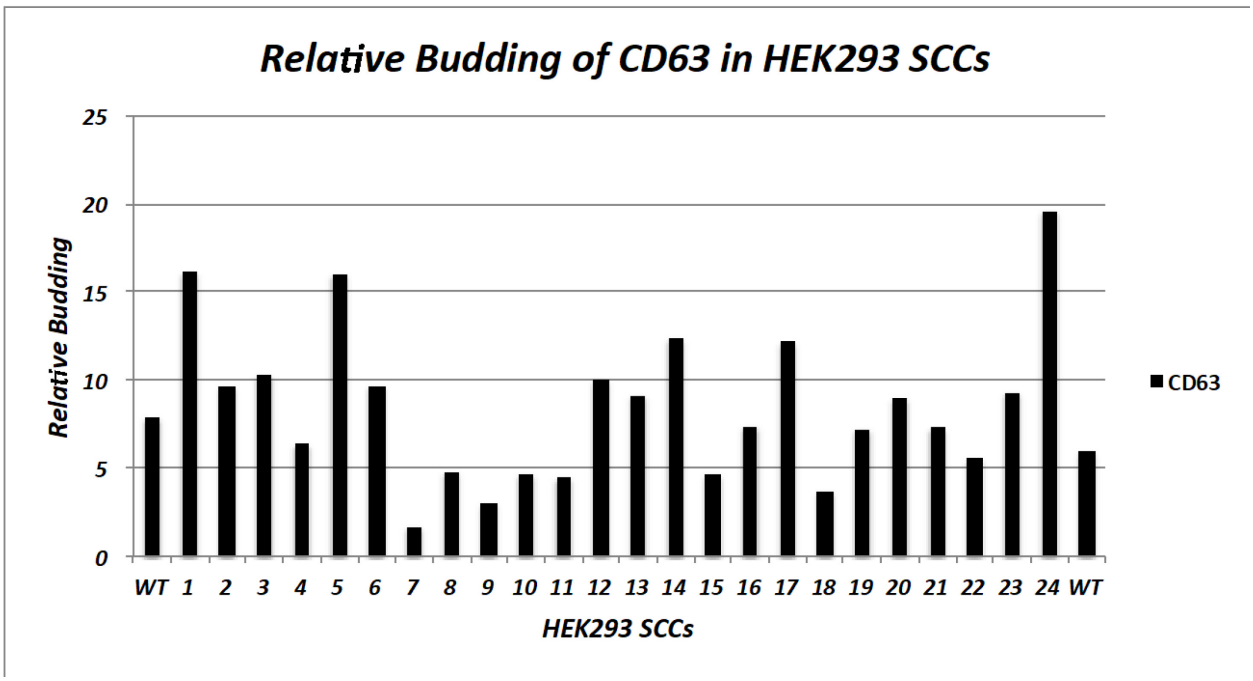

Figure 7: The rate of exosome production varies significantly even in the absence of mutagenesis. Bar graph showing the relative budding of CD63 (measured as percentage of protein in exosomes to the total amount of protein in cell and exosomes) in HEK293 single cell clones.

A

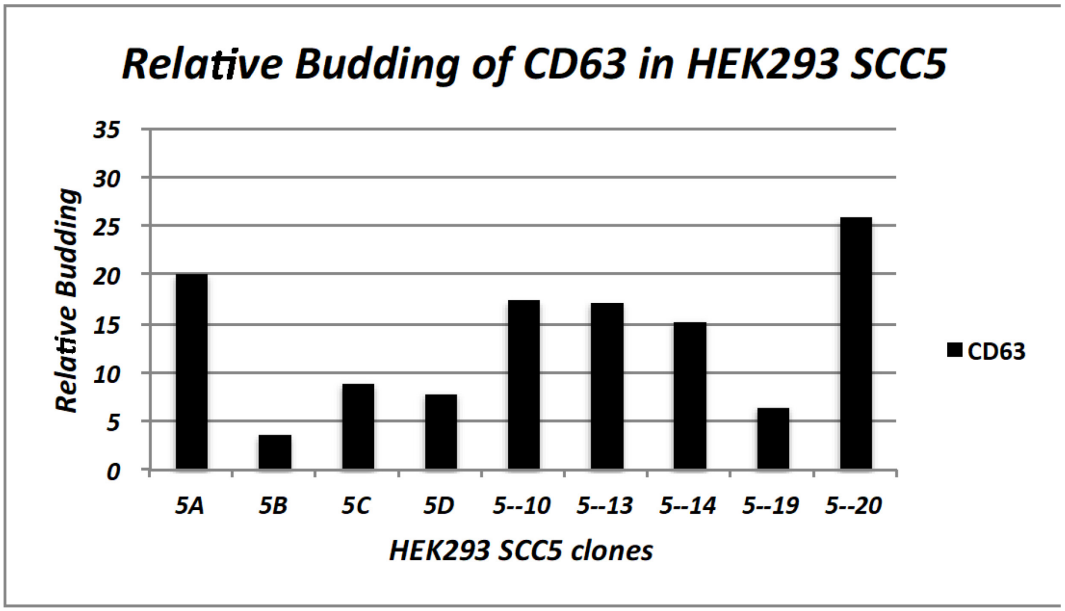

B

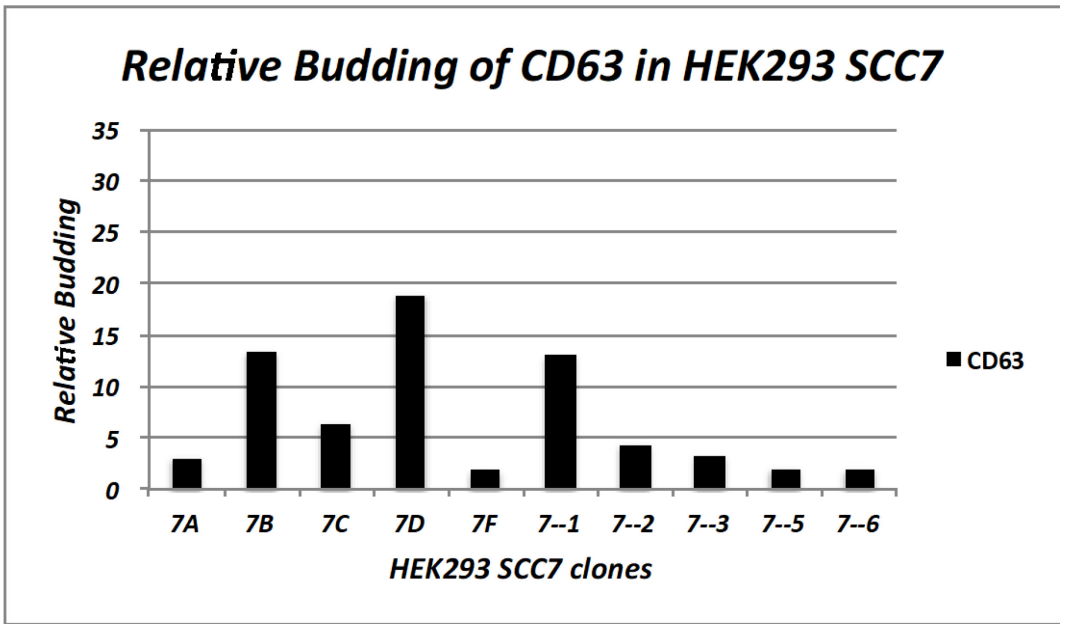

Figure 8: Clonal heterogeneity persists through generations. (A) Bar graph showing the relative budding of CD63 in HEK293 secondary single clones expanded from a primary high exosome producing clone 5 (SCC5), (B) Bar graph showing the relative budding of CD63 in HEK293 secondary single clones expanded from a primary low exosome producing clone 7 (SCC7).

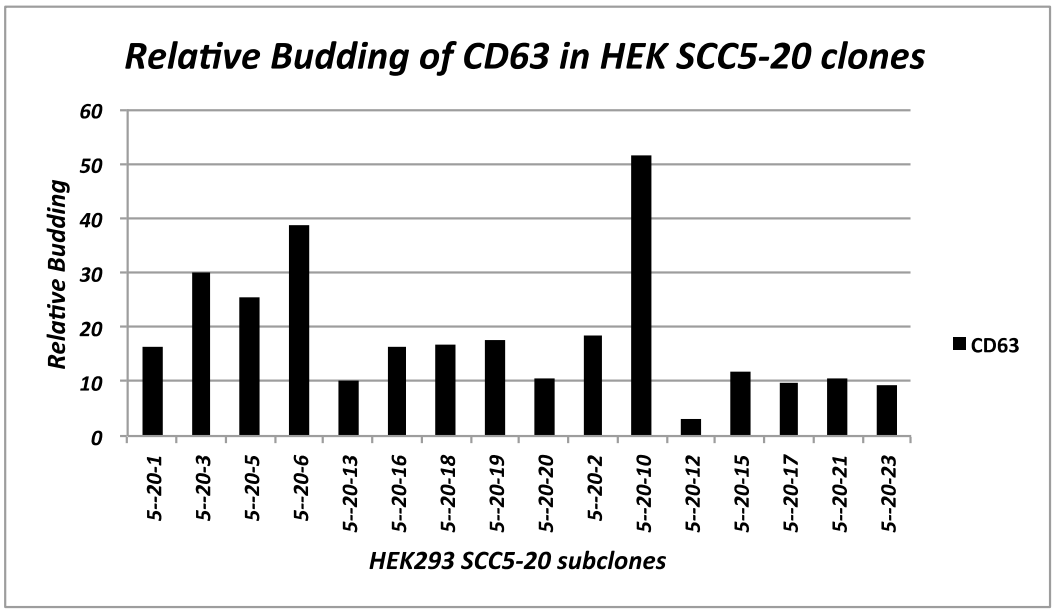

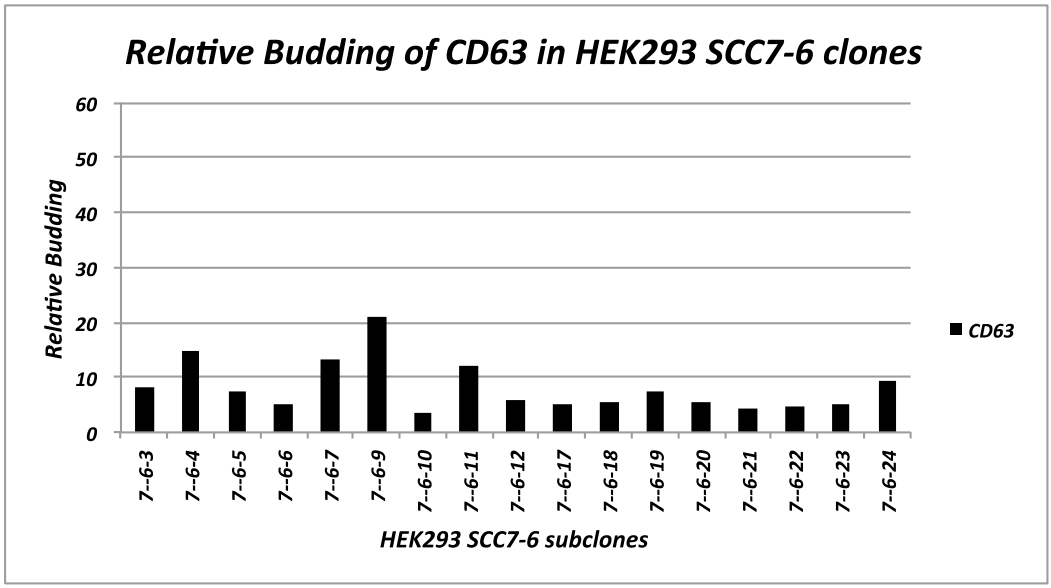

Figure 9: Tertiary clones have varying rates of exosome production. (A), Bar graph showing the relative budding of CD63 in HEK293 tertiary single clones expanded from secondary high exosome producing clone (SCC5-20). (B), Bar graph showing the relative budding of CD63 in HEK293 tertiary single clones expanded from secondary low exosome producing clone (SCC7-6)

A.

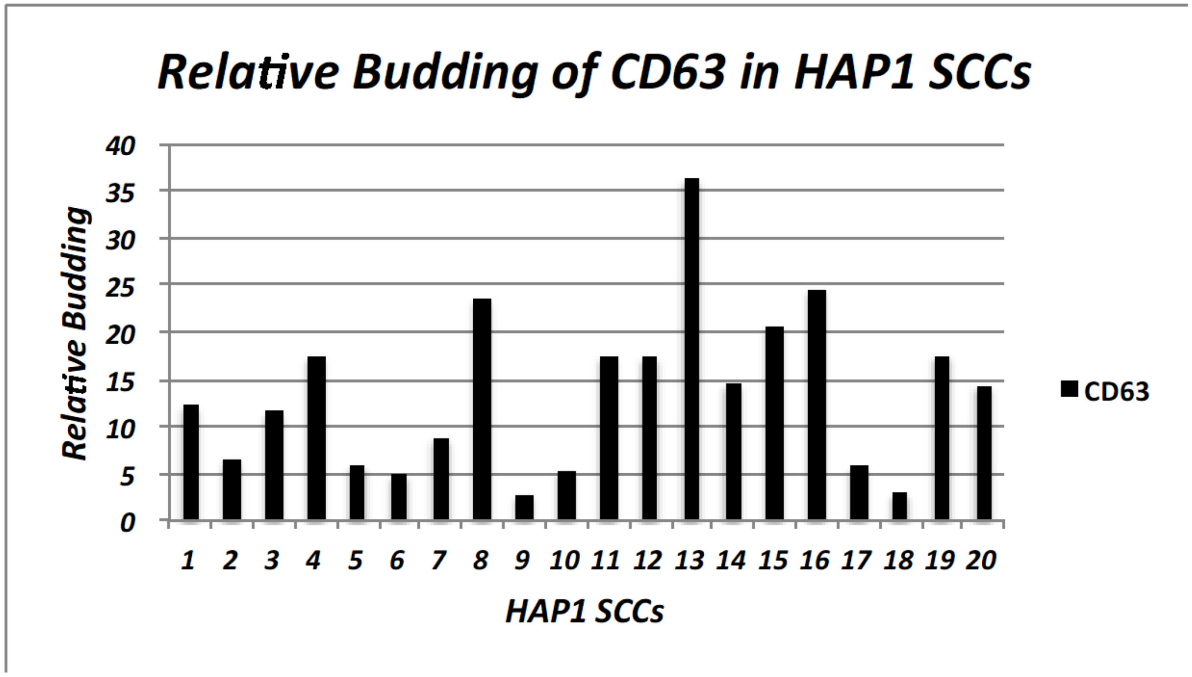

B

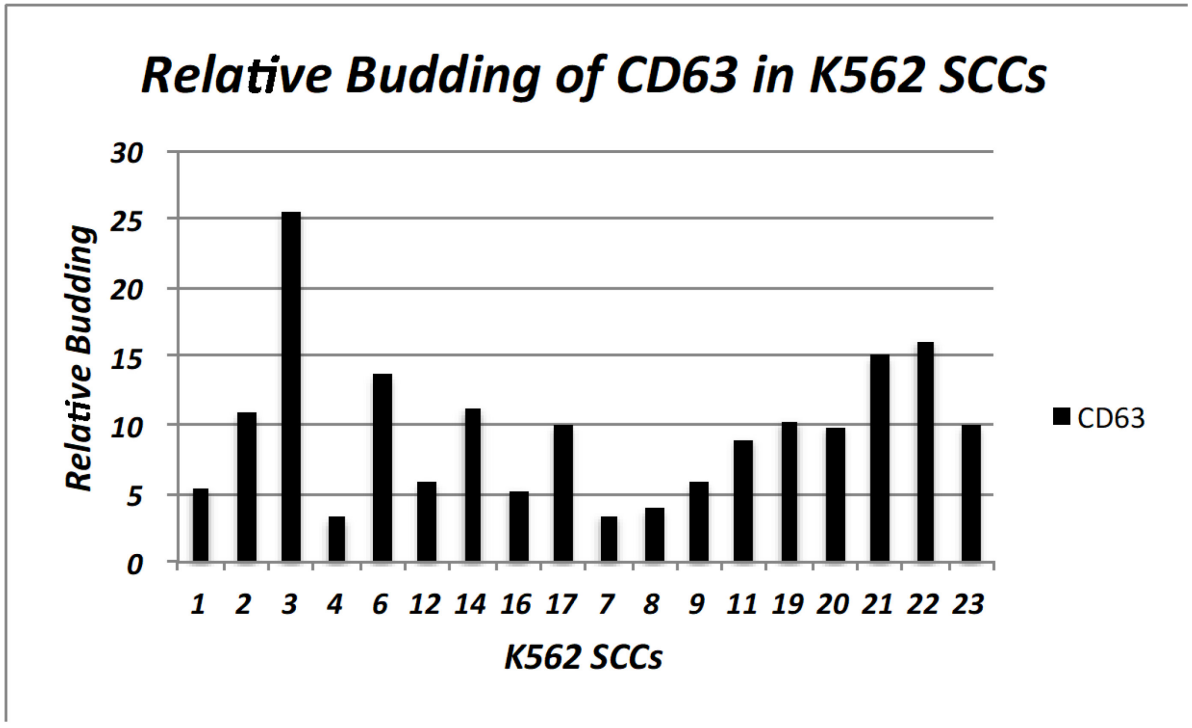

Figure 10: Clonal heterogeneity in exosome biogenesis is observed in multiple cell lines. Bar graph showing the relative budding of CD63 in (A) HAP1 single cell clones, (B) K562 single cell clones

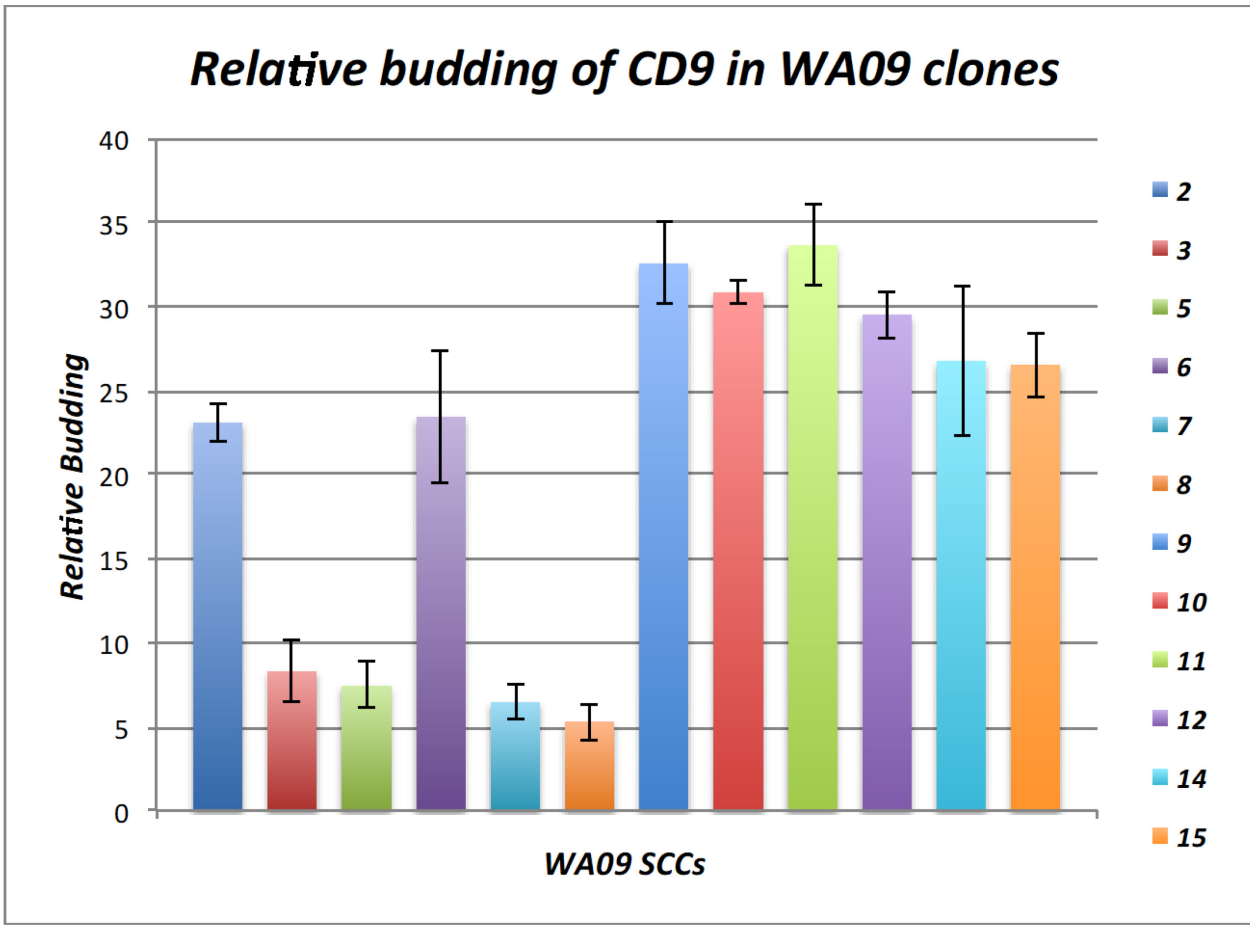

Figure 11: Exosome production varies from clone to clone in stem cells. Bar graph showing the average +/- s.e.m. relative budding of CD63 in single cell clones of human embryonic stem cells WA09.

References

Aird, E.J., Lovendahl, K.N., St Martin, A., Harris, R.S., and Gordon, W.R. (2018). Increasing Cas9-mediated homology-directed repair efficiency through covalent tethering of DNA repair template. Commun Biol *1*, 54.

Baer, M., Nilsen, T.W., Costigan, C., and Altman, S. (1990). Structure and transcription of a human gene for H1 RNA, the RNA component of human RNase P. Nucleic Acids Res *18*, 97-103.

Baietti, M.F., Zhang, Z., Mortier, E., Melchior, A., Degeest, G., Geeraerts, A., Ivarsson, Y., Depoortere, F., Coomans, C., Vermeiren, E*., et al.* (2012). Syndecan-syntenin-ALIX regulates the biogenesis of exosomes. Nat Cell Biol *14*, 677-685.

Colombo, M., Moita, C., van Niel, G., Kowal, J., Vigneron, J., Benaroch, P., Manel, N., Moita, L.F., Thery, C., and Raposo, G. (2013). Analysis of ESCRT functions in exosome biogenesis, composition and secretion highlights the heterogeneity of extracellular vesicles. J Cell Sci *126*, 5553-5565.

Cong, L., Ran, F.A., Cox, D., Lin, S., Barretto, R., Habib, N., Hsu, P.D., Wu, X., Jiang, W., Marraffini, L.A*., et al.* (2013). Multiplex genome engineering using CRISPR/Cas systems. Science *339*, 819-823.

Dragovic, R.A., Gardiner, C., Brooks, A.S., Tannetta, D.S., Ferguson, D.J., Hole, P., Carr, B., Redman, C.W., Harris, A.L., Dobson, P.J*., et al.* (2011). Sizing and phenotyping of cellular vesicles using Nanoparticle Tracking Analysis. Nanomedicine *7*, 780-788.

Fordjour, F.K., S. Owiredu, H. Muendlein, J. Plange, J.C. Morrell, J. Han, and S.J. Gould. 2016. Creation of CD63-deficient HEK293 cell lines using a polycistronic CAS9/EGFP/HSVtk/PuroR expression vector. *Matters*

Gercel-Taylor, C., Atay, S., Tullis, R.H., Kesimer, M., and Taylor, D.D. (2012). Nanoparticle analysis of circulating cell-derived vesicles in ovarian cancer patients. Anal Biochem *428*, 44-53.

Ghossoub, R., Lembo, F., Rubio, A., Gaillard, C.B., Bouchet, J., Vitale, N., Slavik, J., Machala, M., and Zimmermann, P. (2014). Syntenin-ALIX exosome biogenesis and budding into multivesicular bodies are controlled by ARF6 and PLD2. Nat Commun *5*, 3477.

Jinek, M., Chylinski, K., Fonfara, I., Hauer, M., Doudna, J.A., and Charpentier, E. (2012). A programmable dual-RNA-guided DNA endonuclease in adaptive bacterial immunity. Science *337*, 816-821.

Kim, J.H., Lee, S.R., Li, L.H., Park, H.J., Park, J.H., Lee, K.Y., Kim, M.K., Shin, B.A., and Choi, S.Y. (2011). High cleavage efficiency of a 2A peptide derived from porcine teschovirus-1 in human cell lines, zebrafish and mice. PLoS One *6*, e18556.

Kurosaki, T., and Maquat, L.E. (2016). Nonsense-mediated mRNA decay in humans at a glance. J Cell Sci *129*, 461-467.

Mali, P., Yang, L., Esvelt, K.M., Aach, J., Guell, M., DiCarlo, J.E., Norville, J.E., and Church, G.M. (2013). RNA-guided human genome engineering via Cas9. Science *339*, 823-826.

McKnight, S.L. (1980). The nucleotide sequence and transcript map of the herpes simplex virus thymidine kinase gene. Nucleic Acids Res *8*, 5949-5964.

Murphy, S., Tripodi, M., and Melli, M. (1986). A sequence upstream from the coding region is required for the transcription of the 7SK RNA genes. Nucleic Acids Res *14*, 9243-9260.

Ostrowski, M., Carmo, N.B., Krumeich, S., Fanget, I., Raposo, G., Savina, A., Moita, C.F., Schauer, K., Hume, A.N., Freitas, R.P.*, et al.* (2010). Rab27a and Rab27b control different steps of the exosome secretion pathway. Nat Cell Biol *12*, 19-30; sup pp 11-13.

Pegtel, D.M., and S.J. Gould. 2019. Exosomes. *Annu Rev Biochem*. 88:in press.

Perez-Hernandez, D., Gutierrez-Vazquez, C., Jorge, I., Lopez-Martin, S., Ursa, A., Sanchez-Madrid, F., Vazquez, J., and Yanez-Mo, M. (2013). The intracellular interactome of tetraspanin-enriched microdomains reveals their function as sorting machineries toward exosomes. J Biol Chem *288*, 11649-11661.

Roucourt, B., Meeussen, S., Bao, J., Zimmermann, P., and David, G. (2015). Heparanase activates the syndecan-syntenin-ALIX exosome pathway. Cell Res *25*, 412-428.

Savina, A., Vidal, M., and Colombo, M.I. (2002). The exosome pathway in K562 cells is regulated by Rab11. J Cell Sci *115*, 2505-2515.

Trajkovic, K., Hsu, C., Chiantia, S., Rajendran, L., Wenzel, D., Wieland, F., Schwille, P., Brugger, B., and Simons, M. (2008). Ceramide triggers budding of exosome vesicles into multivesicular endosomes. Science *319*, 1244-1247.

Vara, J., Malpartida, F., Hopwood, D.A., and Jimenez, A. (1985). Cloning and expression of a puromycin N-acetyl transferase gene from Streptomyces alboniger in Streptomyces lividans and Escherichia coli. Gene *33*, 197-206.

Zhang, G., Gurtu, V., and Kain, S.R. (1996). An enhanced green fluorescent protein allows sensitive detection of gene transfer in mammalian cells. Biochem Biophys Res Commun *227*, 707-711.

Chapter 4: Transformation Induced Exosome Biogenesis

Abstract

Exosomes are released by almost all eukaryotes. The compositions of exosomes can vary significantly depending on the physiologic state of the cell and in response to hormones, infectious agents, diet and physical activities. We observed about 4-times more CD63, 3-times more CD81, and 1.7 times more CD9 in exosomes of 293T cells than in HEK 293 exosomes. We hypothesized that the increase in exosome production is a result of the transformed phenotype of 293T cells since they are derived from HEK 293 cells via the expression of SV40 large T antigen. As part of our effort to understand why these cells release larger amounts of these exosomal proteins, we screened these cells for the expression and vesicular secretion of numerous exosome-associated proteins. We observed no difference in the expression of most exosome-associated proteins (e.g. HRS, Alix, CD9, TSG101, MFGE8 etc.) but did detect an ~5-fold increase in the expression of nSMase2, raising the possibility that altered ceramide metabolism might underlie the increase in exosomal protein budding of 293T cells.

To test if ceramide plays a role, we assessed the ceramide levels in both cell lines, and found 293T to have significantly higher level of ceramide than HEK293. We also observed another lipid metabolite, diglyceride (DAG) levels to be significantly higher in 293T than in HEK293. DAG is a second messenger that can activate protein kinase C (PKC) and turn on numerous signal transduction pathways(Huang, 1989). We therefore propose that the increase in budding of exosomal classic markers in 293T might be due to the increased levels of ceramide, but also to the increased levels of DAG, and that both molecules may promote exosome biogenesis by a combination of (a) physico-chemical effects on membrane curvature, as both lipids are cone-shaped(Jarsch et al., 2016), and (b) activation of protein kinase signaling

pathways, as both molecules are agonists of one or more isoforms of the protein kinase C family(Huang et al., 1999).

Introduction

Proteins bud from cells in small single-membrane bound vesicles called exosomes. These vesicles bud from endosome and plasma membranes and have the same topology as cells(Pegtel and Gould, 2019). Their sizes range from ~30nm to 200nm, and their compositions can vary significantly depending on their site of budding, physiologic state of cell, and in response to stress and other signals(Gould and Raposo, 2013; Thery et al., 2006). Exosomes have been implicated in many physiological processes and diseases. They have been shown to be involved in cellular homeostasis(Takahashi et al., 2017), cell polarity(Lakkaraju and Rodriguez-Boulan, 2008; Shen et al., 2011) and migration(Shen et al., 2011). The mechanisms by which exosomes are made remain unclear. Exosomes were initially thought to be dependent on the ESCRT machinery because of the similarity of the process to other membrane scission-dependent processes such as MVB biogenesis, virus budding, and cytokinesis(Katzmann et al., 2001). However, several studies have established that blocking the ESCRT machinery causes little to no defect in exosome cargo protein budding(Colombo et al., 2013; Tamai et al., 2010).

Trajkovic et al. reported that Oli-neu cells still secreted exosomes when the ESCRT machinery was silenced. They observed these exosomes to be enriched in ceramide, and that exosome release was reduced following inhibition of the nSMase2 enzyme(Trajkovic et al., 2008). nSMase2 is a member of the neutral sphingomyelinase family that is active in neutral pH and catalyzes the hydrolysis of sphingomyelin (SM), releasing ceramide and the phosphorylcholine (PC) head group(Castro et al., 2014; Hannun and Obeid, 2011; Shamseddine

et al., 2015). A decrease in exosome release has also been reported in response to the inhibition or siRNA induced depletion of nSMase2 in many different systems(Verderio et al., 2018), including HEK293 cells(Kosaka et al., 2010), T cells(Mittelbrunn et al., 2011), hepatocytes(Nojima et al., 2016), astrocytes(Wang et al., 2012), microglial(Asai et al., 2015) and macrophages(Xu et al., 2016). Similar results have been observed in vivo in the context of a transgenic mouse model of Alzheimer's diseases (5XFAD mice), in which exosome reduction was caused by the administration of nSMase2 inhibitor(Dinkins et al., 2014). In their subsequent studies, the nSMase2 KO mice (fro;5XFAD) displayed a phenotype of reduced exosome production in the brain, which lead to the amelioration of Alzheimer's disease pathology and improvement of cognition(Dinkins et al., 2016). Furthermore, elevation of ceramide, either by blocking the conversion of ceramide to SM using sphingomyelin synthase (SMS) inhibitor in 5XFAD mice(Dinkins et al., 2014), or by addition of exogenous C6 ceramide directly to multiple myeloma cells(Cheng et al., 2018), increased exosome secretion.

In this chapter, I explore the differences in budding of exosome cargo proteins in HEK293 and 293T cells. Specifically, I employed an immunoblot-based screen of proteins that have been previously implicated in exosome biogenesis to see if any are expressed at elevated levels in 293T cells. I report here that 293T have significantly higher levels of nSMase2 protein than HEK293 cells, and that 293T cells have higher levels of both ceramide and DAG, raising the possibility that neoplastic transformation, and/or SV40 T antigen expression, induces exosome biogenesis, in part, by increasing the levels of nSMase2 protein and its direct and indirect products, ceramide and DAG.

Results & Discussions

We measured the amount of CD63, CD81 and CD9 in exosome and cell lysates of both HEK293 and 293T cells by immunoblot. We then calculated the relative budding of each protein in these two cell lines. These experiments revealed that 293T buds ~4.2x more CD63, ~3.6x more CD81 and ~1.7x more CD9 than HEK293 cells (Figure 1). To ascertain the mechanisms involved in 293T secreting more exosomal markers than HEK293, we screened for proteins that have been previously implicated in the exosome biogenesis process. We observed no significant difference in the expression of Syntenin, MfgE8, HRS, Alix or Agonaute-2 (Figure 2a). However, we found that 293T cells express ~5-fold more nSMase2 than do HEK293 cells (Figure 2b). nSMase2 catalyzes the breakdown of sphingomyelin to ceramide and has been shown to be involved in a number of physiological processes, including apoptosis, immune responses and cell-cycle(Castro et al., 2014; Hannun and Obeid, 2011; Ogretmen and Hannun, 2004; Verderio et al., 2018). In 2008, Trakjovic et al showed the involvement of nSMase2 in exosome production in Oli-neu cells(Trajkovic et al., 2008). They observed exosome secretion did not depend on the ESCRT machinery as there was no effect on the production of exosomes upon the inhibition of ESCRT. They however observed the secretion of exosomes to be significantly reduced upon the pharmacologic inhibition of nSMase2 enzymatic activity and proposed that the inhibition of this enzyme resulted in a reduction of ceramide level, which may directly affect vesicle formation due to its physico-chemical properties(Jarsch et al., 2016).

Based on this information, we hypothesized that the increase in nSMase2 levels in 293T altered the ceramide levels in the cells which then resulted in the increase in budding of exosomal markers. To test our hypothesis, we measured the amount of the ceramide in both HEK293 and 293T using acidified Bligh and Dyer(Bligh and Dyer, 1959) and quantified by

DGK assay(Hokin and Hokin, 1959). We observed that 293T has 2.5-times more ceramide in the cells than HEK293 cells (Figure 3a). In addition, we observed a significant, nearly 2-fold increase in diacylglycerol (DAG) levels in 293T cell (Figure 3b). This result, which we did not initially expect, makes metabolic sense, as elevated levels of ceramide would be expected to lead to higher metabolite flux through the enzyme sphingomyelin synthase, which catalyzes the reaction of ceramide with phosphatidylcholine, generating sphingomyelin and DAG. These results raise the possibility that the effects of elevating ceramide on exosome biogenesis may be mediated by a combination of both ceramide and DAG, both of which may increase exosome production by physico-chemical mechanisms, and perhaps also by activating one or more isoforms of protein kinase C, for which ceramide and DAG are agonists(Huang et al., 1999; Huang, 1989).

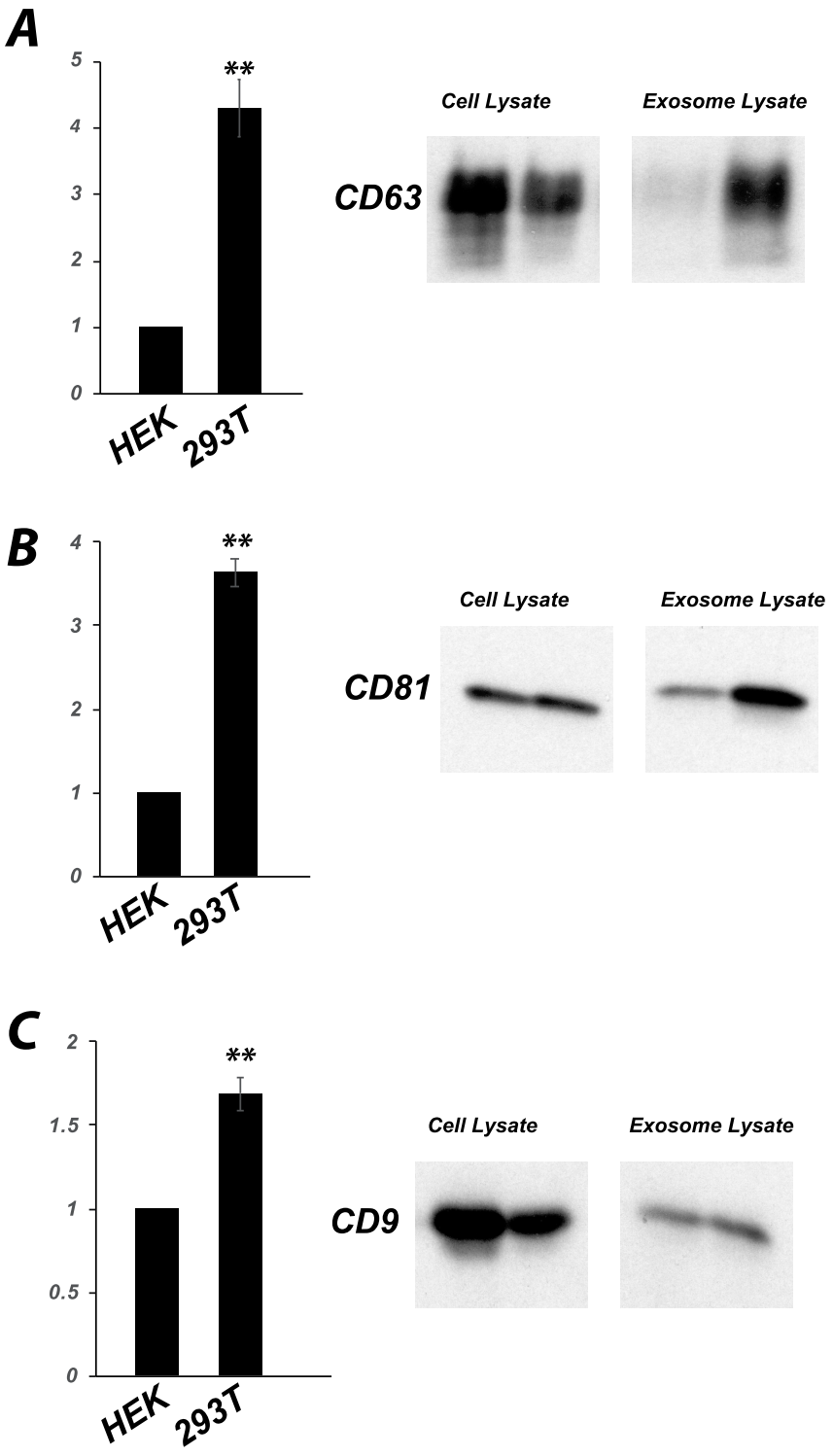

Figure 1: 293T makes more exosomes than HEK293. Bar graphs showing the average +/- s.e.m relative budding of (A) CD63, (B) CD81 and (C) CD9 in HEK293 and 293T. (n=4) ** denotes a *p*-value less than 0.005. Right panel shows immunoblots of cell and exosome lysates of HEK293 and 293T blotted for anti-CD63, anti-CD81 and anti-CD9

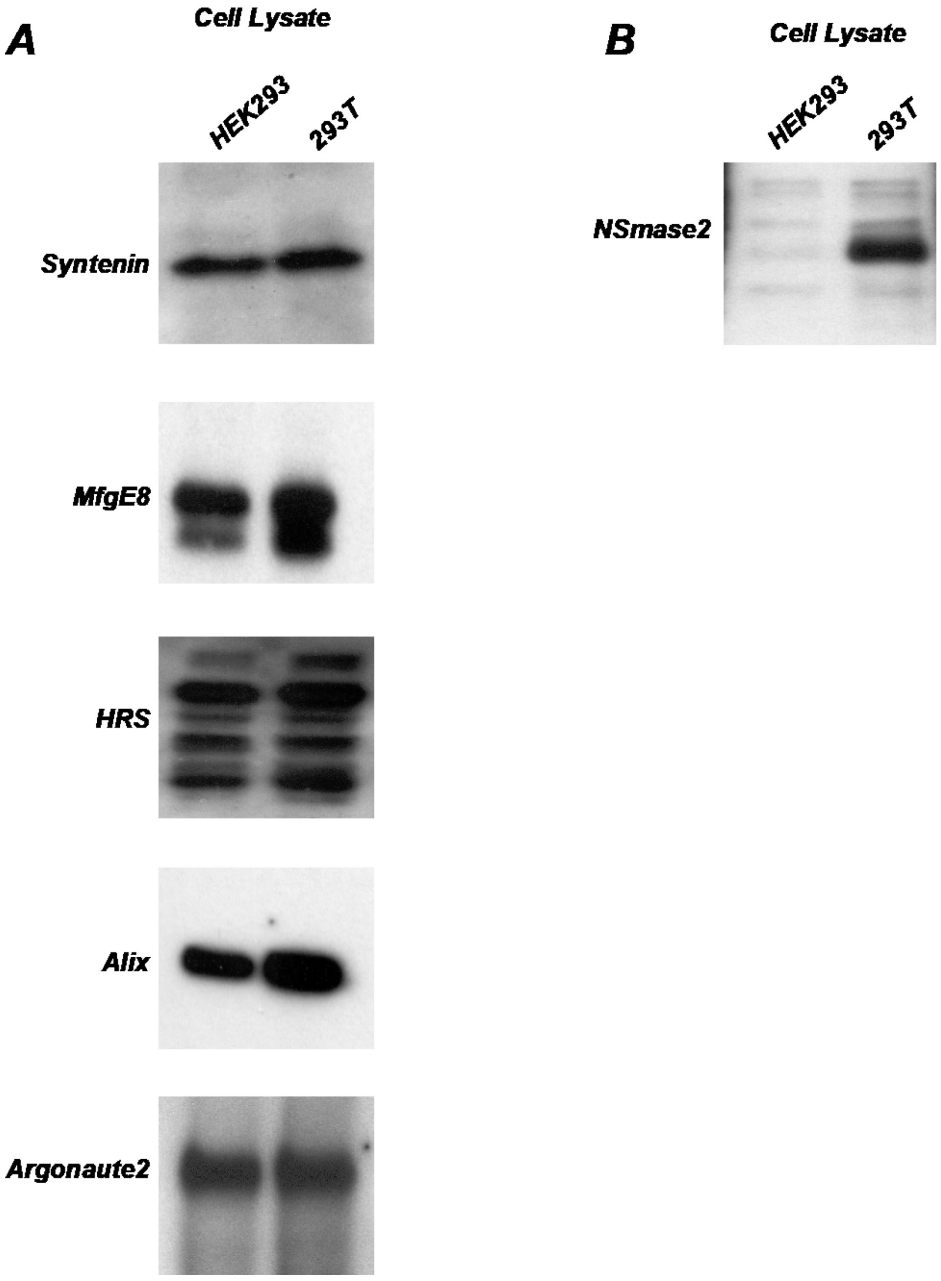

Figure 2: Both cells have similar levels of exosome factors except for nSmase2 (A) (Left panels) Immunoblots of cell lysates of HEK293 and 293T blotted with antibodies specific for syntenin, MfgE8, HRS, Alix and Argonaute-2. (B) (right panel), blotted with antibody specific for nSMase2.

A

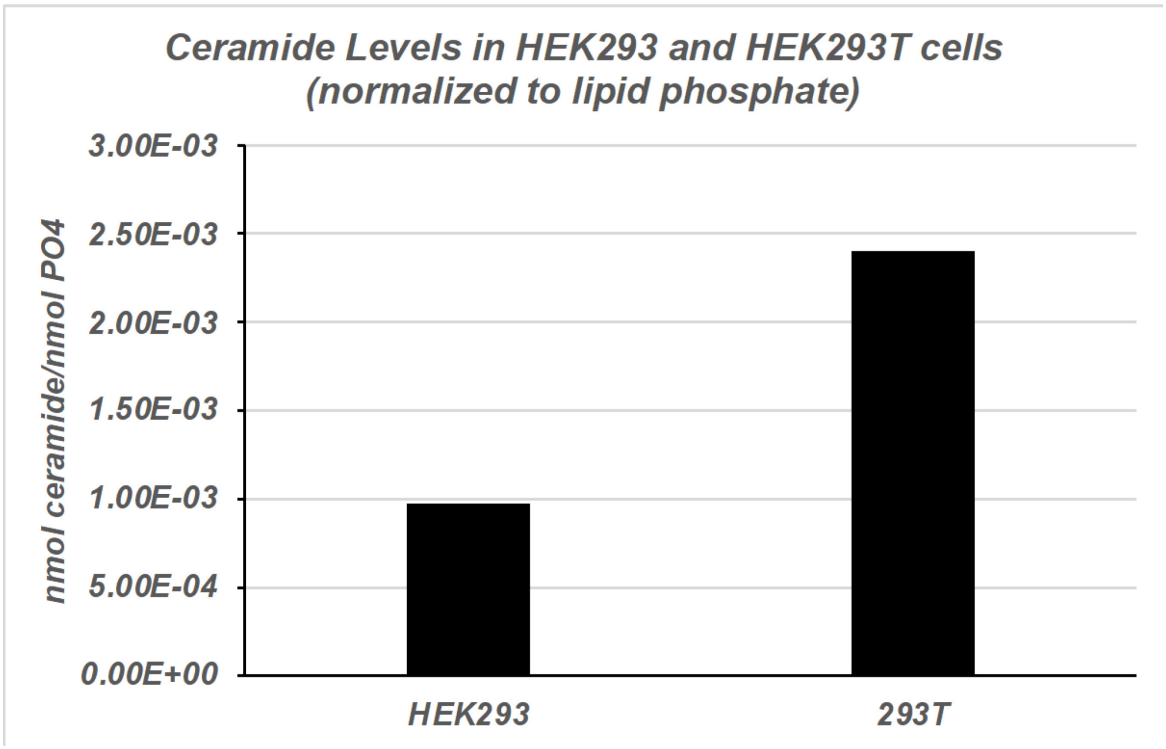
Ceramide Levels in HEK293 and HEK293T cells
(normalized to lipid phosphate)
nmol ceramide/nmol PO4
3.00E-03
2.50E-03
2.00E-03
1.50E-03
1.00E-03
5.00E-04
0.00E+00
HEK293
293T

B

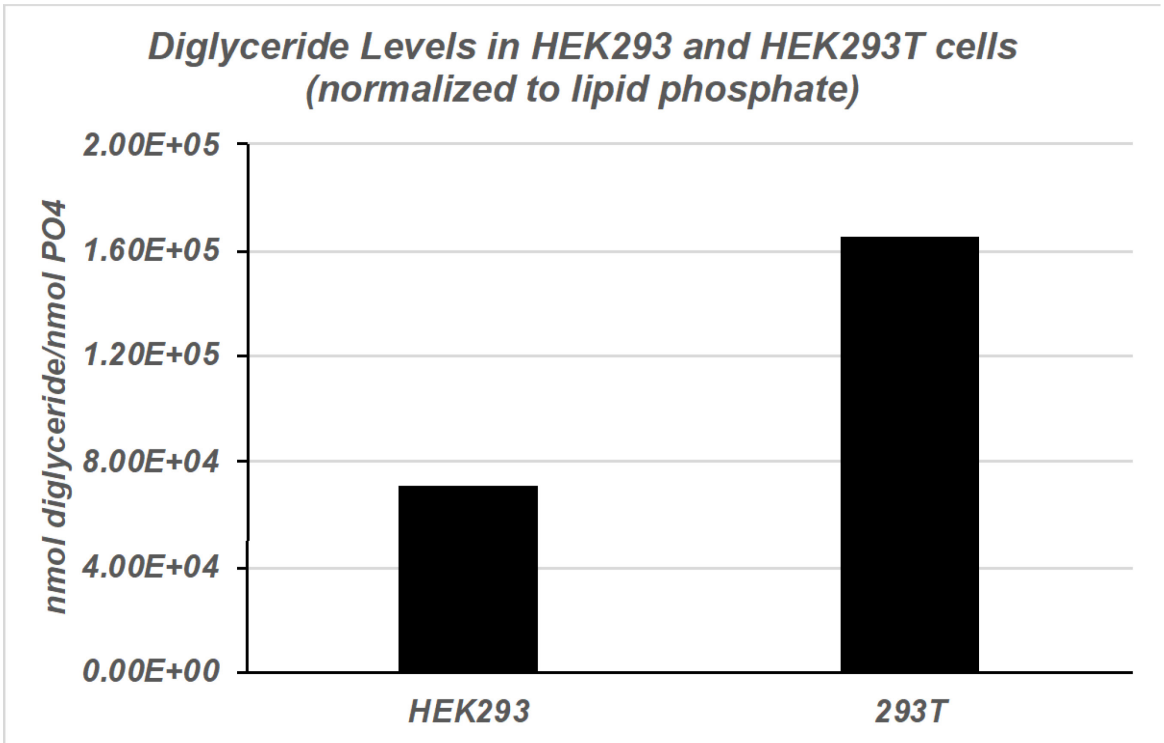
Diglyceride Levels in HEK293 and HEK293T cells
(normalized to lipid phosphate)
nmol diglyceride/nmol PO4
2.00E+05
1.60E+05
1.20E+05
8.00E+04
4.00E+04
0.00E+00
HEK293
293T

Figure 3: 293T has 2.5-fold more ceramide and 2-fold more DAG than HEK293 cells. (A) Bar graph showing ceramide levels in HEK293 and 293T cells, levels are normalized to lipid phosphate. (B): Bar graph showing diglyceride levels in HEK293 and 293T cells, levels are normalized to lipid phosphate.

References

Asai, H., Ikezu, S., Tsunoda, S., Medalla, M., Luebke, J., Haydar, T., Wolozin, B., Butovsky, O., Kugler, S., and Ikezu, T. (2015). Depletion of microglia and inhibition of exosome synthesis halt tau propagation. Nat Neurosci *18*, 1584-1593.

Bligh, E.G., and Dyer, W.J. (1959). A rapid method of total lipid extraction and purification. Can J Biochem Physiol *37*, 911-917.

Castro, B.M., Prieto, M., and Silva, L.C. (2014). Ceramide: a simple sphingolipid with unique biophysical properties. Prog Lipid Res *54*, 53-67.

Cheng, Q., Li, X., Wang, Y., Dong, M., Zhan, F.H., and Liu, J. (2018). The ceramide pathway is involved in the survival, apoptosis and exosome functions of human multiple myeloma cells in vitro. Acta Pharmacol Sin *39*, 561-568.

Colombo, M., Moita, C., van Niel, G., Kowal, J., Vigneron, J., Benaroch, P., Manel, N., Moita, L.F., Thery, C., and Raposo, G. (2013). Analysis of ESCRT functions in exosome biogenesis, composition and secretion highlights the heterogeneity of extracellular vesicles. J Cell Sci *126*, 5553-5565.

Dinkins, M.B., Dasgupta, S., Wang, G., Zhu, G., and Bieberich, E. (2014). Exosome reduction in vivo is associated with lower amyloid plaque load in the 5XFAD mouse model of Alzheimer's disease. Neurobiol Aging *35*, 1792-1800.

Dinkins, M.B., Enasko, J., Hernandez, C., Wang, G., Kong, J., Helwa, I., Liu, Y., Terry, A.V., Jr., and Bieberich, E. (2016). Neutral Sphingomyelinase-2 Deficiency Ameliorates Alzheimer's Disease Pathology and Improves Cognition in the 5XFAD Mouse. J Neurosci *36*, 8653-8667.

Fordjour, F.K., S. Owiredu, H. Muendlein, J. Plange, J.C. Morrell, J. Han, and S.J. Gould. 2016. Creation of CD63-deficient HEK293 cell lines using a polycistronic CAS9/EGFP/HSVtk/PuroR expression vector. *Matters*

Gould, S.J., and Raposo, G. (2013). As we wait: coping with an imperfect nomenclature for extracellular vesicles. J Extracell Vesicles *2*.

Hannun, Y.A., and Obeid, L.M. (2011). Many ceramides. J Biol Chem *286*, 27855-27862.

Hokin, L.E., and Hokin, M.R. (1959). Diglyceride phosphokinase: an enzyme which catalyzes the synthesis of phosphatidic acid. Biochim Biophys Acta *31*, 285-287.

Huang, H.W., Goldberg, E.M., and Zidovetzki, R. (1999). Ceramides modulate protein kinase C activity and perturb the structure of Phosphatidylcholine/Phosphatidylserine bilayers. Biophys J *77*, 1489-1497.

Huang, K.P. (1989). The mechanism of protein kinase C activation. Trends Neurosci *12*, 425-432.

Jarsch, I.K., Daste, F., and Gallop, J.L. (2016). Membrane curvature in cell biology: An integration of molecular mechanisms. J Cell Biol *214*, 375-387.

Katzmann, D.J., Babst, M., and Emr, S.D. (2001). Ubiquitin-dependent sorting into the multivesicular body pathway requires the function of a conserved endosomal protein sorting complex, ESCRT-I. Cell *106*, 145-155.

Kosaka, N., Iguchi, H., Yoshioka, Y., Takeshita, F., Matsuki, Y., and Ochiya, T. (2010). Secretory mechanisms and intercellular transfer of microRNAs in living cells. J Biol Chem *285*, 17442-17452.

Lakkaraju, A., and Rodriguez-Boulan, E. (2008). Itinerant exosomes: emerging roles in cell and tissue polarity. Trends Cell Biol *18*, 199-209.

Mittelbrunn, M., Gutierrez-Vazquez, C., Villarroya-Beltri, C., Gonzalez, S., Sanchez-Cabo, F., Gonzalez, M.A., Bernad, A., and Sanchez-Madrid, F. (2011). Unidirectional transfer of microRNA-loaded exosomes from T cells to antigen-presenting cells. Nat Commun *2*, 282.

Nojima, H., Freeman, C.M., Schuster, R.M., Japtok, L., Kleuser, B., Edwards, M.J., Gulbins, E., and Lentsch, A.B. (2016). Hepatocyte exosomes mediate liver repair and regeneration via sphingosine-1-phosphate. J Hepatol *64*, 60-68.

Ogretmen, B., and Hannun, Y.A. (2004). Biologically active sphingolipids in cancer pathogenesis and treatment. Nat Rev Cancer *4*, 604-616.

Pegtel, D.M., and S.J. Gould. 2019. Exosomes. *Annu Rev Biochem*. 88:in press.

Shamseddine, A.A., Airola, M.V., and Hannun, Y.A. (2015). Roles and regulation of neutral sphingomyelinase-2 in cellular and pathological processes. Adv Biol Regul *57*, 24-41.

Shen, B., Fang, Y., Wu, N., and Gould, S.J. (2011). Biogenesis of the posterior pole is mediated by the exosome/microvesicle protein-sorting pathway. J Biol Chem *286*, 44162-44176.

Takahashi, A., Okada, R., Nagao, K., Kawamata, Y., Hanyu, A., Yoshimoto, S., Takasugi, M., Watanabe, S., Kanemaki, M.T., Obuse, C.*, et al.* (2017). Exosomes maintain cellular homeostasis by excreting harmful DNA from cells. Nat Commun *8*, 15287.

Tamai, K., Tanaka, N., Nakano, T., Kakazu, E., Kondo, Y., Inoue, J., Shiina, M., Fukushima, K., Hoshino, T., Sano, K.*, et al.* (2010). Exosome secretion of dendritic cells is regulated by Hrs, an ESCRT-0 protein. Biochem Biophys Res Commun *399*, 384-390.

Thery, C., Amigorena, S., Raposo, G., and Clayton, A. (2006). Isolation and characterization of exosomes from cell culture supernatants and biological fluids. Curr Protoc Cell Biol *Chapter 3*, Unit 3 22.

Trajkovic, K., Hsu, C., Chiantia, S., Rajendran, L., Wenzel, D., Wieland, F., Schwille, P., Brugger, B., and Simons, M. (2008). Ceramide triggers budding of exosome vesicles into multivesicular endosomes. Science *319*, 1244-1247.

Verderio, C., Gabrielli, M., and Giussani, P. (2018). Role of sphingolipids in the biogenesis and biological activity of extracellular vesicles. J Lipid Res *59*, 1325-1340.

Wang, G., Dinkins, M., He, Q., Zhu, G., Poirier, C., Campbell, A., Mayer-Proschel, M., and Bieberich, E. (2012). Astrocytes secrete exosomes enriched with proapoptotic ceramide and prostate apoptosis response 4 (PAR-4): potential mechanism of apoptosis induction in Alzheimer disease (AD). J Biol Chem *287*, 21384-21395.

Xu, Y., Liu, Y., Yang, C., Kang, L., Wang, M., Hu, J., He, H., Song, W., and Tang, H. (2016). Macrophages transfer antigens to dendritic cells by releasing exosomes containing dead-cell-associated antigens partially through a ceramide-dependent pathway to enhance CD4(+) T-cell responses. Immunology *149*, 157-171.

Curriculum Vitae

CURRICULUM VITAE

The Johns Hopkins University School of Medicine

FRANCIS KUSI FORDJOUR **March 27, 2019**

Educational History:

Ph.D. expected	2019	Program in Biological Chemistry Mentor: Stephen J. Gould, Ph.D.	Johns Hopkins School of Medicine
B.A	2013	Biochemistry	DePauw University

Professional Experiences

Graduate Research Student	07/2013-Present	Lab of Dr. Stephen Gould	Biological Chemistry Johns Hopkins School of Medicine
Global Health Intern	01/2013-02/2013	Dr. Keri Cohn	Massachusetts General Hospital Division of Global Health and Human Rights in partnership with the Harvard College Global Hunger Initiative
Research Assistant	02/2012-05/2013	Lab of Dr. Sharon Crary	Biochemistry and Chemistry Department, DePauw University
Research Assistant	05/2012-08/2012	Lab of Dr. David Price	Biochemistry Department, University of Iowa
Research Assistant	06/2011-12/2012	Lab of Dr. Klass Hellingwerf	Molecular Microbial Physiology Department University of Amsterdam
Research Assistant	06/2011-08/2011	Lab of Dr. Blythe Janowiak	Biology Department, Saint Louis University

Completed Extramural Funding

2012 Douglas B. White Memorial Travel Fund Award
Sponsor: DePauw University
Direct Cost: $4000
PI: Sharon Crary, DePauw University

Role/effort: Global Health Intern/100%

2012 Biochemistry Summer Undergraduate Research Fellowship
Sponsor: University of Iowa
Direct Cost: $4250
PI: David Price, University of Iowa
Role/effort: Research Assistant/100%

2011 The University of Amsterdam Institutional Award for Research
Sponsor: University of Amsterdam
Direct Cost: 2000 Euros
PI: Jeroen van der Steen, University of Amsterdam
Role/effort: Research Assistant/100%

2011 Special Administrative Funds for Summer Research
Sponsor: DePauw University
Direct Cost: $1000
PI: Blythe Janowiak, Saint Louis University
Role/effort: Research Assistant/100%

Awards and Honors

2015 International Society For Extracellular Vesicles Conference Scholarship
2013 Latin Honors-*Cum Laude* DePauw University Commencement
2013 Awesome Dawson Award DePauw University, Biochemistry Department
2013 Thomas Mote Public and Global Health Senior Award, DePauw University
2013 David B. Becker Fellows Award, DePauw University
2012 National Chemistry Honorary Society, DePauw-Wabash University Chapter of Phi Lambda Upsilon
2012 Biochemistry Summer Undergraduate Research Fellow, University of Iowa
2011-2012 Percy Lavon Julian Scholar, DePauw University
2011-2012 Susan Wohlers Pearson Fund for International Study, DePauw University
2011-2012 The University of Amsterdam Institutional Award for Research, University of Amsterdam
2011-2012 Lamar Endowment Fund, DePauw University
2009-2013 DePauw University Dean's List
2009-2013 Information Technology Associate Program, DePauw University
2009-2013 Presidential Award for Excellence, DePauw University
2009-2013 Ruth & Philip Holton Memorial Scholarship, DePauw University

RESEARCH ACTIVITIES

Peer Reviewed Publications

Francis K Fordjour, George Daaboul, Stephen J Gould. (2019) A shared pathway of exosome biogenesis operates at plasma and endosome membranes. bioRxiv

Francis K Fordjour, Shawn Owiredu, Hayley Muendlein, Jerry Plange, James Morrell, Jingnan Han, Stephen J Gould. (2016) Creation of CD63-deficient HEK293 cell lines using a polycistronic CAS9/EGFP/HSVtk/PuroR expression vector. Science Matters

Ling Li, Klaus Piontek, Masaharu Ishida, Michel Fausther, Jonathan A. Dranoff, Rongdang Fu, Esteban Mezey, Stephen J. Gould, **Francis K. Fordjour**, Stephen J. Meltzer, Alphonse E. Sirica, Florin M. Selaru. (2016) Extracellular vesicles carry microRNA-195 to intrahepatic cholangiocarcinoma and improve survival in a rat model. *Hepatology*. DOI: 10.1002/hep.28735

Jiannan Guo, Tiandao Li, Joshua Schipper, Kyle A Nilson, **Francis K Fordjour**, Jeffrey J Cooper, Raluca Gordan, David H Price. (2014) Sequence specificity incompletely defines the genome-wide occupancy of Myc. Genome Biology 15(10): 482

Poster and Talk Presentations

Francis Fordjour. Using CRISPR/Cas9 to Study the Mechanisms for Exosomes Biogenesis (Invited by DePauw University Chemistry & Biochemistry Dept and DePauw Student of Color in Science (SoCiS) to talk on my thesis work and life after DePauw as a minority in STEM, Greencastle, IN-November 14, 2018)

Francis Fordjour, George Daaboul and Stephen Gould. Exosome Biogenesis at the plasma and endosome membranes (Short talk at American Society of Exosomes and Microvesicles Conference, Baltimore, MD-October 2018)

Francis Fordjour and Stephen Gould. Exosome Biogenesis in the absence of CD63, CD81, and CD9 (Short talk at American Society of Exosomes and Microvesicles Conference, Asilomar, CA-October 2017)

Francis Fordjour, Abena Kwaa, Joel Blankson, Stephen Gould. Trojan Exosome Hypothesis (Short talk and poster presentation at Biological Chemistry Annual Retreat, Mt. Washington, MD-September, 2017)

Francis Fordjour, Jerry Plange, Shawn Owiredu, Adrianna Batazzi, James C. Morrell, Stephen Gould Clonal Heterogeneity in Exosome Biogenesis (Short talk and poster presentation at American Society for Exosomes and Microvesicles Conference, Asilomar, CA-October, 2016)

Francis Fordjour, Jerry Plange, Shawn Owiredu, Adrianna Batazzi, James C. Morrell, Stephen Gould. Role of Tetraspanins in Exosome Biogenesis and Function (Short talk at the Biological Chemistry Annual Retreat, Mt. Washington, MD-October, 2016)

Francis Fordjour, Jerry Plange, Shawn Owiredu, Adrianna Batazzi, James C. Morrell, Stephen Gould. Gene Knock-out Cell lines and Plasmids for Studying EV and ex-RNA biogenesis (Short talk presentation at the 6th NIH Ex-RNA Communication Program Investigators Meeting, Washington DC-April, 2016)

Francis Fordjour, Stephen Gould. Tetraspanin budding and Exosome Biogenesis (Short talk presentation at American Society For Exosomes and Microvesicles, Marco Island, FL-October, 2015)

Francis Fordjour and Stephen Gould. Exosomes and Microvesicles Biogeneses: Is Endosomal Targeting Important for Protein Budding? (Short talk at the Biological Chemistry Annual Retreat, Mt. Washington, MD-May, 2015)

Francis Fordjour, Jr-Ming Yang, and Stephen Gould. Biogenesis of exosomal/microvesicular proteins (Abstract submitted to American Society for Exosomes and Microvesicles Conference, Asilomar, CA-October, 2014)

Jr-Ming, **Francis Fordjour**, Michael Wolfgang, and Stephen J. Gould. Exploring the Genetics of Exosome Biogenesis (Abstract submitted to American Society for Exosomes and Microvesicles Conference, Miami FL-September, 2013)

Francis Kusi Fordjour, Lauren E. Salay, Jonathan M. Howard, Lauren M. Guggina, W. Maxwell Hudson, Anne Collier, and Sharon M. Crary. Characterization of the N-terminal Domain of Ebola virus nucleoprotein (Poster presentation at Rustbelt RNA Meeting, Dayton OH-October, 2012)

Tiandao Li, Jiannan Guo, **Francis K. Fordjour**, Jeffrey J. Cooper, and David H. Price. Recruitment of c-Myc to RNA Polymerase II Transcription Complexes (Poster presentation at Summer Undergraduate Research Conference, Iowa City-July, 2012)

Francis K. Fordjour, Jeroen van der Steen, and Klaas Hellingwerf. Light Activation of the General Stress Response of *Bacillus subtilis* (Oral presentation at Euroscholars MidStay Program Conference, Zurich, Switzerland-November, 2011)

Inventions

"High Exosome-producing Cell Lines" JHU reference #C15132 – Co-Inventor

"ExoMap Mice for in vivo Exosome Analysis" JHU reference #C15133 – Co-Inventor

"Bicistronic Mammalian Expression Vectors" JHU reference #C15135 – Co-Inventor

EDUCATIONAL ACTIVITIES

Teaching Experience

2015-2016	Teaching Assistant for graduate students, Molecular Biology and Genomics, Johns Hopkins University School of Medicine
2015	Teaching Assistant for medical students, Cell Physiology section of Scientific Foundations of Medicine, Johns Hopkins University School of Medicine
2012-2013	Science Experiments Tutor for second grade students, Greencastle Middle School, Greencastle, IN
2012-2013	Chemistry Tutor, Greencastle High School, Greencastle, IN

Mentoring Experience

2014-2018	Supervised research of two rotating graduate students and three laboratory technicians Biological Chemistry Department, Johns Hopkins University School of Medicine
2013	Supervised research of a high school student Biological Chemistry Department, Johns Hopkins University School of Medicine
2012	Judge at the Annual Greencastle High School Science Fair Greencastle High School, Greencastle, IN

Scientific Conferences

October 20-24, 2018	Annual Meeting: American Society of Exosomes and Microvesicles, Baltimore MD
October 9-12, 2017	Annual Meeting: American Society of Exosomes and Microvesicles, Asilomar, CA
September 15, 2017	Annual Retreat: Department of Biological Chemistry, Johns Hopkins School of Medicine, Mt. Washington, MD
October 20-24, 2016	Annual Meeting: American Society for Exosomes and Microvesicles, Asilomar, CA
October 14, 2016	Annual Retreat: Department of Biological Chemistry, Johns Hopkins School of Medicine, Mt. Washington, MD (Session Chair)
April 19, 2016	6th NIH Ex-RNA Communication Program Investigators Meeting, Washington DC
October 16-20, 2015	Annual Meeting: American Society for Exosomes and Microvesicles, Marco Island, FL
May 8, 2015	Annual Retreat: Department of Biological Chemistry, Johns Hopkins School of Medicine, Mt. Washington, MD
April 23-26, 2015	Annual Meeting: International Society For Extracellular Vesicles, Washington DC
October 10-13, 2014	Annual Meeting: American Society for Exosomes and Microvesicles, Asilomar, CA
September 6-9, 2013	Annual Meeting: American Society for Exosomes and Microvesicles, Orlando, FL
October 19-20, 2012	Rustbelt RNA meeting, Dayton, OH
November 25, 2011	Euroscholars MidStay Program Conference, Zurich, Switzerland

Professional Societies

2017	American Society of Biochemistry and Molecular Biology, member
2015-present	International Society For Extracellular Vesicles, member
2013-present	American Society of Exosomes and Microvesicles, member
2012-present	Phi Lambda Upsilon National Chemistry Honor Society